CONTRIBUTIONS TO JOINT MONITORING OF

LOCATION AND SCALE PARAMETERS:

SOME THEORY AND APPLICATIONS

by

AMANDA KAYE MCCRACKEN

SUBHABRATA CHAKRABORTI, COMMITTEE CHAIR
B. MICHAEL ADAMS
BRUCE BARRETT
BURCU KESKIN
ROBERT MOORE
MARCUS PERRY

A DISSERTATION

Submitted in partial fulfillment of the requirements for the
degree of Doctor of Philosophy in the Department of
Information Systems, Statistics, and Management
Science in the Graduate School of
The University of Alabama

TUSCALOOSA, ALABAMA

2012

ABSTRACT

Since their invention in the 1920s, control charts have been popular tools for use in monitoring processes in fields as varied as manufacturing and healthcare. Most of these charts are designed to monitor a single process parameter, but recently, a number of charts and schemes for jointly monitoring the location and scale of processes which follow two-parameter distributions have been developed. These joint monitoring charts are particularly relevant for processes in which special causes may result in a simultaneous shift in the location parameter and the scale parameter.

Among the available schemes for jointly monitoring location and scale parameters, the vast majority are designed for normally distributed processes for which the in-control mean and variance are known rather than estimated from data. When the process data are non-normally distributed or the process parameters are unknown, alternative control charts are needed. This dissertation presents and compares several control schemes for jointly monitoring data from Laplace and shifted exponential distributions with known parameters as well as a pair of charts for monitoring data from normal distributions with unknown mean and variance. The normal theory charts are adaptations of two existing procedures for the known parameter case, Razmy's (2005) Distance chart and Chen and Cheng's (1998) Max chart, while the Laplace and shifted exponential charts are designed using an appropriate statistic for each parameter, such as the maximum likelihood estimators.

DEDICATION

This dissertation is dedicated to my closest family members who encouraged me throughout many years of formal education: my parents, Bob and Barbara McMillan; my brother, Robert McMillan; my husband, Will McCracken; and my daughter, Anna McCracken.

ACKNOWLEDGEMENTS

I am pleased to have the opportunity to thank those who helped me during the dissertation development process. I would first like to thank the chairman of my doctoral committee, Dr. Subhabrata Chakraborti, for his continuing guidance. I learned a tremendous amount from him, both during the courses he taught and during the many hours I spent in his office discussing details of this dissertation and my various papers and conference presentations.

I would also like to thank the other faculty members who served on my committee: Dr. Robert Moore, Dr. Michael Adams, Dr. Marcus Perry, Dr. Burcu Keskin, and Dr. Bruce Barrett. Their insightful comments led to significant improvements in this dissertation. Additionally, several of my committee members were instrumental in my success during my undergraduate and graduate coursework. I would particularly like to thank Dr. Moore for his encouragement during my time studying undergraduate mathematics, which helped give me the confidence to major in that subject.

Finally, I would like to thank Dr. Lorne Kuffel and the staff of the Office of Institutional Research and Assessment (OIRA). Throughout my time as a graduate student, I was employed as a research assistant by OIRA. My work there included the opportunity to learn about institutional research, get to know many wonderful people, and complete a number of challenging projects. I am truly grateful for this opportunity and the many learning experiences it provided.

CONTENTS

LIST OF TABLES

LIST OF FIGURES

CHAPTER 1

INTRODUCTION

1.1 Brief Overview of Joint Monitoring

Control charts are widely used for surveillance or monitoring of processes in a variety of industries. These graphical displays are designed to allow a practitioner to determine whether a process is in-control (*IC*) or out-of-control (*OOC*) by taking samples at specified sampling intervals and plotting values of some statistics on a graphical interface which includes decision lines called control limits. The vast majority of control charts are designed to monitor a single process parameter, such as the mean or the variance, but it is often desirable to monitor the mean and the variance simultaneously, since both may shift at the same time and since a change in the variance can affect the control limits of the mean chart. For some processes, special causes can result in a simultaneous change in both the mean and the variance. For example, in circuit manufacturing, an improperly fixed stencil can result in a shift in both the mean and variance of the thickness of the solder paste printed onto circuit boards (Gan et al., 2004). In such cases, simultaneous monitoring of both parameters is a logical approach to process control. As expressed by Gan et al. (2004), "when special causes exist and cause both the mean and variance to shift simultaneously, then it is more reasonable to combine the mean and variance information on one scheme and look at their behavior jointly."

In many cases, practitioners are interested in the general question of whether the process continues to produce results which have the same, specified distribution. The distribution is most commonly assumed to be the normal distribution, which is completely characterized by its mean and variance. Thus, monitoring both mean and variance allows one to determine whether each sample collected appears to be from the specified normal distribution or come from a normal distribution which is different from the *IC* normal distribution in some way. Gan (1995) noted that "the mean and variance charts are virtually always used together." The common practice of using a mean chart together with a variance (or range or standard deviation) chart is one type of joint monitoring scheme. However, as noted by Gan (1997), doing so is "basically looking at a bivariate problem using two univariate procedures." Furthermore, schemes consisting of two independent charts can be affected by the classical 'multiple testing' problem, and if adjustments are not made to these charts' control limits to account for this fact, the false alarm rate (FAR) is inflated, since the process is deemed to be *OOC* whenever a signal occurs on either chart. For example, if each chart is set at a nominal FAR of 0.0027 and the charts operate independently, the overall FAR (the probability of a false alarm on at least one chart) is $1-(1-0.0027)^2 = 0.0054$, a 100% increase from the nominal 0.0027. This FAR inflation can ruin the efficacy of the resulting monitoring procedure. Therefore, practitioners using a two-chart scheme should select control limits for each chart such that the overall FAR is a specified value. In the earlier example, if an overall FAR of 0.01 is desired, each chart should be calibrated at an FAR of 0.005.

1.2 Parametric Charts

As noted earlier, the most typical assumption in statistical process control (SPC) has been that the process output follows a normal distribution. Under this model assumption, joint monitoring of processes involves two parameters, the mean (location) and the variance (scale), and typically uses an efficient statistic for monitoring each parameter. A joint monitoring scheme links these statistics or the corresponding control charts in some way. These schemes can be broadly classified as one- or two-chart control schemes, respectively. Ideally, a monitoring scheme should be "simple to use, easy to understand, and quick to implement" in order to maximize its usefulness (Chao and Cheng, 1996). A joint monitoring scheme should also clearly indicate the parameter or parameters which are *OOC*. We discuss these various schemes and the associated details below.

Though many processes do produce outputs which follow a normal distribution, there are also many which do not. As noted by Yang et al. (2011), many service processes produce non-normally distributed outputs. For example, a variable of interest such as the time to a certain event that is being monitored may follow a righted-skewed exponential distribution; another variable may have an underlying distribution that is symmetric but heavier tailed, such as the logistic distribution. A number of authors have recommended that practitioners avoid using charts based on the normal distribution for processes which are non-normal, since these charts may be quite ineffective or perform rather erratically for other distributions, including highly skewed or heavier tailed processes. Additionally, these existing charting procedures assume the existence and independence of the mean and the variance. It is not clear how these normal theory charts would perform for distributions which lack these traits, such as the skewed gamma distribution, in which the mean and the variance both depend on the scale and the shape parameters, or the Cauchy distribution, which is symmetric and has a finite median but has no finite mean or variance. So far, however, research in the area of parametric joint monitoring has largely overlooked cases in which processes are known to be non-normal. This is an important area for further research, since few non-normal parametric joint monitoring schemes are currently available in the literature.

1.3 Nonparametric Charts

There is not always enough knowledge or information to support the assumption that the process distribution is of a specific shape or form (such as normal). In such cases, nonparametric or distribution-free charts can be useful. These charts also provide a useful approach for monitoring processes which are known to be non-normal. However, this is a relatively new area of research, and only a handful of nonparametric joint monitoring charts are currently available in the literature.

1.4 Focus of Dissertation

1.4.1 Shewhart-Type Control Charts for Simultaneous Monitoring of Unknown Means and Variances of Normally Distributed Processes

A number of joint monitoring schemes have been developed for process data which follow a normal distribution with a known mean and variance. Among these are Chen and Cheng's (1998) Max chart and Razmy's (2005) Distance chart. The performance of these charts, however, is degraded in situations where the mean and/ or variance must be estimated from process data. This can be remedied by adapting the charts to account for the variability in the estimated parameters, a task which can be accomplished by conditioning. The resulting charts are appropriate for use with normally distributed process data with unknown mean and variance, though a different charting procedure should be used if the data are not normally distributed.

1.4.2 Control Charts for Simultaneous Monitoring of Location and Scale of Processes Following a Shifted (Two-Parameter) Exponential Distribution

The shifted, or two-parameter, exponential, is a right-skewed distribution which is often used to model the time to some event which cannot occur prior to a specified point in time, θ. Its two parameters are this location parameter, θ, and a scale parameter, λ.

Like the normal distribution, the shifted exponential distribution is completely described by specifying these two parameters. However, this is essentially the only similarity between the two distributions. Notably, the mean and the variance of the shifted exponential distribution both depend on λ. As a result, it is not appropriate to jointly monitor the mean and variance of data which follow a shifted exponential distribution, as these quantities are correlated. As noted by Ramalhoto and Morais (1999), the mean and standard deviation of process samples are often inefficient summary statistics, and in such cases, using them for process monitoring is both wasteful and unreliable. When process data follow the shifted exponential distribution, this situation occurs, and, as a result, an alternative to monitoring the mean and standard deviation is necessary.

A few control charts for the shifted exponential distribution appear in the literature. Ramalhoto and Morais (1999) studied control charts for the scale parameter of the three-parameter Weibull distribution, which can also be used for the λ parameter of the shifted exponential distribution, since, as mentioned above, the latter is merely a special case of the former. However, using these charts requires the assumption that the location parameter is known and fixed. Sürücü and Sazak (2009) presented a control scheme for this same distribution based on the idea of using moments to approximate the distribution. We propose more exact methods in which θ and λ are monitored jointly, using a well-known estimator for each parameter, in order to determine whether each sample collected appears to be from the specified *IC* shifted exponential distribution or to come from a different shifted exponential distribution.

1.4.3 Control Charts for Simultaneous Monitoring of Location and Scale of Processes Following a Laplace Distribution

The Laplace, or double exponential, distribution is symmetric but heavier-tailed than the normal distribution and is commonly used to model the difference between two exponential distributions with a common scale, for example, differences in flood levels at two different points along a river (Puig and Stephens, 2000; Bain and Engelhardt, 1973). This distribution can be completely described by specifying two parameters, a location parameter, a, and a scale parameter, b. Despite its commonalities with the normal distribution, however, the Laplace distribution is different enough to necessitate its own monitoring schemes. Simulation studies indicate that using normal theory charts for Laplace-distributed process data results in a significantly inflated false alarm rate.

As with the normal distribution, monitoring both location and scale parameters allows one to determine whether each sample collected appears to be from the specified Laplace distribution or come from a normal distribution which is different from the *IC* Laplace distribution in some way. One way to do this is to build control charts based on appropriate statistics, such as the maximum likelihood estimators for these parameters. We propose and compare several monitoring schemes for this distribution.

1.5 Organization of the Dissertation

The dissertation is organized as follows. We present a brief review of parametric and nonparametric joint monitoring schemes in chapter 2. In chapter 3, we study two Shewhart-type control charts for simultaneous monitoring of unknown mean and variances of normally distributed processes. Control charts for simultaneous monitoring of location and scale of processes following a shifted exponential distribution will be considered and studied in chapter 4, and corresponding control charts for simultaneous monitoring of location and scale of processes following a Laplace distribution will be considered and studied in chapter 5. Finally, conclusions and directions for future research will be presented in Chapter 6.

CHAPTER 2

LITERATURE REVIEW

2.1 Parametric Joint Monitoring Schemes for Monitoring Location and Scale

2.1.1 Normal Distribution Joint Monitoring Schemes

Within the control charting literature, the vast majority of joint monitoring schemes are parametric charts designed for monitoring the mean and variance of normally distributed processes. A number of one- and two-chart schemes have been developed for this purpose.

2.1.1.1 One-Chart Joint Monitoring Schemes

Of the two major types of joint monitoring schemes for data from a normal distribution, one-chart schemes have received the most attention in the recent literature. These schemes are appealing for several reasons. First of all, they are simpler than two-chart schemes, in the sense that they allow the practitioner to focus on a sole chart (and, in most cases, a single charting statistic) which makes the operation easier, particularly when the process is *IC* (which it is far more often than not). It is also relatively easy to set the control limits for these charts based on the distribution of the charting statistic, which is often a combination of two statistics, one for the mean and one for the variance. Many of these schemes also have diagnostic capability; that is, they can indicate which of the two parameters may have shifted in case the chart signals. We first discuss some one-chart schemes under the normal distribution when the *IC* mean and variance are specified or known (the so-called standards known case).

2.1.1.1.1 Standards Known, Parametric One-Chart Schemes

There are situations in practice where the *IC* mean and variance of a normally distributed process are known, for example, from external specifications or long-term experience. The term "standards known" or "case K" is often used in the SPC literature for these situations in which all relevant process parameters are known. The development, implementation, and interpretation of control charts are simpler and more straightforward in case K. Thus, although a wide variety of one-chart joint monitoring schemes have been developed over the years, the vast majority of these charts have been proposed for case K.

Among the one-chart joint monitoring schemes in case K, there are two major classes: simultaneous control charts, which use two statistics (one each for mean and variance) plotted on the same chart, and single control charts, which use a single statistic that may actually be a combination of two separate statistics, one each for the mean and the variance (Cheng and Thaga, 2006). Single control charts can further be broken down into those with a two-dimensional control region, wherein the charting statistics are plotted on a two-dimensional plane, and those that have "traditional" control limits (i.e. horizontal line boundaries), wherein the charting statistics are plotted against time. The following three figures use simulated data to illustrate the various categories of one-chart joint monitoring schemes. Figure 2.1 shows an example of a simultaneous control chart developed by Yeh, Lin, and Venkataramani (2004), while Figures 2.2 and 2.3 show examples of single control charts with traditional control limits (Chen and Cheng's (1998) Max chart) and a control region (Chao and Cheng's (1996) semi-circle chart), respectively. These charts will be discussed in more detail in the sections that follow.

Figure 2.1: A simultaneous monitoring scheme

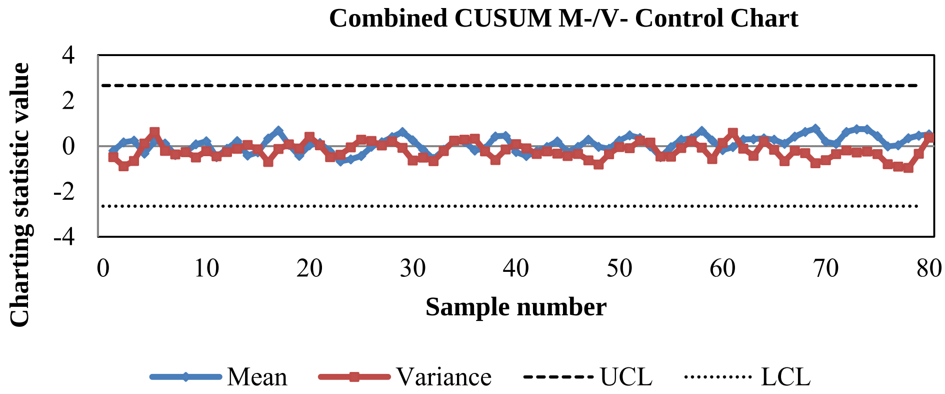

Figure 2.2: A single chart monitoring scheme with a traditional upper control limit

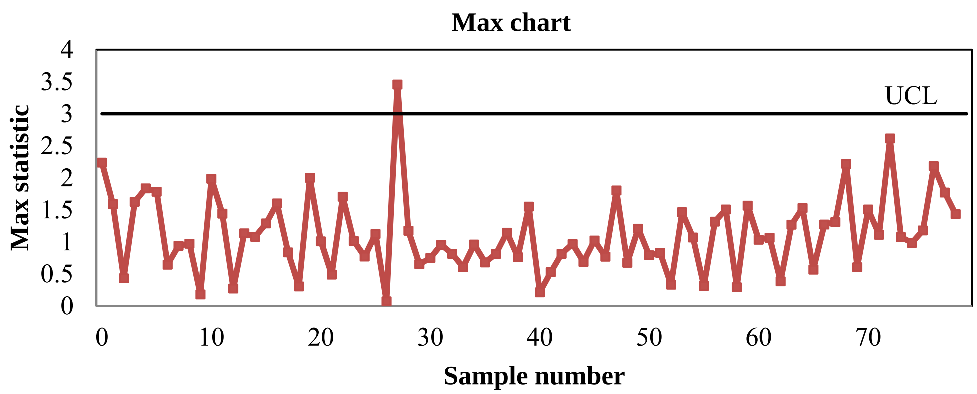

Figure 2.3: A single chart monitoring scheme with a control region

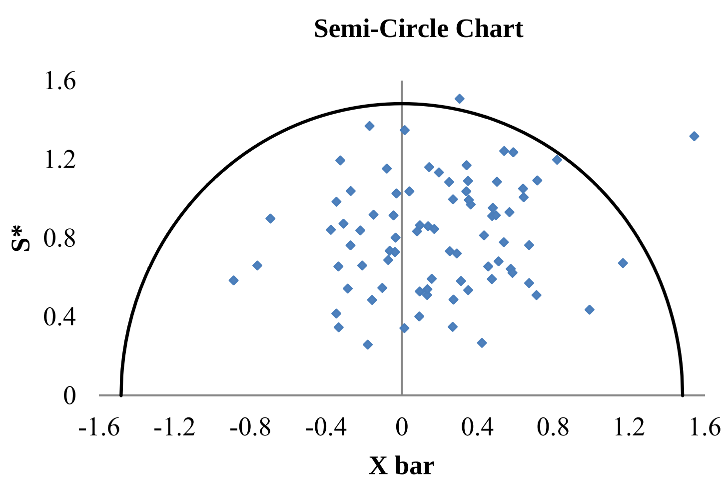

Cheng and Thaga (2006) presented a nice overview of the simultaneous and single control charts available before 2006 and concluded that single charts are typically preferable to simultaneous charts due to their simplicity and clarity. Their article outlined five Shewhart-type charts, six EWMA-type charts, and two CUSUM-type charts (as well as additional charts for multivariate and autocorrelated processes). However, major contributions have been made to the area of joint monitoring in recent years.

2.1.1.1.1.1 Simultaneous charts

A few monitoring schemes exist in the literature in which a mean statistic and a variance statistic are plotted within the same chart. These "simultaneous" charts can be thought of as a compromise between single charts and two-chart schemes, since they maintain separate statistics but only a single graphical interface. A brief discussion of these charts is provided by Cheng and Thaga (2006), who concluded that single charts are more appealing.

2.1.1.1.1.2 Single charts with traditional control limits

Single charts with traditional control limits comprise the area of research in joint monitoring that has seen the most development over the years. These schemes are based on a single charting statistic which is usually some combination (function) of the minimal sufficient statistics $\bar{X}$ and S^2. However, a few charts have been considered that consist of a single charting statistic which is not a direct combination of a mean statistic and a variance statistic. Instead, these schemes incorporate the target process mean and variance (μ_0 and σ_0) directly into the charting statistic. For example, Domangue and Patch (1991) considered an EWMA chart based on the charting statistic $A_i = r\left|\frac{\sqrt{n}(\bar{X}_i-\mu_0)}{\sigma_0}\right|^{\alpha} + (1-r)A_{i-1}$, where r is a weighting constant such that $0 \leq r \leq 1$ and $i = 1,2, \ldots$ denotes the sample number. Later, Costa and Rahim (2004) considered an EWMA non-central chi-square (NCS) chart based on the statistic

$$W_i = \sum_{j=1}^{n} \left(x_{ij} - \mu_0 + \xi_i \sigma_0\right)^2$$

where n is the sample size, $j = 1,2, \ldots, n$ denotes the observation number within each sample, d is a positive constant, $\xi_i = d$ if $(\bar{X}_i - \mu_0) \geq 0$, and $\xi_i = -d$ if $(\bar{X}_i - \mu_0) < 0$. Costa and Rahim (2006) demonstrated that this NCS chart detects changes in the mean and increases in the variance quicker than the $\bar{X} - R$ joint monitoring scheme. However, they did not consider decreases in the variance. Also, it is not clear why the distribution of W_i is a non-central chi-square as claimed by these authors, as the random variable $x_{ij} - \mu_0 + \xi_i \sigma_0$ does not appear to follow a normal distribution.

Among the functions to combine the mean and variance statistics, the maximum has been quite popular. Chen and Cheng (1998) presented the Max chart which combines two normalized statistics, one for the mean and one for the variance, by taking the maximum of the absolute values of the two statistics. The resulting charting statistic is $M = \max(|U_i|, |V_i|)$ where $U_i = \frac{\bar{X}_i - \mu}{\sigma/\sqrt{n_i}}$, $V_i = \Phi^{-1}\left\{H\left[\frac{(n_i-1)S_i^2}{\sigma^2}; n_i - 1\right]\right\}$, $H(w; v)$ is the cumulative distribution function (cdf) of the chi-square distribution with v degrees of freedom, n_i is the size of the ith sample, and $\Phi(.)$ is the cdf of the standard normal distribution. Huang and Chen (2010) provided insight on the economically optimal choice of sample size, sampling interval, and control limits for Max charts. They also compared the economically-designed versions of the Max chart and joint $\bar{X}$ and S charts and determined that they performed similarly. Chen, Cheng, and Xie (2001) proposed a MaxEWMA chart which similarly combines two EWMA statistics for mean and variance, $Y_i = (1 - \lambda)Y_{i-1} + \lambda U_i$ and $Z_i = (1 - \lambda)Z_{i-1} + \lambda V_i, 0 < \lambda \leq 1$, by taking the maximum of the absolute values of the two, where U_i and V_i are the same statistics used in the original Max chart and λ is a specified smoothing constant. However, Costa and Rahim (2004) showed using simulation studies that their NCS chart is preferable to the MaxEWMA chart for detecting increases in process variability, whether or not they are accompanied by a shift in the mean.

The MaxEWMA chart has been a popular chart in the literature. Khoo et al. (2010a) presented a slightly different MaxEWMA chart which utilizes the range R rather than S^2 as the basis for the variance statistic. They stated that this EWMA $\bar{X} - R$ chart is not intended to replace the standard MaxEWMA chart and is simply an attempt to construct a single chart using R instead of S^2. As noted by Chao and Cheng (2008), any approach using R "is bound to be less effective" than the approaches which combine the minimal sufficient statistics. Mahmoud et al. (2010) compared the relative efficiency of S and R and concluded that S is strongly preferable for normally distributed data. Thus, it seems unlikely that a practitioner would choose this chart for process monitoring. As a further modification of the MaxEWMA chart, Khoo et al. (2010b) proposed the Max-DEWMA chart, which combines two double EWMA statistics, $W_i = (1-\lambda)W_{i-1} + \lambda Y_i$ and $Q_i = (1-\lambda)Q_{i-1} + \lambda Z_i$, where Y_i and Z_i are the EWMA statistics used in the MaxEWMA chart. While this chart has an additional layer of complexity, it outperforms the MaxEWMA chart for small and moderate shifts in mean and/or variance, at least when the same smoothing constant λ is used for both the construction of the EWMA statistics Y_i and Z_i and the construction of the DEWMA statistics W_i and Q_i. As is typically the case for EWMA-type charts, choosing a small value for λ increases the sensitivity of both the Max-DEWMA and MaxEWMA charts to small shifts.

Another variation on the MaxEWMA chart is Memar and Niaki's (2011) Max EWMAMS chart, which combines normalized versions of the EWMA $\bar{X}$ statistic, $A_k =$

$(1-\lambda)A_{k-1}+\lambda\bar{X}_k$, and the EWMA mean-squared deviations statistic, $B_k=(1-\lambda)B_{k-1}+\lambda\sum_{j=1}^{n}\frac{\left(X_{kj}-\mu_0\right)^2}{n}$. The resulting charting statistic is

$M_k=\max\left\{\left|\frac{A_k-\mu_0}{\sqrt{\frac{\lambda}{n(2-\lambda)}\left(1-(1-\lambda)^{2k}\right)}\sigma_0}\right|,\left|\Phi^{-1}\left[H\left\{\frac{\nu B_k}{\sigma_0^2};\nu\right\}\right]\right|\right\}$. This chart is effective for most changes in mean and variance but is outperformed by other schemes for decreases in variance.

Other ways of combining a mean statistic and a variance statistic for joint monitoring include using the sum of squares or a weighted loss function or adapting existing tests for comparing the distributions of two samples, such as the likelihood ratio approach. A loss function is an equation which indicates the severity of the difference between a point estimate and the true value it is estimating. Some researchers have proposed charts based on the loss function $L=\frac{\sum_{i=1}^{n}(x_i-\mu_0)^2}{n}=\frac{(2n-1)}{n}\left[\frac{n-1}{2n-1}s^2+\frac{n}{2n-1}(x_i-\mu_0)^2\right]$, but recently, charts based on a general weighted loss function, $WL=\lambda s^2+(1-\lambda)(x_i-\mu_0)^2$ where λ is a appropriate weighing factor between 0 and 1, have been shown to be more effective (Wu and Tian, 2005). Wu and Tian (2005) suggested a CUSUM chart, known as the WLC chart, which is based on this weighted loss function and is useful for jointly monitoring changes in mean and increases (but not decreases) in variance. The statistic used for this chart is $A_t=\max(0,A_{t-1}+WL_t-k_A)$, where k_A is a reference parameter which is determined using a design algorithm, along with the weighting factor λ and the control limit.

While these approaches been rather ad-hoc, the likelihood ratio-based approach appears to be a promising idea, rooted in solid statistical theory, for constructing a single chart, since the joint monitoring problem under an assumed parametric distribution (such as the normal) is analogous to testing the null hypothesis that the most recently taken sample comes from a completely specified population (a simple null hypothesis) versus all alternatives (a composite alternative hypothesis), repeatedly over time as more test samples become available. The exact (finite sample) distribution of the likelihood ratio (LR) (also known as the generalized likelihood ratio (GLR) statistic in this case of composite alternatives) statistic is often difficult to obtain, so in hypothesis testing, the asymptotic properties of this statistic are generally used instead. However, as noted by Hawkins and Deng (2009), in the control charting setting, practitioners rarely use sample sizes large enough to make the asymptotic distribution useful, so the efficacy of this approach could be a concern.

Hawkins and Deng (2009) proposed a pair of new charts: a generalized likelihood ratio (GLR) chart which has the charting statistic $G = \left(\frac{\sqrt{n}(\bar{X}-\mu_0)}{\sigma_0}\right)^2 + \frac{(n-1)S^2}{\sigma_0^2} - n\ln\left(\frac{(n-1)S^2}{\sigma_0^2}\right) + n\ln n - n$ and a Fisher chart based on the statistic $W = -2\log A_1 A_2$ where A_1 is the p-value given by the $\bar{X}$ chart for a specified mean and A_2 is the p-value given by the S chart for a specified standard deviation. They then compared the performance of these two charts to that of the Max chart and found that the GLR chart has superior performance for detecting decreases in variance, though another chart performs better for any mean increase not accompanied by a variance decrease. Additionally, they noted that the Max chart and the Fisher chart both exhibit bias, that is, the *OOC* average run length (*ARL*) is larger than the *IC ARL*, while the GLR chart does not share this problem.

A few other authors have also utilized the likelihood ratio approach to control charting. Zhou, Luo, and Wang (2010) proposed a GLR-based chart for detecting non-sustained shifts in mean and/or variance, which may occur, for example, in healthcare settings. Zhang, Zou, and Wang (2010) developed a likelihood ratio-based EWMA (ELR) chart which likewise is able to detect decreases in variance. Conveniently, setting up the GLR and ELR charts does not require specification of an additional parameter such as α in Domangue and Patch's chart or d in Costa and Rahim's NCS chart. However, the limits for the ELR chart are obtained using a complicated Markov chain approximation, making it difficult to implement in general, though the authors did provide a table of control limits for certain sample sizes, *IC ARL*s, and EWMA weight smoothing parameters.

Another method which is sometimes used for detecting an impending change is the Shiryaev–Roberts test. This test "has been proved to be optimal for detecting a change that occurs at distant time horizon when the observations are i.i.d. and the pre- and post-change distributions are known" and is based upon the likelihood ratio between the two specified distributions (Zhang, Zou, and Wang, 2011). A Shiryaev–Roberts chart based upon this test was proposed by these authors and was shown to perform comparably to the ELR and WLC charts.

2.1.1.1.1.3 Single charts with control regions

Some researchers have developed joint monitoring schemes in which the process data are plotted on a two-dimensional plane and are considered *IC* if they fall within some defined control region. Otherwise, the process is declared *OOC*. A variety of these single control charts have been developed, with semi-circular, circular, and elliptical control regions. As noted by Chao and Cheng (2008), "the combined visual effect of points that fall in/out of a certain closed region is more striking than points just crossing the lines." While visually appealing, a disadvantage of such control schemes is that the time-ordered nature of the data is lost, removing the opportunity for the practitioner to spot time-related trends.

Charts with semi-circular control regions have been popular in the literature. Takahashi (1989) studied several possible control regions (rectangular, sectorial, and elliptic) and noted that each has advantages in detecting a particular type of change: rectangular for changes in mean only, sectorial for changes in variance only, and elliptic for changes in both. He developed a very complex chart for which the control region is the common area of a rectangle and a sectorial.

Chao and Cheng (1996) developed a control chart in which the points $(\bar{X}_i, S_i^*)$ are plotted on the $(\bar{X}, S^*)$ plane, where $S^* = \sqrt{\frac{1}{n}\sum_{i=1}^{n}(X_i - \bar{X})^2}$. The control region for the chart is based on the statistic $= (\bar{X} - \mu_0)^2 + S^{*2}$. If the sample data are normally distributed, $\frac{n}{{\sigma_0}^2}T$ has a chi-square distribution with n degrees of freedom. Furthermore, the equation for the statistic T neatly defines a circular region. However, since S^* must be non-negative, only half of the region is needed, and this scheme is known as a semicircle (SC) chart. Chao and Cheng (2008) expanded upon this concept to construct an SC chart with minimum coverage area. Chen, Cheng, and Xie (2004) utilized this T statistic as the basis for an EWMA-SC chart. However, despite the chart's name, the control region for this chart is the area under a line, not a semi-circle. The T statistic is decomposed into mean and variance components, $\left[\frac{n(\bar{X}_i-\mu_0)^2}{\sigma_0^2} - 1\right]$ and $\left[(n-1)\left(\frac{S_i^2}{\sigma_0^2} - 1\right)\right]$, respectively, which are used to form the EWMA statistics, U_i and V_i. The sample points are then plotted in the U, V-plane (rather than sequentially), and all points falling below a specified line are taken to be *IC*.

2.1.1.1.2 Standards Unknown, Parametric One-Chart Schemes

Nearly all of the joint mean/ variance control charts available in the literature are designed under the assumption of normality of the process distribution with specified parameters (case K). However, in practice, more often than not, one or more of these parameters are unknown and unspecified. This is referred to as the "standards unknown" case or "case U."

Devising and interpreting control charts in case U is more interesting and challenging, because even under the assumption of a known process distribution, such as the normal, the estimation of the mean and variance parameters from the data and the use of them to construct the trial control limits result in statistical dependency (see for example, Chakraborti, Human, and Graham, 2009). This dependency can affect the performance of the chart in a significant way (such as resulting in many more false alarms than expected), to such a large extent that the practitioner might lose faith in the whole endeavor. Thus, the effect of parameter estimation on the performance of control charts has become an important area of research.

A little background is in order. The development of control charts for statistical monitoring of a process is typically undertaken in two stages: Phase I, which involves retrospective examination of the process, and Phase II, which focuses on prospective monitoring. In Phase II, data are collected at regular intervals, and a charting statistic of interest is calculated from the data and placed on a control chart. When a charting statistic plots above the upper control limit (*UCL*) or below the lower control limit (*LCL*), a signal occurs, and the process is said to be *OOC*. In case U, a major objective of the Phase I study is to obtain a set of *IC* process data (i.e. a reference sample) from which the parameters needed to determine the control limits for the Phase II charts can be estimated. The size and the quality of this reference sample can and do greatly impact the performance of the chart. This has been an active area of research for the last decade or so. Jensen et al. (2006) presented a comprehensive review of the literature on the effects of parameter estimation on various types of control charts, noting that it is particularly problematic when a small Phase I sample is utilized. Although they did not explicitly mention joint monitoring schemes, their observations on the impact of parameter estimation almost certainly extend to these charts. Further work is necessary to better understand the precise impact of parameter estimation on joint monitoring schemes.

Traditionally, obtaining the reference sample is accomplished using an iterative procedure in Phase I in which trial limits are first constructed from the data (several subgroups or a number of observations), and then some charting statistics are placed on a control chart. It may be noted that the construction of Phase I control charts has different objectives (see for example the 2009 review article by Chakraborti et al.) from those in Phase II. Phase II control charts are designed to have a specific *IC ARL*, while Phase I control charts should be constructed based on a specified *IC* false alarm probability (FAP), which requires consideration of the joint distribution of the charting statistics. In any case, subgroups corresponding to the charting statistics which are located outside the control limits are generally considered *OOC* and removed from the analysis, and new limits are estimated from the remaining data.[1] This step is repeated until no more charting statistics appear *OOC* so that the remaining data is taken to be *IC*, at which point the final control limits may be constructed for Phase II monitoring.

However, control charts for joint monitoring in Phase I, case U, have been largely absent from the literature so far. This is an important problem since if the Phase I chart used to identify this *IC* data is incorrect or ineffective at identifying the *OOC* samples for removal, the resulting parameter estimates may not be very accurate, which will affect the performance of the Phase II chart. In fact, several researchers have demonstrated the pitfalls of estimating the parameters using data which contains *OOC* samples. The resulting control limits may be too tight or too

[1] There are two competing schools of thought concerning the handling of subgroups which plot *OOC*. Some practitioners automatically discard these subgroups, while others remove them only if they can be attributed to "assignable causes." In our discussion, we focus primarily on the former approach; however, problems can arise with either method. In the case of the latter approach, the practitioner may fail to identify the cause of a particular subgroup which plots *OOC* and therefore not discard it. If, however, the subgroup was, in fact, *OOC*, failure to remove it could likewise result *IC* limits which are too tight or too loose.

loose, causing an inflated FAR or a higher-than-nominal *IC ARL*, respectively. On this point, for example, Mabouduo-Tchao and Hawkins (2011) noted, "Plugging in parameter estimates… fundamentally changes the run length distribution from those assumed in the known-parameter theory and diminishes chart performance, even for large calibration samples." Jensen et al. (2006) pointed out that "the impact of parameter estimation…depends on the direction of the estimation error." Clearly, then, in case U situations, it is important to have very good Phase I charts; otherwise, the resulting Phase II charts will suffer.

A few case U charts for joint monitoring are present in the literature. A recent example is the simultaneous chart proposed by Yeh, Lin, and Venkataramani (2004) which involves a pair of CUSUM mean and variance statistics which have the same scale and then plots them on one control chart with a single set of control limits.[2] The CUSUM mean and variance statistics are computed by taking appropriate functions of $\bar{X}$ and S^2 and applying the probability integral transformation (PIT) to each, producing statistics which have the uniform distribution. Because the PIT is used, this chart can be extended for processes with known, non-normal distributions as well.

A substantial amount of recent research has demonstrated that in case U, a large quantity of reference data is needed before the Phase II charts actually display their expected (nominal) behavior. Jensen et al. (2006) noted that depending on the type of control chart being utilized, hundreds or even thousands of reference data points may be necessary. However, it is not always possible to have such a large "clean" dataset. In these situations an alternative class of control charts may be useful. Among these are the self–starting charts (Hawkins, 1987) and the Q-charts (Quesenberry, 1991). For the joint monitoring problem, Li, Zhang, and Wang (2010) recently

[2] The statistics can also be placed on separate charts, resulting in a two-chart scheme.

proposed a self-starting EWMA likelihood-ratio (SSELR) chart which has this advantage. However, this chart is only appropriate for univariate data.

Hawkins and Zamba (2005) presented a single chart based on a “changepoint” model which also avoids the problem of needing a large reference dataset. In this model, the “changepoint” is the unknown instant at which a special cause brings about a shift in one or both of the parameters; as a result, the observations taken prior to the changepoint have a different mean and/ or variance than the observations taken after it. A GLR test can be used to determine whether the samples before and after a suspected changepoint seem to have the same parameters. However, the time of the true changepoint is unknown, and it could occur between any two samples. Thus, the chart proposed by Hawkins and Zamba (2005) uses the maximum of the GLR statistics resulting from considering all possible changepoints. They demonstrated that this chart is effective when as few as three Phase I data points are available. However, they acknowledge that their procedure is inadequate for non-normal distributions.

2.1.1.1.3 Disadvantages of One-Chart Monitoring Schemes

In general, one-chart schemes are not without some weaknesses. As noted by Chao and Cheng (2008), one-chart schemes lack a desirable feature present in two-chart schemes, that is, they lose either the time-sequential presentation of the data, in the case of single charts with control regions, or the separate treatment of the mean and variance statistics, in the case of single charts with traditional control limits. In the former case, the charts do not indicate the order in which the data are collected, making it difficult to spot time-related trends. In the latter case, there is a reduction in the information to be gleaned by looking at the charting scheme. A signal on a single mean-variance chart with traditional control limits cannot be attributed to variance or mean without diagnostic follow-up.[3] Single charts with control regions, however, do not share this limitation.

Another disadvantage of one-chart joint monitoring schemes is that they often utilize very complex charting statistics. Additionally, many single charts have some chart-specific "tuning" parameters, such as α in Domangue and Patch's (1991) chart or d in Costa and Rahim's (2004) non-central chi-square chart, which must be specified and which greatly affect the chart's performance (Zhang, Zou, and Wang, 2010). Choosing appropriate values for these parameters can be quite complex. Some one-chart schemes also have the disadvantage of being insensitive to large or small shifts in the parameters or to decreases in variance. While individual one-chart schemes have been shown to have performance advantages over two-chart schemes, it is inaccurate to claim that one-chart schemes always have superior performance.

2.1.1.2 Two-Chart Joint Monitoring Schemes

Since the early days of SPC, there have been joint monitoring schemes, used either implicitly or explicitly, consisting of two charts. For normally distributed data, these two-chart monitoring schemes are made up of a mean chart (such as the $\bar{X}$ chart) and a variance chart (such as the S^2 chart or the R chart). They can consist of a pair of Shewhart, CUSUM, or EWMA charts, one for the mean and one for the variance, or even a combination of one CUSUM and one EWMA chart. The mean charts utilized in these schemes are typically two-sided, while the variance charts may be either one-sided or two-sided. Figure 2.4 shows an example of a two-

[3] In contrast, a signal on the variance chart of a two-chart scheme is immediately attributable to a shift in variance, although the same cannot be said of a signal on the mean chart. This fact will be discussed in greater detail later in this dissertation, but the main point here is that neither two-chart nor one-chart schemes with traditional control limits can immediately indicate whether a chart signal is caused by the mean, the variance, or both, though two-chart schemes do provide slightly more information.

chart monitoring scheme, constructed using simulated data. The mean of the process appears to go *OOC* around subgroup 70.

Figure 2.4: A two-chart monitoring scheme consisting of two EWMA charts

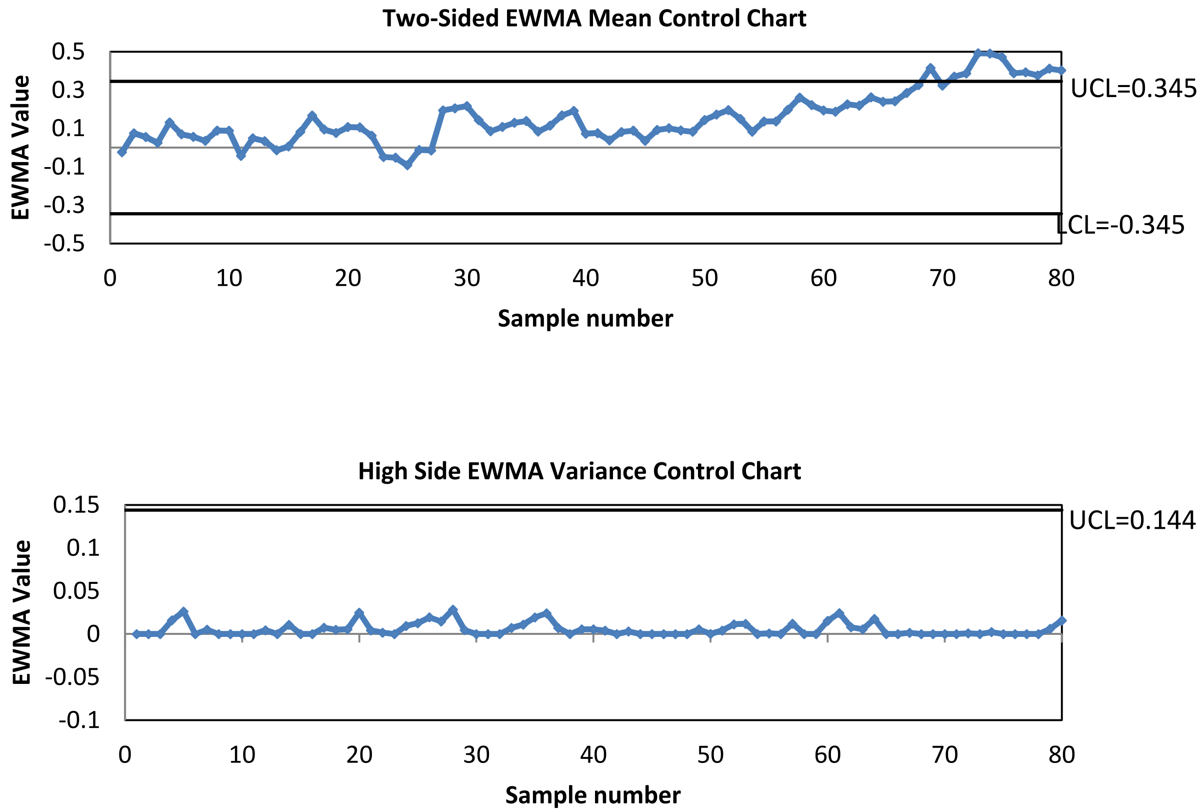

A major advantage of two-chart monitoring schemes is their familiarity and the apparent ease of visual interpretation. Such schemes have been used for many years. Furthermore, it seems natural to some practitioners to monitor the mean and the variance separately and simultaneously, since the statistics $\bar{X}$ and S are independent.

2.1.1.2.1 Standards Known, Parametric Two-Chart Schemes

As with one-chart monitoring, the vast majority of two-chart monitoring schemes presented in the literature are for data from a specified distribution, such as the normal, for which the true parameters are specified. Several authors have considered the construction and improvement of these schemes. Gan (1995) discussed scheme CC, consisting of a two-sided CUSUM mean chart and a two-sided CUSUM variance chart; scheme EE_u, consisting of a two-sided EWMA mean chart and a high-sided EWMA variance chart; and scheme EE, consisting of a two-sided EWMA mean chart and a two-sided EWMA variance chart, comparing these to Domangue and Patch's (1991) omnibus chart. He demonstrated that EE performs similarly to scheme CC and is slightly more sensitive than CC when there is a small shift in the mean concurrent to a slight decrease in the variance. The other schemes performed poorly in comparison. Reynolds and Stoumbos (2004) also investigated and compared popular Shewhart, EWMA, and CUSUM schemes, likewise recommending a pair of EWMA (or CUSUM) charts, though with a different variance statistic than the one discussed by Gan (1995). Reynolds and Stoumbos (2005) expanded upon this work, comparing a variety of other two- (and three-) chart combinations, including some Shewhart-EWMA schemes. They, too, ultimately recommended a pair of EWMA (or CUSUM) charts).

2.1.1.2.2 Standards Unknown, Parametric Two-Chart Schemes

The standards unknown situation presents even more complex problems for two-chart monitoring schemes than it does for one-chart schemes. Perhaps for this reason, such charts (for both Phases I and II) have not yet been studied in the literature. In the Phase I setting, a major problem which needs to be addressed is how to conduct the iterative, parameter estimation procedure for a two-chart scheme.[4] Should trial limits be constructed for the two charts simultaneously and a subgroup discarded if it plots *OOC* on either chart? Alternatively, should the iterative procedure be conducted first for the variance chart (since it is independent of the mean parameter) and then for the mean chart using only the data not already discarded? If this second method is utilized, should the final control limits be recomputed for the variance chart using only those samples not discarded during the estimation of the process mean? Another difficulty is designing the scheme so that it has a specified FAP. Further research is needed to address all of these issues and make two-chart joint monitoring schemes a viable option for case U. For the Phase II problems, there is also a current shortage of charts that account for parameter estimation from a Phase I reference data set. Since the impact of parameter estimation on Phase II charts can be serious and parameters are estimated based on reference data obtained by the use of appropriate Phase I charts, two-chart schemes for both settings should be an area of further research.

2.1.1.2.3 Disadvantages of Two-Chart Monitoring Schemes

Two-chart schemes also have some disadvantages. Cheng and Thaga (2006) noted that these schemes utilize more personnel, time, and other resources than do one-chart schemes. Typical two-chart schemes give the illusion of clearly showing whether a process is *OOC* with respect to mean, variance, or both, since a signal on the mean chart appears to indicate that mean is *OOC*, a signal on the variance chart appears to indicate that variance is *OOC*, and signals on both charts seem to indicate that both are *OOC*. Contrary to popular perception, this can actually be quite misleading. As noted by Hawkins and Deng (2009), since the control limits for an $\bar{X}$

[4] The appropriate approach may depend, in part, on whether practitioner chooses the discard all subgroups which plot *OOC* or only those for which "assignable causes" can be identified.

chart are functions of the *IC* standard deviation, an increase in the variability may lead to a false signal on the $\bar{X}$ chart, and likewise, a decrease in variability may cause the $\bar{X}$ to fail to signal even though a shift in the mean has also occurred. Furthermore, in many two-chart monitoring schemes, the mean and variance charts are constructed completely independently, so that each has a specified *ARL*. Appropriate two-chart joint monitoring schemes, however, should have control limits which have been adjusted so that the overall *ARL* of the scheme is a specified value.

2.1.2 Shifted Exponential Distribution Monitoring Schemes

The shifted exponential distribution has a prominent place in reliability and life testing research, particularly in the context of guarantee times. As noted by Basu (2006), this distribution can be useful for predicting the life expectancy of a cancer patient or the life span of light bulbs. Many research problems arising from the shifted exponential distribution have been addressed in the literature, particularly those that relate to reliability, which, in a statistical context, is the probability that a random variable exceeds some value. Parameter estimation from censored and uncensored data, hypothesis testing, reliability sampling plans, and prediction of future data points are among the topics for which research on this distribution has been conducted. A few control charts for shifted exponential data also appear in the literature, but much more work in this area is needed.

Parameter estimation is one of the relevant areas of research regarding this distribution. Varde (1969) derived Bayesian point estimates for both parameters. Kececioglu and Li (1985) presented a method for calculating an optimum confidence interval for the location parameter of a shifted exponential distribution. Lam et al. (1994) presented a method for estimating both parameters in situations where the sample data can be ranked but not precisely measured, and Basu (1971) provided a sequential rule for estimation of the location parameter when the scale parameter is unknown.

Several other authors have considered parameter estimation from censored data, including Epstein (1960), Varde (1969), Viveros and Balakrishnan (1994), and Balakrishnan and Sandhu (1996). Epstein (1960) derived sufficient statistics and interval estimates for progressively censored data from this distribution, and Balakrishnan and Sandhu (1996) derived the best linear unbiased estimators and the maximum likelihood estimators for these parameters. Viveros and Balakrishnan (1994) derived exact confidence intervals for these parameters. Thiagarajah and Paul (1997) developed confidence intervals for the scale parameter based of Type I censored data.

In addition to estimating the parameters of this distribution, several researchers have focused their efforts on estimating $P(X < Y)$, the probability that one random variable, X, that follows the shifted exponential distribution is smaller than another random variable, Y, from another shifted exponential distribution. One application of this problem is the estimation of stress-strength reliability, that is, the probability that the strength of an object exceeds the stress placed upon it (Baklizi, 2008). An example of this is the situation is which the breakdown voltage of a capacitor must exceed the output voltage of a transverter (Hall, 1985). Beg (1980) provided both minimum variance unbiased and Bayesian estimators for $P(X < Y)$. Baklizi (2008) provided point estimates and confidence intervals for this probability in the cases where two shifted exponential distributions share a common scale or location parameter.

Ramalhoto and Morais (1999) studied control charts for the scale parameter of the three-parameter Weibull distribution, which can also be used for the λ parameter of the shifted exponential distribution, since, as mentioned above, the latter is merely a special case of the former. However, using these charts requires the assumption that the location parameter is known and fixed. Sürücü and Sazak (2009) presented a control scheme for this same distribution based on the idea of using moments to approximate the distribution.

There has also been research in a number of other areas. Wright et al. (1978) developed hypothesis tests for these parameters for Type I censored data. A few authors have considered the problem of predicting future data points from a shifted exponential distribution, including Ahsanullan (1980) and Ahmadi and MirMostafaee (2009). Reliability sampling plans have also been a popular research area. Balasooriya and Saw (1998) considered reliability sampling plans for progressively censored shifted exponential data.

While the shifted exponential distribution is most commonly identified with guarantee times, a number of other types of processes follow this distribution. Some examples in manufacturing and healthcare settings are given by Kao (2010). Furthermore, any process which follows the one-parameter exponential distribution also follows the shifted exponential with location parameter zero. If there is any possibility that an assignable cause could effect a change in that location parameter, then a chart for the shifted exponential distribution is needed to monitor it.

2.1.3 Laplace Distribution Monitoring Schemes

The symmetric Laplace, or double exponential, distribution occurs whenever the random variable of interest is the difference between a pair of exponentially distributed random variables with a common scale parameter (Piug and Stephens, 2000). As noted by Kotz et al. (2001), the Laplace distribution typically appears in the literature as a counterexample in discussions of the normal distribution. However, it has numerous practical applications and is therefore deserving of careful study in its own right. Examples include differences in flood levels at two different points along a river (Puig and Stephens, 2000; Bain and Engelhardt, 1973), daily and weekly observations of individual stocks in the Finnish stock market (Linden, 2001), and sunspot cycles (Sabarinath and Anilkumar, 2008). Kotz et al. (2001) provided an in-depth overview of the distribution, outlining its distribution, characteristics, and properties, as well as providing examples of applications in finance, engineering, operations management, and the natural sciences. Their extensive work provides the reader a handy reference which synthesizes the extensive literature on the Laplace distribution into a convenient, usable form. Many research problems arising from the Laplace distribution have been addressed in the literature, including parameter estimation, reliability estimation, construction of tolerance limits, and hypothesis testing. However, extensive contributions are needed in the area of process monitoring.

Most recent work has been undertaken for Type II censored samples. Balakrishnan and Chandramouleeswaran (1996a) developed BLUEs for each of the distribution's parameters for samples with this type of censoring. Balakrishnan and Chandramouleeswaran (1996b) extended these results to produce a reliability function estimator. They also presented tolerance limits for the Laplace distribution. Childs and Balakrishnan (1996) constructed confidence intervals for each of the distribution's parameters by conditioning on values of some statistics used in the calculation. Ioliopoulos and Balakrishnan (2011) constructed maximum likelihood-based exact confidence intervals and hypothesis tests for the distribution's parameters, likewise for Type II censored samples.

Tests of fit for the Laplace distribution have been an area of recent research interest. Puig and Stephens (2000) developed goodness-of-fit tests for this distribution based on the empirical distribution function. Choi and Kim (2006) developed goodness-of-fit tests which are instead based on maximum entropy.

2.2 Nonparametric Joint Monitoring Schemes

All of the methodologies discussed above, and indeed, the vast majority of available work in the area of joint monitoring, have focused on data with a known or assumed parametric distribution. Given the existing literature on the performance of individual normal theory charts for the mean and the variance, it is reasonable to believe that departures from these parametric assumptions can have a dramatic impact on the effectiveness of at least some such charts. This can be remedied by applying a nonparametric or a distribution-free control chart that does not require the assumption of a specific form of the underlying distribution. A recent review of nonparametric control charts can be found in Chakraborti et al. (2011); however, the literature in the area of nonparametric joint monitoring, both one- and two- chart schemes, is currently very limited and thus presents a great opportunity for research and development.

The few nonparametric joint monitoring schemes available in the literature are all one-chart schemes. Zou and Tsung (2010) proposed an EWMA control chart based on a goodness-of-fit test. They showed that this chart is effective for detecting changes in location, scale, and shape. Mukherjee and Chakraborti (2011) adapted a well-known nonparametric test for location-scale which combines the Wilcoxon rank-sum location statistic with the Ansari-Bradley scale statistic and constructed a chart based on it. Their Shewhart-type chart is called the Shewhart-Lepage (SL) chart, and it has post-signal diagnostic capability for determining the nature of the shift. Within the nonparametric joint monitoring literature, their paper appears to be the first major foray into the standards unknown case, though more work is currently in progress.

While there is no doubt that nonparametric two-chart monitoring schemes could be developed, as far as we know, there are none in the current SPC literature. However, Reynolds and Stoumbos (2010) presented some schemes consisting of a pair of CUSUM charts which are robust to the normality assumption.

2.3 Summary

A variety of control charting schemes are currently available for jointly monitoring the mean and the variance of a normal distribution. Both one- and two-chart schemes exist in the literature and can be useful to the practitioners. Though all available schemes have advantages and disadvantages, one-chart schemes appear to be the more promising option, particularly since there are many unanswered questions regarding the practical implementation of two-chart schemes when parameters are estimated in a Phase I study.

Joint monitoring schemes for other parametric distributions, including the shifted exponential and Laplace distributions, are largely absent from the literature.

CHAPTER 3

SHEWHART-TYPE CONTROL CHARTS FOR SIMULTANEOUS MONITORING OF UNKNOWN MEANS AND VARIANCES OF NORMALLY DISTRIBUTED PROCESSES

3.1 Introduction

Since their invention in the 1920s by W.A. Shewhart, Shewhart-type control charts have been popular tools for use in statistical process control (Montgomery, 2005). These charts are well-known to be able to detect moderate to large and transient shifts. Most of these charts are designed to monitor a single process parameter, typically the mean (μ) or the variance (σ^2), but more recently, a number of charts have been developed for jointly monitoring the mean and variance of normally distributed processes. The issue of joint monitoring is particularly relevant for processes in which special causes may result in a simultaneous shift in the mean and the variance. An example given by Gan et al. (2004) is an improperly fixed stencil in circuit manufacturing which can cause such a shift in the mean and the variance of the thickness of the solder paste printed onto circuit boards.

Two major classes of joint monitoring schemes have been developed in the literature: those which monitor the mean and the variance simultaneously on a single chart, and those which use two separate charts, one each for monitoring the mean and the variance. Costa and Rahim's (2004) NCS chart is an example of the former, while Gan's (1995) scheme EE is an example of the latter. Though both types of joint monitoring schemes have advantages and disadvantages, one-chart schemes seem to be preferable for both practical and statistical reasons.

In particular, the one-chart schemes typically require fewer process control resources and are more straightforward to implement. Moreover, they seem to be more useful in situations when the process is mostly in-control and fewer out-of-control events are anticipated. Cheng and Thaga (2006) provided a review of the joint monitoring literature until about 2005; McCracken and Chakraborti (2011) gave a more recent overview.

Among the available one-chart schemes for jointly monitoring the mean and the variance, the vast majority are designed for situations in which the true parameters are known rather than estimated from data. The term "standards known" or "case K" is typically used for situations in which all relevant process parameters are known, while the term "standards unknown" or "case U" is used for situations in which one or more process parameters are unknown. When one or both of the parameters are unknown and must be estimated, it is well known that the estimation has a big impact on the performance of the case K charts, particularly in terms of the *ARL* and the FAR, in that many more false alarms are observed. Thus, when parameters are estimated, the case K control charts must be modified (both in terms of the plotting statistic and the control limits) to correctly account for parameter estimation, so that the charts perform at a specified nominal *IC ARL*.

In this chapter, we consider the modification of a pair of existing joint monitoring procedures for case K to case U. These are both Shewhart-type one-chart joint monitoring schemes, useful for detecting large shifts in process parameters: Chen and Cheng's (1998) Max chart and Razmy's (2005) Distance chart. These charts are similar in that both are based on the idea of combining the estimators $\bar{X}$ and S^2 (minimal sufficient statistics) of the mean (μ) and the variance (σ^2) to construct a single charting statistic capable of monitoring the mean and the variance simultaneously. Additionally, once there is a signal, these charts allow the practitioner to easily determine both the direction of the shift and which of the two parameters has shifted. Furthermore, charts of this type have played a pivotal role in the joint monitoring literature. For example, many currently available joint monitoring charts are based on the Max chart, including Chen, Cheng, and Xie's (2001) MaxEWMA chart; Cheng and Thaga's (2010) Max-CUSUM chart; Khoo et al's (2010a) EWMA $\bar{X} - R$ chart; Khoo et al's (2010b) Max-DEWMA chart; and Memar and Niaki's (2011) Max-EWMAMS chart. The Max chart is a Shewhart-type chart, and as noted by Cheng and Thaga (2006), this chart is more effective for detecting large shifts.

For purposes of comparison, we also consider a similarly-modified two-chart ($\bar{X}/S$) scheme in various parts of this chapter.

3.2 Background

It has long been recognized that using estimated parameters in control charts designed for situations in which the true parameters are known introduces additional variability into a monitoring scheme. In their well-written review, Jensen et al. (2006) summarized the effects of parameter estimation on the performance of a variety of control charts. In particular, they noted that problems abound when a small Phase I sample is utilized. Although they did not explicitly mention joint monitoring schemes, their observations on the impact of parameter estimation can be shown to extend to these charts.

To understand the degree of potential impact of parameter estimation on case K joint monitoring charts, first consider the Max chart. This chart has a plotting statistic $M = \left\{\left|\frac{\bar{X}_i-\mu_0}{\sigma_0/\sqrt{n}}\right|, \left|\Phi^{-1}\left\{F_{\chi^2_{(n-1)}}\left(\frac{(n-1)S_i^2}{\sigma_0^2}\right)\right\}\right|\right\}$, where Φ is the cdf of the standard normal distribution, $F_{\chi^2_{(n-1)}}$ is the cdf of the chi-square distribution with $(n-1)$ degrees of freedom, and $\bar{X}_i$ and S_i^2 are the mean and the variance of the ith sample of size n. When the desired *IC ARL* for this chart is 500, the appropriate *UCL*, 3.29, can easily be calculated using Mathcad or estimated using Monte Carlo simulations; the corresponding type I error probability (false alarm rate) is 0.002.[5]

Next, consider the Shewhart distance chart studied in Razmy (2005). The plotting statistic of this chart is $D = \sqrt{\left(\frac{\bar{X}_i-\mu_0}{\sigma_0/\sqrt{n}}\right)^2 + \left(\Phi^{-1}\left\{F_{\chi^2_{(n-1)}}\left(\frac{(n-1)S_i^2}{\sigma_0^2}\right)\right\}\right)^2}$. When the desired *IC ARL* for this chart is 500, the appropriate *UCL*, 3.52, can be obtained using Monte Carlo simulations, and the corresponding FAR is 0.002.

Finally, consider the two-chart joint monitoring scheme which consists of an $\bar{X}$ chart and an S chart.[6] The plotting statistic of the $\bar{X}$ chart is $\bar{X}_i$, and the plotting statistic of the S chart is S_i. When the desired *IC ARL* for this scheme is 500, each of these charts should have an *IC ARL* of 999.5. When $n = 5$, the appropriate control limits for the $\bar{X}$ chart are $\mu_0 - \frac{\Phi\left(1-\left(1-\sqrt{1-\frac{1}{500}}\right)/2\right)\sigma_0}{\sqrt{n}} = -1.47$ and $\mu_0 + \frac{\Phi\left(1-\left(1-\sqrt{1-\frac{1}{500}}\right)/2\right)\sigma_0}{\sqrt{n}} = 1.47$, while the appropriate control limits for the S chart are $\sqrt{\frac{\sigma_0^2 F_{\chi^2_{(n-1)}}\left(\left(1-\sqrt{1-\frac{1}{500}}\right)/2\right)}{\mathrm{n}-1}} = 0.13$ and $\sqrt{\frac{\sigma_0^2 F_{\chi^2_{(n-1)}}\left(1-\left(1-\sqrt{1-\frac{1}{500}}\right)/2\right)}{\mathrm{n}-1}} = 2.24$. As with the Max and Distance charts, the FAR for the $(\bar{X}, S)$ scheme is 0.002.

Now, suppose that the true *IC* mean and variance are unknown. In practice, one would typically estimate these parameters from an *IC* reference sample of size m prior to implementing a monitoring scheme. Then, one might "plug in" these estimates for the parameters when

[5] Note that in the known parameter case, the FAR is the reciprocal of the *IC ARL*.

[6] The $\bar{X}$ and S charts discussed in this paper are based on probability limits rather than the 3-sigma control limits given by Montgomery (2005). The differences between the 3-sigma method and the probability limits method of constructing these charts is discussed in greater detail in A.4 in the Appendix.

calculating M and D, resulting in estimated plotting statistics $\widehat{M}$ and $\widehat{D}$, respectively. However, if one then uses the same control limits that were used with M and D, the chart performance will be degraded. In fact, it is expected that the *IC ARL* for the charts using the parameter estimates would decrease from the nominal value so that more false alarms would occur.

Likewise, for the $(\bar{X}, S)$ monitoring scheme, if the true *IC* mean and variance are unknown, one might "plug in" parameter estimates to compute the control limits for the $\bar{X}$ and S charts. However, doing so without accounting for the additionally variability caused by the parameter estimation will likewise cause the charts' performances to be degraded. As for the Max and Distance charts, it is expected that the *IC ARL* for the for the $(\bar{X}, S)$ scheme using the parameter estimates would decrease from the nominal value so that more false alarms would occur.

To examine the extent of the effect of parameter estimation on the Max and the Distance charts and the $(\bar{X}, S)$ scheme, a simulation study was undertaken. The nominal *IC ARL* was set at 500, and 25,000 simulations were done.[7] Table 3.1 shows values of the observed *ARL* for various combinations of *m* and *n*, where *m* is the total size of the Phase I reference sample and *n* is the size of each Phase II monitoring sample.

It is well known that in the standards known case, increasing n decreases the probability of type II error for control charts, just as is the case for hypothesis tests (see, for example, Montgomery, 2005). This is true because larger values of n improve the chart's ability to recognize differences between the given parameters and the mean and standard deviation of a particular process sample. When the true mean and standard deviation are unknown and are instead estimated from a Phase I sample, increasing n likewise improves the charts' ability to

[7] Throughout this dissertation, the number of simulations is selected to ensure a low standard error of estimation.

recognize differences between the mean and standard deviation of the Phase I sample and the mean and standard deviation of a given Phase II sample. However, since the Phase I mean and standard deviation are estimates rather than the true process parameters, identifying differences between these values and the mean and standard deviation of the Phase II sample can result in false alarms. Thus, for a fixed m, increasing n results in a decrease in the nominal *ARL*. On the other hand, when n is fixed, increasing m causes the Phase I mean and standard deviation estimates to converge toward the true mean and standard deviation. Thus, for a fixed n, larger m's result in *ARL*s which are closer to the nominal *ARL*.

From Table 3.1, it is seen that the Max and Distance charts and the $(\bar{X}/S)$ scheme are all affected by parameter estimation. When parameters are estimated, the observed *ARL* values can be considerably lower than 500, even when a fairly large reference sample (m = 100) is used. The departure from the nominal *IC ARL* is greater when smaller, more typically recommended, reference samples ($m \approx 30$) are used. Thus, it is clear that for typical situations in practice ($m < 100$), modifications and adjustments to the "standards known" charts must be made before they can be used correctly in the "standards unknown" case. This is so that the *IC ARL* will be close to the nominal value; otherwise, there can be a large number of false alarms that will diminish the utility of these charts in practical situations.

Table 3.1: Observed *IC ARL* for the Max and the Distance charts when the mean and the standard deviation of a Phase I sample are used to estimate μ and σ

m	n	Max Chart Observed *ARL*	Distance Chart Observed *ARL*	$(\bar{X}, S)$ Scheme Observed *ARL*
500	5	493.68	506.62	490.52
400	5	483.07	495.16	486.84
300	5	482.16	491.82	486.03
200	5	476.21	490.90	476.98
150	5	474.02	488.10	468.57
100	5	457.58	471.17	453.99
75	5	444.51	461.56	441.31
50	5	424.94	447.26	419.76
30	5	383.86	408.51	382.09
100	15	324.51	332.96	328.96
75	15	301.91	307.06	299.15
50	15	259.84	260.63	254.84
30	15	206.17	205.47	204.52
100	25	266.95	263.15	263.10
75	25	233.84	233.17	233.39
50	25	177.73	188.90	188.54
30	25	151.22	153.19	140.82

Although from Table 3.1 one can see the effect of the size of the Phase I sample on the *IC ARL*, note that these figures are unconditional; that is, they are obtained by averaging over all possible values of the mean and the standard deviation estimates. Since the sample mean and standard deviation are random variables with their own probability distributions, the values of these estimates would vary in practice even though the Phase I sample is obtained from an *IC* process. The magnitudes of these estimates can affect the performance of the chart, and hence it is fair to examine, in addition to the unconditional performance, the "conditional" performance of the charts, i.e. what happens when specific values of the estimators are used in setting up the chart. In order to study this phenomenon, a second simulation uses specific quantiles of the distributions of $\bar{x}$ and s^2 to simulate their values, to show the effects that high, low, and medium estimates can have on the resulting *IC ARL*. These *ARL* values, obtained for some specific values of the estimators, are called conditional *ARL* values. Table 3.2 shows the conditional *ARL* values which shed interesting light on the effect of parameter estimation on these joint monitoring charts.

Based on the results in Table 3.2, it is clear that the particular estimates, obtained from different samples from an *IC* process, can have a dramatic impact on the observed *IC ARL* of the charts. Depending on the values (quantiles) of $\bar{x}$ and s^2 used, the *IC ARL* may be either greatly higher or lower than what is nominally expected, and in some cases, the results of particular combinations are not intuitive. For certain quantiles, the impact is greatest on the $(\bar{X}/S)$ scheme, while for other quantiles, the impact is greatest on the Distance chart. "Plugging in" estimates for μ and σ in the traditional Max chart, Distance chart, or $(\bar{X}/S)$ scheme would therefore lead to unpredictable chart performance. It is thus desirable to modify each chart so that the unconditional *IC ARL* is correctly maintained at a specified nominal value.

Table 3.2: Conditional *IC ARL* for the Max and Distance charts when specified quantiles of $\bar{x}$ and s^2 are used as estimates for μ and , $m = 30$, and $n = 5$[8]

Mean Quantile	Variance Quantile	Max Chart Observed *ARL*	Distance Chart Observed *ARL*	$(\bar{X}, S)$ Scheme Observed *ARL*
5th	5th	22.23	20.20	5.06
5th	25th	34.56	31.35	6.23
5th	50th	38.34	34.81	6.55
5th	75th	34.52	31.25	6.27
5th	95th	22.28	20.18	5.08
25th	5th	71.39	67.06	29.80
25th	25th	139.07	128.84	49.27
25th	50th	165.41	154.35	55.69
25th	75th	138.98	130.40	49.49
25th	95th	70.87	66.68	30.07
50th	5th	164.85	162.13	148.86
50th	25th	362.47	350.77	324.26
50th	50th	445.20	435.53	396.66
50th	75th	360.37	352.05	322.87
50th	95th	164.62	160.77	148.42
75th	5th	357.70	343.11	578.11
75th	25th	718.09	728.67	880.58
75th	50th	855.02	886.17	944.86
75th	75th	723.74	726.47	872.09
75th	95th	352.78	345.27	576.97

[8] The nominal IC ARL is 500.

95th	5th	651.80	615.69	440.06
95th	25th	834.43	991.63	437.48
95th	50th	877.19	1098.48	441.65
95th	75th	845.33	988.03	442.50
95th	95th	648.65	621.72	439.01

3.3 Statistical Framework and Preliminaries

Let $U_1, U_2, \dots, U_m$ be a random sample of size m from normal distribution with mean μ_1 and variance σ_1^2, respectively. Further, let $V_1, V_2, \dots, V_n$ be a random sample of size n, likewise from the normal distribution, with mean μ_2 and variance σ_2^2, respectively, and let the U's and the V's be mutually independent. The parameters μ_1, μ_2, σ_1^2, and σ_2^2 are all assumed unknown with $-\infty < \mu_1, \mu_2 < \infty$ and $0 < \sigma_1^2, \sigma_2^2 < \infty$. When the process is *IC*, $\mu_1 = \mu_2 = \mu$ and $\sigma_1^2 = \sigma_2^2 = \sigma^2$ so that the two populations have the same normal distribution, with unknown mean μ and unknown variance σ^2. When the process is *OOC*, the normality assumption is still assumed to hold, but one or both of these equalities among the parameters is violated; in other words, in the *OOC* case, either the means, the variances, or both would differ for the two normal distributions.

Now, let $\bar{U} = \frac{1}{m}(U_1 + U_2 + \cdots + U_m)$ and $\bar{V} = \frac{1}{n}(V_1 + V_2 + \cdots + V_n)$ be the respective sample means, and also let $S_U^2 = \frac{1}{m-1}\sum_{j=1}^{m}(U_j - \bar{U})^2$ and $S_V^2 = \frac{1}{n-1}\sum_{j=1}^{n}(V_j - \bar{V})^2$ be the respective sample variances. It is well known that $\bar{U}$ is normally distributed with mean μ_1 and variance and $\frac{\sigma_1^2}{m}$, while $\frac{(m-1)S_U^2}{\sigma_1^2}$ is distributed as a chi-square with $(m-1)$ degrees of freedom. Furthermore, it is well known that $\bar{U}$ and S_U^2 are mutually independent. Similarly, $\bar{V}$ is normally distributed with mean μ_2 and variance $\frac{\sigma_2^2}{n}$, and $\frac{(n-1)S_V^2}{\sigma_2^2}$ is distributed as a chi-square with $(n-1)$ degrees of freedom, independently of $\bar{V}$. Additionally, $(\bar{U},\ S_U^2)$ and $(\bar{V},\ S_V^2)$ are mutually independent. Letting $N = m + n$, denote $W_1 = \sqrt{\frac{mn}{N}}\frac{(\bar{V}-\bar{U})}{S_U}$ and $W_2 = \frac{S_V^2}{S_U^2}$.

Next, consider modifying the Max and the Distance charts using the estimators from a reference sample. The proposed plotting statistics and the resulting control charts are constructed in the same spirit as in the original case K charts, in that they use the probability integral transformation, but suitable modifications are made to account for estimation of parameters and the correct application of the resulting statistical distribution theory. Suppose the U sample corresponds to an *IC* or reference sample. Much of what follows is based on correctly accounting for the impact of the reference sample on the plotting statistics and the chart performance. To this end, we first consider the distribution of various statistics given (or conditionally on) $U_1, U_2, \dots, U_m$, or, equivalently, on the minimal sufficient statistics, $\bar{U}$ and S_U^2. First, it can be seen that conditionally, W_1 follows a normal distribution with mean $\sqrt{\frac{mn}{N}}\frac{(\mu_2-\bar{U})}{S_U}$ and variance $\frac{m}{N}\frac{\sigma_2^2}{S_U^2}$, and $\frac{(n-1)S_U^2}{\sigma_2^2}W_2$ follows a chi-square distribution with $(n-1)$ degrees of freedom. Moreover, W_1 and W_2 are mutually independent. Next, it can be shown that unconditionally, when the process is *IC*, W_1 follows a *t* distribution with $(m-1)$ degrees of freedom, and W_2 follows an *F* distribution with $(n-1)$ and $(m-1)$ degrees of freedom. However, W_1 and W_2 are not mutually independent. As a result, the two statistics ${W_1}^* = \Phi^{-1}\{\zeta_{m-1}(W_1)\}$, and ${W_2}^* = \Phi^{-1}\{F_{m-1,n-1}(W_2)\}$, where $\zeta_\upsilon(.)$ and $F_{\upsilon_1,\upsilon_2}(.)$ denote, respectively, the cdf of a *t* distribution with υ degrees of freedom and an *F* distribution with υ_1 and υ_2 degrees of freedom, are also dependent. As we see next, our plotting statistics are functions of ${W_1}^*$ and ${W_2}^*$, and their dependence plays a crucial role in the correct implementation of the proposed charts. They are:

i. The Modified Max chart plotting statistic: $\widehat{\Psi}_i = \max\{|W_{1i}^*|, |W_{2i}^*|\}$. The corresponding Shewhart-type chart is called the Modified Max chart. The process is declared *OOC* when $\widehat{\Psi}_i > H_M$ where the upper control limit H_M is obtained so that the *IC ARL* is some given nominal value.

ii. The Modified Distance chart plotting statistic: $\widehat{\Delta}_i = \sqrt{W_{1i}^{*2} + W_{2i}^{*2}}$. The corresponding chart is called the Modified Distance chart, which is also a Shewhart-type chart. The process is declared *OOC* when $\widehat{\Delta}_i > H_D$, where the upper control limit H_D is obtained so that the *IC ARL* is equal to some given nominal value.

In order to implement the charts we need to find the control limits, so we next study the distributions of the plotting statistics.

3.4 Distribution of Plotting Statistics

Distribution of $\widehat{\Psi}$

With the Modified Max chart, the process is declared *OOC* when for the ith test sample, $\widehat{\Psi}_i > H_M$ where the upper control limit H_M is obtained so that the *IC ARL* is some given nominal value. Since when parameters are estimated, the statistics W_1^* and W_2^* that are components of the Max chart plotting statistic are dependent, a derivation of the run length distribution is more complicated. However, this problem can be conveniently solved by conditioning on the reference sample as demonstrated by Chakraborti (2000). The details of the derivation are given in the Appendix. It is shown that the (unconditional) cdf of the plotting statistic $\widehat{\Psi}$ is given by

$$P\left(\widehat{\Psi} \leq g\right) = \int_0^\infty \int_{-\infty}^\infty p(z_U, y_U)\phi(z_U) f_{\chi^2_{(m-1)}}(y_U) dz_U dy_U,\ g > 0$$

where

$$p(Z_U, Y_U) = \left\{\Phi\left[\tau\left(\sqrt{\frac{N}{n}}\ k\sqrt{\frac{Y_U}{m-1}} + \sqrt{\frac{n}{m}} Z_U + \Delta\right)\right] - \Phi\left[\tau\left(\sqrt{\frac{N}{n}}\ h\sqrt{\frac{Y_U}{m-1}} + \sqrt{\frac{n}{m}} Z_U + \Delta\right)\right]\right\}$$

$$\times \left\{F_{\chi^2_{(n-1)}}\left[\frac{(n-1)}{(m-1)} d\tau Y_U\right] - F_{\chi^2_{(n-1)}}\left[\frac{(n-1)}{(m-1)} c\tau Y_U\right]\right\},$$

$h = \zeta_{m-1}^{-1}\{\Phi(-g)\}, k = \zeta_{m-1}^{-1}\{\Phi(g)\}, c = F_{n-1,m-1}^{-1}\{\Phi(-g)\}, d = F_{n-1,m-1}^{-1}\{\Phi(g)\}, \tau = \sigma_1^2/\sigma_2^2$,

$\Delta = \sqrt{n}(\mu_1 - \mu_2)/\sigma_1, Z_U = \sqrt{m}(\bar{U} - \mu_1)/\sigma_1$, and $Y_U = (m-1)S_U^2/\sigma_1^2$.

The run length distribution and the associated characteristics, such as the moments and percentiles, can all be obtained similarly by conditioning. For example, conditionally on Z_U and Y_U, the run length random variable, R, follows a geometric distribution with probability of success (signal) $1 - p(Z_U, Y_U)$, where $g = H_M$. Thus,

$$P(R = r|\ Z_U, Y_U) = [1 - p(Z_U, Y_U)][p(Z_U, Y_U)]^{r-1}, r = 1,2,3, \ldots$$

As a result, the unconditional run length distribution can be obtained by calculating the expectation of the conditional run length distribution over the distributions of Z_U and Y_U:

$$P(R = r) = \int_0^\infty \int_{-\infty}^\infty [1 - p(z_U, y_U)][p(z_U, y_U)]^{r-1} \phi(z_U) f_{\chi^2_{(m-1)}}(y_U) dz_U dy_U$$

Similarly, the conditional *ARL* of the Modified Max chart equals $[1 - p(Z_U, Y_U)]^{-1}$ and the unconditional *ARL* is given by

$$ARL = \int_0^\infty \int_{-\infty}^\infty [1 - p(z_U, y_U)]^{-1} \phi(z_U) f_{\chi^2_{(m-1)}}(y_U) dz_U dy_U.$$

Other moments and percentiles of the run length distribution can be calculated in a similar manner, that is, first conditionally and then unconditionally, over the joint distribution of Z_U and Y_U.

Note that when the process is *IC*, we have $\Delta = 0$ and $\tau = 1$, so that

$$p(Z_U, Y_U|IC) = \Phi\left[\sqrt{\frac{N}{n}}\, k\sqrt{\frac{Y_U}{m-1}} + \sqrt{\frac{n}{m}}Z_U\right] - \Phi\left[\sqrt{\frac{N}{n}}\, h\sqrt{\frac{Y_U}{m-1}} + \sqrt{\frac{n}{m}}Z_U\right]$$

$$\times\left[F_{\chi^2_{(n-1)}}\left[\tfrac{(n-1)}{(m-1)}dY_U\right] - F_{\chi^2_{(n-1)}}\left[\tfrac{(n-1)}{(m-1)}cY_U\right]\right].$$

Hence, the *IC* unconditional *ARL* is given by

$$\int_0^\infty \int_{-\infty}^\infty 1 - [p(z_U, y_U|IC)]^{-1}\phi(z_U) f_{\chi^2_{(m-1)}}(y_U) dz_U dy_U$$

where $g = H_M$, the *UCL* of the Max chart. The same expression can be used to find the *UCL* for a given nominal value of the *IC* unconditional *ARL*, such as 500. Note that since $p(Z_U, Y_U|IC)$ is free of Δ and τ, both the conditional and the unconditional *IC* run length distributions (and hence all the unconditional and conditional run length distribution characteristics such as the *ARL* and the percentiles) are free of the nuisance parameters when the process is *IC*. This is an important practical feature of the Modified Max chart.

Distribution of $\widehat{\Delta}$

For the Shewhart Modified Distance chart, the process is declared *OOC* when for the ith test sample $\widehat{\Delta}_i > H_D$ where the *UCL* H_D is obtained so that the *IC ARL* is equal to some given nominal value. As in the case of the Modified Max chart, the plotting statistic $\widehat{\Delta}$ is a function of W_1^* and W_2^*, and since the joint distribution (cdf) of W_1^* and W_2^* can be obtained by conditioning (as shown in the Appendix), the conditional and the unconditional distribution of $\widehat{\Delta}$ can be obtained from it. For example, it is shown that the (unconditional) cdf of $\widehat{\Delta}$ is given by

$$P(\widehat{\Delta} \le g) = \int_0^\infty \int_{-\infty}^\infty \int_{-\infty}^\infty \int_{-\sqrt{g^2-v_2}}^{\sqrt{g^2-v_2}} f_{W_1^*,W_2^*}(v_1, v_2|z_U, y_U)\, dv_1 dv_2\, \phi(z_U) f_{\chi^2_{(m-1)}}(y_U) dz_U dy_U$$

where $f_{W_1^*,W_2^*}(v_1, v_2|z_U, y_U)$denotes the conditional joint pdf of (W_1^*, W_2^*).

Again, as in the case of the Modified Max chart, the run length distribution of the Modified Distance chart can be conveniently obtained, along with the moments and percentiles, by conditioning on the reference sample. For example, writing

$$p^*(z_U, y_U) = \int_{-\infty}^{\infty} \int_{-\sqrt{g^2-v_2}}^{\sqrt{g^2-v_2}} f_{W_1^*,W_2^*}(v_1, v_2 | z_U, y_U) dv_1 dv_2 \text{ where } g = H_D$$

and following the same lines of argument as with the Modified Max chart, the run length distribution and the associated characteristics, such as moments and percentiles, for the Modified Distance chart can be obtained. Hence, conditionally on Z_U and Y_U, the run length, R^*, follows a geometric distribution, with probability of success (signal) $1 - p^*(Z_U, Y_U)$. Therefore

$$P(R^* = r | Z_U, Y_U) = [1 - p^*(Z_U, Y_U)][p^*(Z_U, Y_U)]^{r-1}, r = 1,2,3 \ldots$$

and the unconditional run length distribution can be obtained by calculating expectation over the distribution of Z_U and Y_U:

$$P(R^* = r) = \int_0^{\infty} \int_{-\infty}^{\infty} [1 - p^*(z_U, y_U)][p^*(z_U, y_U)]^{r-1} \phi(z_U) f_{\chi^2_{(m-1)}}(y_U) dz_U dy_U.$$

As in the case of the Modified Max chart, the unconditional *ARL* of the Modified Distance chart can be calculated by finding the expectation of $[1 - p^*(Z_U, Y_U)]^{-1}$ over the distribution of Z_U and Y_U:

$$ARL = \int_0^{\infty} \int_{-\infty}^{\infty} [1 - p^*(z_U, y_U)]^{-1} \phi(z_U) f_{\chi^2_{(m-1)}}(y_U) dz_U dy_U.$$

Other moments and percentiles can be calculated in a similar manner. Again, note that when the process is *IC*, we have $\Delta = 0$ and $\tau = 1$ so that the unconditional run length distribution is free of "nuisance" parameters.

Note further that the conditional joint pdf $f_{W_1^*,W_2^*}(v_1, v_2 | z_U, y_U)$ needed in the calculation of $p^*(z_U, y_U)$ can be obtained by differentiating the conditional joint cdf $F_{W_1^*,W_2^*}(v_1, v_2 | z_U, y_U)$ given in (*) in Appendix A. Hence

$$p^*(z_U, y_U) = \int_{-\infty}^{\infty}\int_{-\sqrt{g^2-v_2}}^{\sqrt{g^2-v_2}}\left\{\frac{\partial^2}{\partial v_1 \partial v_2}\left\{\left\{\Phi\left[\tau\left(\sqrt{\frac{N}{n}}\, b\sqrt{\frac{y_U}{m-1}} + \sqrt{\frac{n}{m}} z_U + \Delta\right)\right] - \right.\right.\right.$$

$$\left.\left.\left.\Phi\left[\tau\left(\sqrt{\frac{N}{n}}\, a\sqrt{\frac{y_U}{m-1}} + \sqrt{\frac{n}{m}} z_U + \Delta\right)\right]\right\}\left\{F_{\chi^2_{(n-1)}}\left[\frac{(n-1)}{(m-1)} d\tau y_U\right] - F_{\chi^2_{(n-1)}}\left[\frac{(n-1)}{(m-1)} c\tau y_U\right]\right\}\right\}\right\} dv_1 dv_2.$$

3.5 Proposed Charting Procedures

We propose the following methods for constructing appropriately Modified Distance and Max charts to monitor the mean and variance when they are unknown:

Phase II Modified Max Chart

Step 1. Collect a reference sample of size *m* from an *IC* process:

$$\boldsymbol{X_m} = (X_1, X_2, \dots, X_m)$$

Step 2. Let $\boldsymbol{Y_{i,n}} = (Y_{i1}, Y_{i2}, \dots, Y_{in})$ be the ith Phase II (test) sample of size *n*, $i = 1,2, \dots$

Step 3A: Identify the *U*'s with the *X*'s and the *V*'s with the *Y*'s, respectively. Calculate the statistics $|W_1^*|$ and $|W_2^*|$ for the ith test sample, for $i = 1,2, \dots$

Step 4A. Calculate the Shewhart max-type plotting statistic: $\widehat{\Psi}_{\mathrm{i}} = \max\{W_{1i}^*|, |W_{2i}^*|\}$.

Step 5A. Plot $\widehat{\Psi}_{\mathrm{i}}$ against the *UCL* H_M. Note that $\widehat{\Psi}_i \geq 0$ by definition and larger values of $\widehat{\Psi}_i$ suggest an *OOC* process.

Step 6A. If $\widehat{\Psi}_i$ exceeds H_M, the process is declared *OOC* at the ith test sample. If not, the process is thought to be *IC*, and testing continues to the next test sample.

Step 7A. Follow-up: The Modified Max chart requires no additional charting constants for its follow-up procedure, making it simple to implement. When the process is declared *OOC* at the ith test sample, compare each of $|W_{1i}^*|$ and $|W_{2i}^*|$ with H_M.

(i) If $|W_{2i}^*| < H_M < |W_{1i}^*|$, a shift in mean is indicated.

(ii) If $|W_{1i}^*| < H_M < |W_{2i}^*|$, a shift in variance is indicated.

(iii) If $|W_{1i}^*|$ and $|W_{2i}^*|$ both exceedH_M, a shift in both mean and variance is indicated.

Phase II Modified Distance Chart

Steps 1-2 Same as before.

Step 3B. Identify the *U*'s with the *X*'s and the *V*'s with the *Y*'s, respectively. Calculate the statistics $W_{1i}^{*2}$and W_{2i}^{*2} for the ith test sample, for $i = 1,2, \ldots$

Step 4B. Calculate the Shewhart distance-type plotting statistic: $\hat{\Delta}_i = \sqrt{W_{1i}^{*2} + W_{2i}^{*2}}$

Step 5B. Plot $\hat{\Delta}_i$ against a *UCL* H_D. Note that $\hat{\Delta}_i \geq 0$ by definition and larger values of $\hat{\Delta}_i$ suggest an *OOC* process.

Step 6B. If $\hat{\Delta}_i$ exceeds H_D, the process is declared *OOC* at the ith test sample. If not, the process is considered to be *IC*, and testing continues to the next test sample.

Step 7B. Follow-up: The following procedure is recommended. When the process is declared *OOC* at the ith test sample, calculate $p_1 = P[W_1^{*2} > w_{1i}^{*2} \,|IC]$ and $p_2 = P[W_2^{*2} > w_{2i}^{*2} \,|IC]$. Note that since W_1^{*2} and W_2^{*2} each follow a chi-square distribution with 1 degree of freedom, both of these probabilities can be obtained directly from a chi-square table.

(i) If both $p_1, p_2 < 0.01$, a shift in both mean and variance is indicated.

(ii) If both $p_1, p_2 > 0.05$, a false alarm is indicated.

(iii) If $p_1 < 0.01$ and $p_2 > 0.05$, a shift in mean is indicated.

(iv) If $p_2 < 0.01$ and $p_1 > 0.05$, a shift in variance is indicated.

(v) If $p_1 < 0.01$ and $0.01 \leq p_2 \leq 0.05$, a major shift in mean with possible associated shift is variance is indicated.

(vi) If $p_2 < 0.01$ and $0.01 \leq p_1 \leq 0.05$, a major shift in variance with possible associated shift is mean is indicated.

3.6 Implementation

The proposed Modified Max and Distance charts are designed such that the appropriate *UCL* is found based on the sample sizes and the desired nominal *IC ARL*. Although one can use the analytical expressions for the *IC ARL* given in the earlier sections to find (solve for) the control limits, this is bound to be tedious as the formulas involve evaluations of multi-dimensional integrals. Instead we use simulations in R to calculate the control limits. Note that we also use the software Mathcad to evaluate the integrals and thus spot check the simulation results in a number of cases. In Table 2, we provide the appropriate *UCL* values for both of these charts for various combinations of m and n, for a nominal *IC ARL* of 500.

From Table 3.3 it can be seen that the standard unknown values for H_M and H_D approach the corresponding standards known values 3.29 and 3.52, respectively. Additionally, *H* does not change much once the reference sample size m is sufficiently high. It increases only slightly when n is fixed and m increases from 150. However, when m is fixed and n increases, *H* actually decreases slightly. For other values of *m* and *n* within the range of the table, approximations to the control limit can be obtained. For example, for the Modified Max chart, a simple polynomial fit for *n* = 5 yields, y = 6E-09x^3 - 6E-06x^2 + 0.0019x + 3.0626, where $y = H$ and $x = m$. This fit has a remarkably high $R^2 = 0.9802$.

Table 3.3: The *H* values for the Modified Max and Distance charts for a nominal *IC ARL* of 500

m	n	H_M	H_D
500	5	3.27	3.50
400	5	3.26	3.49
300	5	3.25	3.49
200	5	3.24	3.47
150	5	3.23	3.45
100	5	3.20	3.43
75	5	3.18	3.41
50	5	3.15	3.37
30	5	3.10	3.31
100	15	3.17	3.39
75	15	3.13	3.35
50	15	3.06	3.28
30	15	2.93	3.14
100	25	3.11	3.33
75	25	3.05	3.26
50	25	2.94	3.14
30	25	2.73	2.93

3.7 Illustrative Example

Montgomery (2005) presents a data set for an automotive manufacturing process which involves a Phase I data set consisting of twenty-five samples of five piston ring diameters and a Phase II data set consisting of an additional fifteen samples of five piston ring diameters. We use this example to illustrate the effectiveness of the Modified Max and Modified Distance charts for jointly monitoring the mean and the variance of the process. Here, $m = 125$, and $n = 5$. Suppose we wish to use an *IC ARL* of 500. Then, using simulations, the control limits are found to be $H_M = 3.216$ for the Modified Max chart and $H_D = 3.450$ for the Modified Distance chart. The resulting control charts with the plotted statistics are shown in Figures 3.1 and 3.2, respectively.

Though the two charts look very similar, the signal occurs at the 12$^{\text{th}}$ sample for the Max chart and at the 13$^{\text{th}}$ sample for the Distance chart, indicating that the Max chart is somewhat superior in this particular instance. Since the charts both signal, we use the proposed follow-up post-signal diagnostic procedures and see that both charts indicate a shift in mean only. This is because for the Max chart, $\left|W_{1,12}^*\right| = 3.239$ exceeds $H_M = 3.216$, while $\left|W_{2,12}^*\right| = 0.624$ does not. Likewise, for the Distance chart, we calculate the two p-values $p_1 = 0.0001$ and $p_2 = 0.7391$ using R and reach the same conclusion. It is interesting to note that for the same data set, Mukherjee and Chakraborti's (2011) Shewhart-Lepage nonparametric control chart also signalled at the 12$^{\text{th}}$ sample, but their post-signal diagnostic procedure concluded that there was evidence of both a location and a scale shift. On the parametric side, based on a two-chart scheme made up of a traditional 3-sigma $\bar{X}$ and a 3-sigma *R* chart as in Montgomery (2005), one would conclude that there was evidence of a mean shift at sample 12 but no variance shift. Our normal theory one-chart procedures reach the same conclusion and are correctly designed for a specified *IC ARL* of 500 in the presence of estimated parameters.

Montgomery's (2005) piston ring data

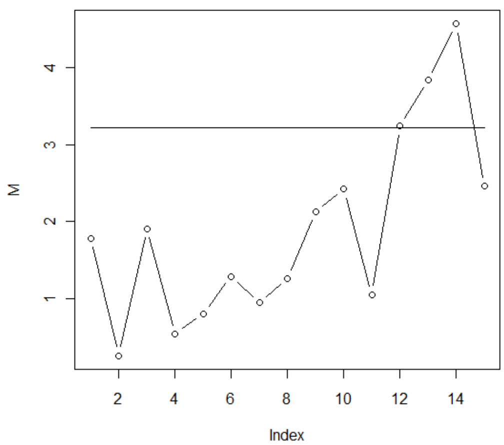

Figure 3.1: Modified Max Chart

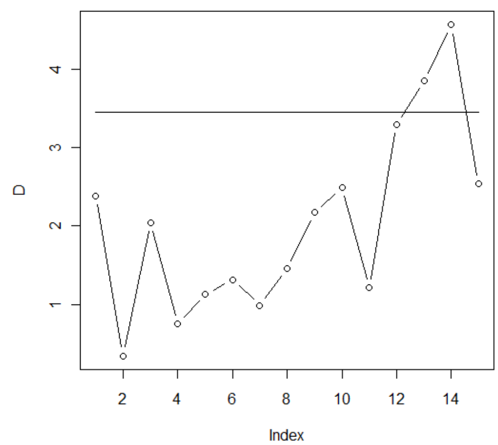

Figure 3.2: Modified Distance Chart

Next we examine the performance of the proposed charts through a study of their run length properties.

3.8 Performance Comparisons

The performance of the Modified Max and Distance charts is evaluated in a simulation study. The tables and plots in Appendix B compare the performance of the two charts for various mean and variance shifts and sample sizes, providing the *ARL*, the run length standard deviation, and specified quantiles of the run length distribution. Note that the underlying distribution is normal and that $\mu = 0$ and $\sigma = 1$ represents the *IC* case. For purposes of comparison, the modified $(\bar{X}/S)$ scheme discussed in Appendix A.4 is also included in the simulation. It is important to realize that the control limits for this $(\bar{X}/S)$ scheme are determined by taking the parameter estimation into account. The Montgomery (2005) ($\bar{X}/S$) scheme is not directly comparable to the Modified Max and Distance charts.

Since joint monitoring of the mean and variance of a normal distribution is analogous to testing the null hypothesis that the sample at hand comes from a completely specified normal distribution (a simple null hypothesis) versus all alternatives (a composite alternative hypothesis), a likelihood ratio-based joint monitoring scheme appears to be a promising alternative. Several researchers have considered control charts based on the likelihood ratio, including Hawkins and Deng (2009); Zhou, Luo, and Wang (2010); Zou and Tsung (2010); and Zhang, Zou, and Wang (2010). Following this line of argument, we considered a chart based on the two-sample likelihood ratio statistic (the LR chart) and compared its performance to that of the Modified Max and Distance charts in the simulations. However, the LR chart was found to have the uniformly worst performance, often taking more than twice as long as the Max and Distance charts to detect a shift. This relatively poor performance may result from the fact that the many small changes in mean and variance which are detected by the W_1^* and W_2^* statistics (and therefore produce a signal in that Max and Distance charts) are not large enough to produce a significant change in the likelihood ratio statistic. As a result, the LR chart for joint monitoring was deemed to be too conservative to be useful in practice and will not be discussed any further in this chapter.

From the tables and the figures, it is seen that the Modified Max and Distance charts perform rather similarly, though the Distance chart slightly outperforms the Max chart in most cases. The Max chart has slightly superior performance in detecting moderate to large shifts in the mean (0.75 to 3.0) accompanied by smaller or absent shifts in the variance. For example, when $m = 100, n = 5$, and the mean shifts from 0 to 1 and there is no shift in the variance, the

ARL of the Modified Max chart is 9.55, while that of the Modified Distance chart is about 6% larger. However, the Modified Distance chart has a shorter *ARL* in the majority of the cases, including small shifts in the mean (less than .05) with no shift in the variance and moderate-to-large shifts in the mean accompanied by any shift in the variance. Note that the Max chart is easier to apply since it has a simpler follow-up post-signal diagnostic procedure. The similarity in performance of the two charts is not surprising, given that both of these charts are based upon functions of the same basic statistics W_1^* and W_2^*. Both charts quickly detect moderate to large changes in the mean and/or variance.

The $(\bar{X}/S)$ scheme exhibits very promising performance, though its performance is greatly influenced by the size of the reference sample m. The scheme outperforms the Max chart for all of the shifts studied. When $n = 30$, this two-chart scheme also outperforms the Distance chart for all of the shifts studied. However, when a larger set of reference data is used, we see that the Distance chart outperforms the $(\bar{X}/S)$ scheme when a medium-to-large shift in the variance occurs.

Next, an important question about all normal theory control charts is their robustness to normality, that is, how their performance is affected or degraded by a departure from the normality assumption upon which the methodology is based. We now examine this issue for the proposed charts.

3.9 Robustness to Departures from Normality

It is of interest to examine the performance of the Modified Max and Distance charts when the underlying process distribution is non-normal. This is particularly important in the *IC* case so that one can understand the effect of non-normality on the *IC ARL*. To study this, we performed simulations in which both the Phase I and Phase II data come from the same non-normal distribution. We considered both skewed and symmetric distributions, as well as the "normal-like" Laplace and *t* distributions. The results appear in Tables 3.4 and 3.5.

Table 3.4. The *IC* run length characteristics for the normal theory Modified Distance chart where $m = 50, n = 5, IC\ ARL = 500$, and $H_D = 3.37$.[1]

Distribution (Scaled to mean 0 and variance 1)	ARL	VAR	5th Percentile	1st Quartile	Median	3rd Quartile	95th Percentile
Laplace	72.88	9471.88	4	15	38	91	258
Gamma (1,1)	27.77	966.47	3	7	17	36	89
Gamma (3,1)	82.36	11800.07	4	17	44	104	297
t(5)	69.93	8239.04	4	16	39	88	245
t(4)	48.71	3732.66	3	11	27	61	168

[1]*H* is calculated on the basis of normal distribution.

Table 3.5. The IC run length characteristics for the normal theory Modified Max chart where $m = 50, n = 5, IC\ ARL = 500$, and $H_M = 3.15$.[2]

Distribution (Scaled to mean 0 and variance 1)	ARL	VAR	5th Percentile	1st Quartile	Median	3rd Quartile	95th Percentile
Laplace	76.31	8370.85	4	17	44	100	263
Gamma (1,1)	37.21	1661.33	3	10	23	50	119
Gamma (3,1)	129.54	27521.56	6	26	70	166	463
t(5)	81.56	9810.29	4	19	48	105	276
t(4)	56.15	4514.14	4	13	33	73	187

[2]*H* is calculated on the basis of normal distribution.

From Tables 3.4 and 3.5, it is clearly seen that non-normality presents a major problem for both of these charts, in that the *IC* run length distribution is heavily impacted. For example, the *ARL* is seen to be far lower than the nominal *IC ARL*, which indicates the presence of a high FAR. Other run length distribution characteristics such as the median and the percentiles are impacted similarly. Though the Max chart fares somewhat better than the Distance chart, both fall far short of the nominal *IC ARL*. This means that when the data arise from such distributions a large number of false alarms will be generated, which can ruin the utility and the purpose of control charts. It has long been known that single-parameter charts based on the normal distribution, such as the $\bar{X}$ and S^2 charts, are non-robust for some distributions including the skewed and the heavier tailed, so it is no surprise that this problem extends to mean-variance charts, such as the ones considered in this paper. From the tables, it can be seen that that the charts have especially poor performance for the skewed Gamma (1,1) distribution. In fact, the 95^{th} percentile of the *IC* run length distribution in this case was only 119. The (*IC*) non-robustness of normal (parametric) theory based charts should be a matter of considerable concern to practitioners.

An alternative class of control charts, known as nonparametric or distribution-free control charts are *IC* robust by definition, and they can be useful in situations where the underlying distribution is unknown or is expected to be non-normal. These charts have the same *IC* distribution for all continuous distributions, which means, for example, they have the same known false alarm rate. A number of researchers have contributed to the literature of nonparametric control charts; for a recent overview, see Chakraborti et al. (2011). However, only a few nonparametric joint monitoring charts are currently available; these include Mukherjee and Chakraborti's (2011) Shewhart-Lepage (SL) chart and Zou and Tsung's (2010) goodness-of-fit test-based EWMA control chart. Clearly, more research in this area is necessary.

Finally, we study the effects of parameter estimation on the performance of the proposed charts.

3.10 Effects of Estimation of Parameters

In order to examine the impact of the Phase I estimation of μ and σ on the *IC* performance of the Modified Max and Distance charts, we perform a simulation study to investigate the actual or the observed *ARL* resulting from using particular estimates (in a similar fashion to the simulation study we presented earlier for the original Max and Distance charts). We find and use the appropriate control limits such that the nominal *IC ARL* of each chart is 500 when $m = 30$ and $n = 5$. For the Distance chart, the *UCL* is 3.31; for the Max chart, the *UCL* is 3.10. For purposes of comparison, the $(\bar{X}, S)$ scheme was also included in this simulation. When conditioning is used to find the proper control limits for these charts, the control limits for the $\bar{X}$ chart are $\bar{U} \pm \frac{\Phi\left(1-\frac{p_0}{2}\right)S_U}{\sqrt{n}}$, and the control limits for the S chart are $\sqrt{\frac{S_U^2 F_{\chi^2_{(n-1)}}\left(\frac{p_0}{2}\right)}{n-1}}$ and $\sqrt{\frac{S_U^2 F_{\chi^2_{(n-1)}}\left(1-\frac{p_0}{2}\right)}{n-1}}$. When $m = 30$ and $n = 5$, this $p_0 = .000763$.

Table 3.6: Conditional *IC ARL* for the Modified Max and Distance charts when specified quantiles are used as estimates for μ and σ^2, $m = 30$, and $n = 5$[9]

Mean Quantile	Variance Quantile	Modified Max Chart Observed *ARL*	Modified Distance Chart Observed *ARL*	Modified $(\bar{X}, S)$ Scheme Observed *ARL*
5th	5th	54.56	41.78	5.49
5th	25th	99.06	74.46	6.83
5th	50th	116.10	86.89	7.12
5th	75th	99.28	74.19	6.81
5th	95th	53.96	41.73	5.49

[9] The nominal *IC ARL* is 500.

25^{th}	5th	195.29	161.76	35.02
25^{th}	25th	416.67	339.78	58.28
25^{th}	50th	508.60	414.30	66.08
25^{th}	75th	420.70	338.89	58.81
25^{th}	95th	194.30	161.58	34.99
50^{th}	5th	407.85	350.42	186.30
50^{th}	25th	726.26	666.76	414.86
50^{th}	50th	822.15	782.59	516.07
50^{th}	75th	729.87	667.71	416.16
50^{th}	95th	407.83	349.21	184.73
75^{th}	5th	579.48	507.34	769.77
75^{th}	25th	742.46	785.59	1167.05
75^{th}	50th	770.43	864.29	1249.41
75^{th}	75th	741.35	784.15	1163.95
75^{th}	95th	584.09	509.40	769.53
95^{th}	5th	496.72	515.00	573.72
95^{th}	25th	512.54	659.63	575.32
95^{th}	50th	515.63	689.37	578.05
95^{th}	75th	510.73	653.66	578.41
95^{th}	95th	498.48	514.55	574.12

It is seen that the values in Table 3.6 still vary greatly from the nominal *IC ARL* of 500, indicating that the particular estimates (quantiles) of $\bar{x}$ and s^2 obtained from the Phase I sample at hand and used in the chart will greatly affect the charts' performance.

In many cases, the conditional *IC ARL*s for the modified $(\bar{X}/S)$ scheme are further from the nominal value than those of the Max and Distance charts. The modified $(\bar{X}/S)$ scheme has particularly poor performance in this respect when low quantiles of $\bar{x}$ are used. On the other hand, when a very high quantile of $\bar{x}$ is used, the modified $(\bar{X}/S)$ scheme has a closer-to-nominal *IC ARL* than the other two charts.

The conditional *IC ARL* values in Table 3.6 are typically somewhat closer to the nominal value than those shown in Table 3.2, indicating that the modifications have improved the charts' robustness to error in the estimation of the parameters. In particular, note that when the 25th percentile estimate is used for both $\bar{x}$ and s^2, the conditional *IC ARL* for the Modified Max chart (416.67) is nearly three times as large as the corresponding *IC ARL* for the original Max chart (139.07), and, similarly, the conditional *IC ARL* for the Modified Distance chart (339.78) is more than two-and-a-half times as large as the corresponding *IC ARL* for the original Distance chart (128.84). Furthermore, between the two one-chart schemes, the Max chart appears to exhibit superior performance when a lower estimate (quantile) of the variance is used, while the Distance chart seems preferable when a higher estimate is used. Nevertheless, the results are not entirely satisfactory, as it is clear that the Phase I estimate of the mean and variance can greatly impact the *IC* performance of the Phase II chart, particularly when *m* is small to moderate as is currently recommended in the literature. This is an important problem which would benefit from further research.

3.11 Summary and Conclusions

Monitoring the mean and variance is an important problem in statistical process control. Chen and Cheng's (1998) Max chart and Razmy's (2005) Distance chart are applicable when the *IC* mean and variance of the underlying normal distribution are known or specified. However, when these parameters are unknown, it is necessary to estimate them from an *IC* reference (or a Phase I) sample. This estimation introduces additional variability which needs to be properly taken into account in order to apply the charts correctly. Otherwise, the *IC ARL* can vary greatly and is usually much lower than what is nominally expected, which means excessive false alarms which can vastly diminish the utility of the charts in practice. We consider modifications of the Max chart and the Distance chart for the unknown parameter case and study their implementation and run length properties. It is shown that the two modified charts perform similarly, with the Distance chart having a slight advantage in most cases. The modified charts can be used in practice whenever a Shewhart-type chart for jointly monitoring unknown mean and variance is desirable. Further refinements, such as using averages-type charts including the CUSUM and the EWMA charts that can be useful for detecting small and sustained changes will be considered elsewhere in the future.

Finally, Hawkins and Zamba (2005) proposed an alternative methodology for jointly monitoring the mean and variance of a normal distribution when the parameters are unknown based on what is called a changepoint formulation. The "changepoint" is the unknown instant at which a shift occurs in one or both of the parameters, such that the observations taken before the changepoint have a different mean and/ or variance than those taken after it. The changepoint approach to joint monitoring can be attractive in situations where practitioners do not have access to or prefer not to collect a reference sample prior to starting prospective process monitoring. Our approach, on the other hand, is a more traditional one based on current practice which allows practitioners to use control charts with which they are familiar while making the necessary adjustments to correct the control limits that account for estimation of parameters. Moreover, there are situations in practice where it is common to conduct a Phase I study as a part of routine process analysis before starting prospective monitoring.

CHAPTER 4

CONTROL CHARTS FOR SIMULTANEOUS MONITORING OF KNOWN LOCATION AND SCALE PARAMETERS OF PROCESSES FOLLOWING A SHIFTED (TWO-PARAMETER) EXPONENTIAL DISTRIBUTION

4.1 Introduction

Often manufacturers of consumer products offer a guarantee that some product, if used properly, will work for a particular amount of time. For example, an automobile may come with a three-year/30,000 mile guarantee, under which the manufacturer agrees to fix any defects which occur during that specified period. In order to determine an appropriate guarantee period, a manufacturer would typically utilize a relevant statistical distribution to model the lifetime of the product. The two-parameter exponential distribution is often an appropriate statistical model for such circumstances. Under this model, the assumed distribution of the lifetime, x, of the product is $f(x;\ \theta,\lambda) = \frac{1}{\lambda}e^{-(x-\theta)/\lambda}$ where $\theta < x$ is a period during which no failure can occur, i.e. the guarantee period, and $\lambda > 0$ is the scale parameter (Epstein, 1960). Thus, the determination of a guarantee period can be accomplished by estimating the parameter θ.

A manufacturer may also want to engage in prospective monitoring to determine whether the distribution of the product's lifetime has remained unchanged or whether some shift has occurred in one or both of the distribution's parameters. He needs a control scheme capable of accurately determining whether each sample taken comes from the specified shifted exponential distribution or one that differs from the specified one in some way. External factors, such as pollution or changes in the materials used to pave roads, could alter the distribution of the product's lifetime by changing one or both of the distribution's parameters. Control charts are a useful tool for engaging in such process monitoring. However, the majority of control charts are designed for situations in which the data are known or assumed to be normally distributed. When the data are actually non-normal, however, the use of such charts is inappropriate and can be quite misleading. Instead of using normal theory charts, practitioners should use charts designed for the correct distribution, in this case, the shifted exponential distribution.

The monitoring of guarantee times is far from the only situation in which one might need a control chart for the shifted exponential distribution. Kao (2010) provides examples of processes which follow this distribution in both manufacturing and healthcare settings. Notably, he demonstrates that time between MSRA infections in patients at a particular hospital, which might reasonably be expected to follow a one-parameter exponential distribution, actually has a location parameter and follows a shifted exponential distribution.

Furthermore, in practice many processes are assumed to follow the one-parameter exponential distribution, which is simply a special case of the shifted exponential distribution. It is often plausible that a process whose *IC* distribution is exponential could experience a location shift, in which case a control chart for the shifted exponential distribution is needed to monitor it. For example, suppose that Steve, a preschool student, occasionally bites his classmates. Also assume that every time Steve bites another child, he is scolded by his teacher and that the time between Steve's biting episodes follows a one-parameter exponential distribution. Now, suppose that following complaints from other's children's parents, Steve's exasperated teacher begins placing him in seclusion for five minutes immediately following each biting episode. This intervention by the teacher is an assignable cause which will undoubtedly result in a location shift, since Steve cannot bite another student for at least five minutes, but it may or may not result in a shift in the scale parameter.

A large body of research on testing and estimation for the shifted exponential distribution has been developed over the years. Researchers including Epstein (1960), Varde (1969), Kececioglu and Li (1985), and Lam et al. (1994) have developed point and interval estimates for the location and scale parameters of this distribution. Ahsanullah (1980) and Ahmadi and MirMostafaee (2009) made contributions to predicting future data points from the shifted exponential distribution.

Unfortunately, however, while parameter estimation, hypothesis testing, reliability sampling plans, and prediction of future data points are addressed in the literature, the research on control charts for data from this distribution is much sparser. Ramalhoto and Morais (1999) developed a control chart for monitoring only the scale parameter, and Sürücü and Sazak (2009) presented a control scheme for this distribution in which moments are used to approximate the distribution. Neither method is entirely satisfactory for the purposes described above. Instead, the product manufacturer needs a control scheme capable of jointly monitoring the location and scale parameters.

At first, it might seem tempting to construct a chart which jointly monitors the process mean and standard deviation, using the mean and standard deviation of process samples to monitor the distribution, as is typically done in normal theory situations. However, these summary statistics can be inefficient and unreliable in this case, as noted by Ramalhoto and Morais (1999). They point out that “a more reliable alternative is to identify or fit a distributional model for the output that is more appropriate than the normal model, and then to construct control charts based on that model.”

Here, we discuss and compare several possibilities for one-chart schemes for jointly monitoring the parameters of the shifted exponential distribution. First, we propose a pair of joint monitoring schemes similar to Chen and Cheng's (1998) Max chart for normally distributed data. These schemes transform the estimators for each parameter so that they each have the standard normal distribution and then combine them together using a max function. The Shifted Exponential MLE Max (SEMLE-Max) chart utilizes the maximum likelihood estimators (MLEs) of the location and scale parameters, while the Shifted Exponential MVUE Max (SEMVUE-Max) chart utilizes the minimum variance unbiased estimators (MVUEs). As mentioned previously, there are other ways of constructing joint monitoring schemes, but max-type charts have been popular in the literature and with practitioners, due to their straightforwardness and relative simplicity. Next, we suggest a max-type joint monitoring scheme similar to the SEMLE-Max chart except that it transforms the estimators so that both have the chi-square distribution with two degrees of freedom. Here, we transform the estimators to the chi-square distribution rather than the normal distribution in effort to address a problem with ARL bias that occurs in the SEMLE-Max and SEMVUE-Max charts. We call this the Shifted Exponential MLE Chi-square Max (SEMLE-ChiMax) chart. Finally, we consider a likelihood ratio-type chart, which we will refer to as the Shifted Exponential Likelihood Ratio (SE-LR) chart.

Additionally, we consider a two-chart joint monitoring scheme made up of a control chart for monitoring the location and a separate control chart for monitoring the scale. Each of these component charts utilizes the MLE of the parameter that it monitors, and the control limits for the two charts are selected individually so that the overall *IC ARL* of the scheme is a specified value. We refer to this as the SEMLE-2 joint monitoring scheme.

4.2 Statistical Framework and Preliminaries

Let us first consider the case where the *IC* parameters, θ_0 and λ_0, are known or specified. Let $V_1, V_2, \dots, V_n$ be a random sample of size n from the shifted exponential distribution, with location parameter θ_2 and scale parameter λ_2.[10] The parameters θ_2 and λ_2 are unknown; however, when the process is *IC*, $\theta_2 = \theta_0$ and $\lambda_2 = \lambda_0$. When the process is out-of-control (*OOC*), one or both of these equalities is violated; in other words, either the location parameter, the scale parameter, or both differ from the specified *IC* parameters, θ_0 and λ_0, respectively. However, at the outset, it is unclear whether or not the distributions are the same.

4.3 The SEMLE-Max Chart

Let $\hat{\theta}_2 = V_{(1)}$ be the first order statistic of the sample. This is known to be the MLE for the location parameter (Johnson and Kotz, 1970). Also, let $\hat{\lambda}_2 = \frac{\sum_{i=1}^{n}(V_i - \hat{\theta}_2)}{n} = \frac{\sum_{i=1}^{n} V_i}{n} - \hat{\theta}_2 = \bar{V} - \hat{\theta}_2$. This is the MLE of the scale parameter (Johnson and Kotz, 1970). Furthermore, $\hat{\theta}_2$ and $\hat{\lambda}_2$ are independent (see Johnson and Kotz, 1970; Govindarajulu, 1966; Tanis, 1964). However, they are not unbiased, since $E(\hat{\theta}_2) = \theta_2 + \frac{\lambda_2}{n}$ and $E(\hat{\lambda}_2) = \lambda_2(1 - n^{-1})$.

Since $\hat{\theta}_2$ is simply the first order statistic of the $V_1, V_2, \dots, V_n$ sample, its distribution is well known to be the shifted exponential distribution with location parameter θ_2 and scale parameter λ_2/n. As a result, $\frac{2n(\hat{\theta}_2 - \theta_2)}{\lambda_2}$ has a chi-square distribution with 2 degrees of freedom.

The distribution of $\hat{\lambda}_2$ is less straightforward but still obtainable. First, observe that $\sum_{i=1}^{n}(V_i - \hat{\theta}_2) = \sum_{i=1}^{n}(V_i - V_{(1)}) = \sum_{i=2}^{n}(n - i + 1)(V_{(i)} - V_{(i-1)})$. Now, $\frac{2}{\lambda_2}\sum_{i=2}^{n}(n - i +$

[10] For consistency across chapters of this dissertation, we use θ_0 and λ_0 for known *IC* parameters and θ_2 and λ_2 for Phase 2 parameters. θ_1 and λ_1 are reserved for use in discussion of Phase I parameters.

$1)\left(V_{(i)}-V_{(i-1)}\right)$ has a chi-square distribution with $2n-2$ degrees of freedom (Tanis, 1964). Thus, $\frac{2n\widehat{\lambda}_2}{\lambda_2}=\frac{2}{\lambda_2}\sum_{i=2}^{n}(n-i+1)\left(V_{(i)}-V_{(i-1)}\right)$ has a chi-square distribution with $2n-2$ degrees of freedom.

Now, let $B_1=\Phi^{-1}\left\{G\left(\frac{2n(\widehat{\theta}_2-\theta_0)}{\lambda_0},2\right)\right\}$ where $G(.,\upsilon)$ denotes the cdf of a chi-square distribution with υ degrees of freedom, and let $B_2=\Phi^{-1}\left\{G\left(\frac{2n\widehat{\lambda}_2}{\lambda_0},2n-2\right)\right\}$. Note that both B_1 and B_2 have a standard normal distribution when the process is *IC*. We will use these two statistics to construct the SEMLE-Max chart.

4.3.1 Proposed Charting Procedure for the SEMLE-Max chart

We propose the following method for constructing SEMLE-Max charts when the location and scale parameters, θ_0 and λ_0, are known or specified:

Step 1. Let $Y_{i,n}=(Y_{i1},Y_{i2},\dots,Y_{in})$ be the ith Phase II sample of size $n, i=1,2,\dots$

Step 2. Identify the $V's$ with the $Y's$. Calculate the statistics B_{1i} and B_{2i} for the ith test sample, for $i=1,2,\dots$

Step 3: Calculate the plotting statistic $\mathcal{M}_i=\max\{|B_{1i}|,|B_{2i}|\}$.

Step 4. Plot $\mathcal{M}_i$ against a *UCL* $H_{\mathcal{M}}$. Note that $\mathcal{M}_i\geq 0$ by definition so that the *LCL* is 0 and that larger values of $\mathcal{M}_i$ suggest an *OOC* process.

Step 5. If $\mathcal{M}_i$ exceeds $H_{\mathcal{M}}$, the process is declared *OOC* at the ith test sample. If not, the process is considered to be *IC*, and testing continues to the next sample.

Step 6. Follow up: When the process is declared *OOC* at the ith test sample, compare each of $|B_{1i}|$ and $|B_{2i}|$ with $H_{\mathcal{M}}$.

(i) If $|B_{2i}|< H_{\mathcal{M}}<|B_{1i}|$, a shift in the location parameter is indicated.

(ii) If $|B_{1i}| < H_{\mathcal{M}} < |B_{2i}|$, a shift in the scale parameter is indicated.

(iii) If $|B_{1i}|$ and $|B_{2i}|$ both exceed $H_{\mathcal{M}}$, a shift in both the location and scale parameters is indicated.

4.3.2 Distribution of the Plotting Statistic for the SEMLE-Max chart

For the SEMLE-Max chart, the process is declared *OOC* when $\mathcal{M} > H_{\mathcal{M}}$ where the *UCL* $H_{\mathcal{M}}$ is obtained so that the *IC ARL* is some given nominal value. B_1 and B_2 are independent because $\hat{\theta}_2$ and $\bar{V} - \hat{\theta}_2$ are, and as mentioned previously, both have the standard normal distribution when the process is *IC*. The cdf of the plotting statistic $\mathcal{M}$ is given by $P(\mathcal{M} \le g) = P(\max\{|B_{1i}|, |B_{2i}|\} \le g) = P\{(|B_{1i}| \le g)\,\&(|B_{2i}| \le g)\} = \left\{G\left(\frac{2n}{\lambda_2}\left(\frac{\lambda_0}{2n}G^{-1}(\Phi(g),2) + \theta_0 - \theta_2\right),2\right) - G\left(\frac{2n}{\lambda_2}\left(\frac{\lambda_0}{2n}G^{-1}(\Phi(-g),2) + \theta_0 - \theta_2\right),2\right)\right\} \times \left\{G\left(\frac{\lambda_0}{\lambda_2}G^{-1}(\Phi(g),2n-2),2n-2\right) - G\left(\frac{\lambda_0}{\lambda_2}G^{-1}(\Phi(-g),2n-2),2n-2\right)\right\}$.[11]

When the process is *IC*, the cdf of the plotting statistic $\mathcal{M}$ simplifies to $P(\mathcal{M} \le g|IC) = \{\Phi(g) - \Phi(-g)\}^2$. The *IC ARL* is $\frac{1}{P(\mathcal{M}>g)} = \frac{1}{1-\{\Phi(g)-\Phi(-g)\}^2} = \frac{1}{1-\{2\Phi(g)-1\}^2}$. Thus, the *UCL* $H_{\mathcal{M}} = \Phi^{-1}\left(\frac{1+\sqrt{1-\frac{1}{IC\ ARL}}}{2}\right)$.

4.4 The SEMLE-ChiMax Chart

Next, let $D_1 = \frac{2n(\hat{\theta}_2-\theta_0)}{\lambda_0}$ and $D_2 = \mathrm{G}^{-1}\left\{\mathrm{G}\left(\frac{2n\hat{\lambda}_2}{\lambda_0}, 2n-2\right), 2\right\}$ where $\hat{\theta}_2$ and $\hat{\lambda}_2$ are the maximum likelihood estimators given above. Note that both D_1 and D_2 have a chi-square

[11] Further details are given in section C.3 of the Appendix.

distribution with two degrees of freedom when the process is *IC*. These are the two statistics that we will use to construct the SEMLE-ChiMax chart.

4.4.1 Proposed Charting Procedure for the SEMLE-ChiMax chart

We propose the following method for constructing SEMLE-ChiMax charts when the location and scale parameters, θ_0 and λ_0, are known or specified:

Step 1. Let $Y_{i,n} = (Y_{i1}, Y_{i2}, \ldots, Y_{in})$ be the ith Phase II sample of size $n, i = 1,2, \ldots$

Step 2. Identify the $V's$ with the $Y's$. Calculate the statistics D_{1i} and D_{2i} for the ith test sample, for $i = 1,2, \ldots$. Note that if the process is *IC*, both of these quantities should be positive. If $D_{1i} \leq 0$, the process is declared *OOC* at the *i*th test sample. If $D_{1i} > 0$, continue to step 3.

Step 3: Calculate the plotting statistic $\mathrm{T}_i = \max\{D_{1i}, D_{2i}\}$.

Step 4. Plot T_i against a *UCL* H_{T}. Note that $\mathrm{T}_i \geq 0$ so that the *LCL* is 0 and large values of T_i suggest an *OOC* process.[12]

Step 5. If T_i is greater than H_T or less than 0, the process is declared *OOC* at the *i*th test sample. If not, the process is considered to be *IC*, and testing continues to the next sample.

Step 6. Follow up: When the process is declared *OOC* at the *i*th test sample, compare each of D_{1i} and D_{2i} with H_{T}.

(i) If $D_{2i} < H_{\mathrm{T}} < D_{1i}$, a shift in the location parameter is indicated.

(ii) If $D_{2i} < H_{\mathrm{T}}$ and $D_{1i} < 0$, a shift in the location parameter is indicated.

(iii) If $D_{1i} < H_{\mathrm{T}} < D_{2i}$ and $D_{1i} \geq 0$, a shift in the scale parameter is indicated.

[12] By its design, the SEMLE-ChiMax chart is able to detect both increases and decreases in the location parameter, though only increases in the scale parameter. In this sense, it is not particularly different from numerous normal theory schemes which detect increases and decreases in the mean but only increases in the variance.

(iv) If D_{1i} and D_{2i} both exceed H_{T}, a shift in both the location and scale parameters is indicated.

(v) If $D_{2i} > H_{\mathrm{T}}$ and $D_{1i} < 0$, a shift in both the location and scale parameters is indicated.

4.4.2 Distribution of the Plotting Statistic for the SEMLE-ChiMax chart

For the SEMLE-ChiMax chart, the process is declared *OOC* when $\mathrm{T} \leq 0$ or $\mathrm{T} > H_{\mathrm{T}}$ where the *UCL* H_{T} is obtained so that the *IC ARL* is some given nominal value. D_1 and D_2 are independent because $\hat{\theta}_2$ and $\bar{V} - \hat{\theta}_2$ are, and as mentioned previously, both have the chi-square distribution with two degrees of freedom when the process is *IC*. The cdf of the plotting statistic T is given by

$$\begin{aligned}P(T \leq g \,\&\, D_1 > 0) &= P(\max\{ D_1, D_2\} \leq g \,\&\, D_1 > 0)\\ &= \left\{G\left[\frac{2n}{\lambda_2}\left(\frac{\lambda_0 g}{2n} + \theta_0 - \theta_2\right), 2\right] - G\left[\frac{2n}{\lambda_2}(\theta_0 - \theta_2), 2\right]\right\}\\ &\times \left\{G\left\{\frac{\lambda_0}{\lambda_2} G^{-1}[G(g,2), 2n-2], 2n-2\right\}\right\}.\end{aligned}$$ [13]

When the process is *IC*, the cdf of the plotting statistic T simplifies to $P(\mathrm{T} \leq g \,\&\, D_1 > 0|IC) = \{G(g,2)\}\{G(g,2)\} = \{G(g,2)\}^2$. The *IC ARL* is $\frac{1}{P(\mathrm{T}>g \text{ or } D_1 \leq 0)} = \frac{1}{1-\{G(g,2)\}^2}$. Thus, the *UCL* $H_{\mathrm{T}} = G^{-1}\left(\sqrt{1 - \frac{1}{IC\ ARL}}, 2\right)$.

[13] Further details are given in section C.4 of the Appendix.

4.5 The SEMVUE-Max Chart

Next, let $\tilde{\theta}_2 = \frac{nV_{(1)}-\bar{V}}{n-1}$ and $\tilde{\lambda}_2 = \frac{n(\bar{V}-V_{(1)})}{n-1}$. These are the minimum variance unbiased estimators for θ_2 and λ_2, respectively, though unlike $\hat{\theta}_2$ and $\hat{\lambda}_2$, they are not independent (Cohen and Helm, 1973). In fact, they have covariance $\frac{-\lambda^2}{n(n-1)}$. The distribution of $\tilde{\lambda}_2$ is clearly proportional to the distribution of $\hat{\lambda}_2$, so that $\frac{2(n-1)\tilde{\lambda}_2}{\lambda_2}$ has a chi-square distribution with $2n-2$ degrees of freedom. The distribution of $\tilde{\theta}_2$ is much more complicated to obtain, and we could find no references to it in the literature. However, using the Jacobian method (see Appendix C.1), we find that the joint distribution of $\tilde{\theta}_2$ and $\tilde{\lambda}_2$ is

$$f_{\tilde{\theta}_2,\tilde{\lambda}_2}(y_1, y_2) = \frac{n(n-1)^{n-1}}{\lambda_2^n \Gamma(n-1)} y_2^{n-2} e^{-\frac{n}{\lambda_2}(y_1+y_2-\theta_2)}, y_1 > \theta_2 - \frac{y_2}{n}, y_2 > 0.$$

It can easily be shown that $\int_0^\infty \int_{\theta_2-\frac{y_2}{n}}^\infty f_{\tilde{\theta}_2,\tilde{\lambda}_2}(y_1, y_2) dy_1 dy_2 = 1$. The marginal distributions can be obtained by integrating this pdf. Doing so, we confirm that $\frac{2(n-1)\tilde{\lambda}_2}{\lambda_2}$ has the distribution specified above. The pdf of $\tilde{\theta}_2$is

$$f_{\tilde{\theta}_2}(y_1) = \int_0^\infty \frac{n(n-1)^{n-1}}{\lambda_2^n \Gamma(n-1)} y_2^{n-2} e^{\frac{-n(y_2+y_1-\theta_2)}{\lambda_2}} dy_2\, I_{(\theta_2,\infty)}(y_1)$$
$$+ \int_{n(\theta_2-y_1)}^\infty \frac{n(n-1)^{n-1}}{\lambda_2^n \Gamma(n-1)} y_2^{n-2} e^{\frac{-n(y_2+y_1-\theta_2)}{\lambda_2}} dy_2\, I_{(-\infty,\theta_2]}(y_1).$$

The details of the derivations can be found in Appendix C.2. When $n = 5$, one can easily obtain the cdf,

$$F_{\tilde{\theta}_2}(y_1) = \begin{cases} .59 - \frac{256}{625}\left[e^{(5\theta_2-5y_1)/\lambda_2} - 1\right] & \theta_2 \le y_1 < \infty \\ a & -\infty < y_1 < \theta_2 \end{cases}$$

where $a = \frac{1}{375\lambda_2^3} e^{(20y_1 - 20\theta_2)/\lambda_2}[-100{,}000{y_1}^3 + 27{,}000\lambda_2{y_1}^2 + 300{,}000\theta_2{y_1}^2 - 300{,}000\theta_2^2 y_1 - 54{,}000\lambda_2\theta_2 y_1 - 3{,}660\lambda_2^2 y_1 + 100{,}000\theta_2^3 + 27{,}000\lambda_2\theta_2^2 + 3{,}660\lambda_2^2\theta_2 + 221.4\lambda_2^3]$, by integrating $f_{\tilde{\theta}_2}(y_1)$. It is easy to see that this distribution has two parameters, θ_2 and λ_2.

Now, let $C_1 = \Phi^{-1}\left\{G\left(\frac{2(n-1)\tilde{\lambda}_2}{\lambda_0}, 2n-2\right)\right\}$, and let $C_2 = \Phi^{-1}\{A(\tilde{\theta}_2, \theta_0, \lambda_0)\}$ where $A(.,\mathrm{a},\mathrm{b})$ denotes the cdf of $\tilde{\theta}_2, F_{\tilde{\theta}_2}(y_1)$, with parameters a and b. Note that both $C_1$and C_2 have a standard normal distribution when the process is *IC*. We will use these two statistics to construct the SEMVUE-Max chart.

4.5.1 Proposed Charting Procedure for the SEMVUE-Max chart

We propose the following method for constructing SEMVUE-Max charts when the location and scale parameters, θ_0 and λ_0, are known or specified:

Step 1. Let $Y_{i,n} = (Y_{i1}, Y_{i2}, \ldots, Y_{in})$ be the *i*th Phase II sample of size $n, i = 1,2,\ldots$

Step 2. Identify the $V's$ with the $Y's$. Calculate the statistics C_{1i} and C_{2i} for the ith test sample, for $i = 1,2,\ldots$

Step 3: Calculate the plotting statistic $\aleph_i = \max\{|C_{1i}|, |C_{2i}|\}$.[14]

Step 3. Plot $\aleph_i$ against a *UCL* $H_\aleph$. Note that $\aleph_i \geq 0$ by definition so that the *LCL* is 0 and that larger values of $\aleph_i$ suggest an *OOC* process.

Step 4. If $\aleph_i$ exceeds $H_\aleph$, the process is declared *OOC* at the *i*th test sample. If not, the process is considered to be *IC*, and testing continues to the next sample.

[14] Although C_1 and C_2 are correlated, the distribution of the plotting statistic can be obtain be using their joint distribution.

Step 5. Follow up: When the process is declared *OOC* at the *i*th test sample, compare each of $|C_{1i}|$ and $|C_{2i}|$ with $H_{\aleph}$.

(i) If $|C_{2i}| < H_{\aleph} < |C_{1i}|$, a shift in the location parameter is indicated.

(ii) If $|C_{1i}| < H_{\aleph} < |C_{2i}|$, a shift in the scale parameter is indicated.

(iii) If $|C_{1i}|$ and $|C_{2i}|$ both exceed $H_{\aleph}$, a shift in both the location and scale parameters is indicated.

4.5.2 Distribution of the Plotting Statistic for the SEMVUE-Max chart

For the SEMVUE-Max chart, the process is declared *OOC* when $\aleph > H_{\aleph}$ where the *UCL* $H_{\aleph}$ is obtained so that the *IC ARL* is some given nominal value. Note that C_1 and C_2 are not independent; however, both have the standard normal distribution when the process is in-control. The cumulative distribution function of the plotting statistic $\aleph$ is given by

$$P(\aleph \le g) = P(\max\{|C_{1i}|, |C_{2i}|\} \le g) = P\{(|C_{1i}| \le g)\,\&(|C_{2i}| \le g)\}$$

$$= \int_{\left[\frac{\lambda_0}{2(n-1)}G^{-1}(\Phi(-g),2n-2)\right]}^{\left[\frac{\lambda_0}{2(n-1)}G^{-1}(\Phi(g),2n-2)\right]} \int_{\theta_2}^{[A^{-1}(\Phi(g),\theta_0,\lambda_0)]} f_{\tilde{\theta}_2,\tilde{\lambda}_2}(y_1, y_2)dy_1dy_2$$

$$+ \int_{[A^{-1}(\Phi(-g),\theta_0,\lambda_0)]}^{\theta_2} \int_{n(\theta_2-y_1)}^{\left[\frac{\lambda_0}{2(n-1)}G^{-1}(\Phi(g),2n-2)\right]} f_{\tilde{\theta}_2,\tilde{\lambda}_2}(y_1, y_2)dy_2dy_1.$$

4.6 The SE-LR Chart

Since joint monitoring of the location and scale is analogous to repeatedly testing the null hypothesis that the sample at hand comes from a completely specified shifted exponential population (a simple null hypothesis) versus all alternatives (a composite alternative hypothesis), we also wish to consider a chart based upon the perspective of a likelihood ratio statistic. It can be shown (see the appendix) that the likelihood ratio statistic for the shifted exponential distribution is given by $\Lambda = e^n \left(\frac{\bar{V} - V_{(1)}}{\lambda_0}\right)^n \exp\{-n(\bar{V} - \theta_0)/\lambda_0\}$. This will be a plotting statistic used to define the SE-LR chart.

4.6.1 Proposed Charting Procedure for the SE-LR chart

We propose the following method for constructing SE-LR charts when the location and scale parameters, θ_0 and λ_0, are known or specified:

Step 1. Let $Y_{i,n} = (Y_{i1}, Y_{i2}, \dots, Y_{in})$ be the *i*th Phase II sample of size $n, i = 1,2, \dots$

Step 2. Identify the $V's$ with the $Y's$. Calculate the statistics Λ_i for the ith test sample, for $i = 1,2, \dots$

Step 3: Step 3. Plot Λ_i against a *LCL* H_Λ. Note that $\Lambda_i \leq 1$ by definition so that the *UCL* is 1 and that smaller values of Λ_i suggest an *OOC* process.

Step 4. If Λ_i is lower than H_Λ, the process is declared *OOC* at the *i*th test sample. If not, the process is considered to be *IC*, and testing continues to the next sample.

Step 5. Follow up: When the process is declared *OOC* at the *i*th test sample, calculate $\frac{2n(\hat{\theta}_2 - \theta_0)}{\lambda_0}$ and $\frac{2n\hat{\lambda}_2}{\lambda_0}$. When the process is *IC*, each has a chi-square distribution (with 2 and $2n - 2$ degrees of freedom, respectively). Let $p_1 = P[\chi^2_2 > \frac{2n(\hat{\theta}_2 - \theta_0)}{\lambda_0}]$ and $p_2 = P[\chi^2_{2n-2} > \frac{2n\hat{\lambda}_2}{\lambda_0}]$. Both can be obtained directly from a chi-square table.

(i) If both $p_1, p_2 < 0.01$, a shift in both the location and scale parameters is indicated.

(ii) If both $p_1, p_2 > 0.05$, a false alarm is indicated.

(iii) If $p_1 < 0.01$ and $p_2 > 0.05$, a shift in the location parameter is indicated.

(iv) If $p_2 < 0.01$ and $p_1 > 0.05$, a shift in the scale parameter is indicated.

(v) If $p_1 < 0.01$ and $0.01 \leq p_2 \leq 0.05$, a major shift in the location parameter with possible associated shift in the scale parameter is indicated.

(vi) If $p_2 < 0.01$ and $0.01 \leq p_1 \leq 0.05$, a major shift in the scale parameter with possible associated shift in the location parameter is indicated.

4.6.2 Distribution of the Plotting Statistic for the SE-LR chart

For the SE-LR chart, the process is declared *OOC* when $\Lambda < H_\Lambda$, where the *LCL* H_Λ is obtained so that the *IC ARL* is equal to some given nominal value. However, the distribution of Λ is rather intractable.

When m and n are large, it is useful to consider the asymptotic properties of Λ. Consider a function of Λ, $-2\ln\Lambda = -2\ln\left\{e^n\left(\frac{\bar{V}-V_{(1)}}{\lambda_0}\right)^n \exp\{-n(\bar{V}-\theta_0)/\lambda_0\}\right\}$. It can be shown (see for example Hogg, McKean and Craig (2005)) that $-2\ln\Lambda$ converges in distribution to a chi-square random variable with 2 degree of freedom. Using this property, it is simple to obtain H_Λ as long as m and n are appropriately large. However, when m and n are small or moderate as is typically the case in control charting, H_Λ can easily be obtained through Monte Carlo simulation.

4.7 The SEMLE-2 Scheme

Let $E_1 = \frac{2n(\hat{\theta}_2-\theta_0)}{\lambda_0}$ and $E_2 = \frac{2n\hat{\lambda}_2}{\lambda_0}$. Note that when the process is *IC*, both E_1 and E_2 have a chi-square distribution (with 2 and $2n-2$ degrees of freedom, respectively). These are the two statistics that we will use to construct the charts which make up the SEMLE-2 scheme.

4.7.1 Proposed Charting Procedure for the SEMLE-2 scheme

We propose the following method for constructing SEMLE-2 schemes when the location and scale parameters, θ_0 and λ_0, are known or specified:

Step 1. Let $Y_{i,n} = (Y_{i1}, Y_{i2}, \dots, Y_{in})$ be the *i*th Phase II sample of size $n, i = 1,2, \dots$

Step 2. Identify the $V's$ with the $Y's$. Calculate the plotting statistics E_{1i} and E_{2i} for the ith test sample, for $i = 1,2, \dots$. Note that if the process is *IC*, both of these quantities should be positive. If $E_{1i} \leq 0$, the process is declared *OOC* at the *i*th test sample. If $E_{1i} > 0$, continue to step 3.

Step 3. Plot E_{1i} against a *UCL* H_{E_1}. Note that the *LCL* is 0, and large values of E_{1i} suggest an *OOC* process.

Step 4. On a separate chart, plot E_{2i} against an *UCL* $H_{E_{2U}}$ and *LCL* $H_{E_{2L}}$.

Step 5. If E_{1i} is greater than $H_{E_1}$and/or E_{2i} is greater than $H_{E_{2U}}$or less than $H_{E_{2L},}$ the process is declared *OOC* at the *i*th test sample. If not, the process is considered to be *IC*, and testing continues to the next sample.

Step 6. Follow up: When the process is declared *OOC* at the *i*th test sample, compare E_{1i} with H_{E_1} and E_{2i} with $H_{E_{2U}}$ and $H_{E_{2L}}$.

(i) If $\mathrm{E}_{1i} > H_{E_1}$ and $H_{E_{2L}} < \mathrm{E}_{2i} < H_{E_{2U}}$, a shift in the location parameter is indicated.

(ii) If $H_{E_{2L}} < \mathrm{E}_{2i} < H_{E_{2U}}$ and $\mathrm{E}_{1i} < 0$, a shift in the location parameter is indicated.

(iii) If $\mathrm{E}_{2i} > H_{E_{2U}}$ and $0 < \mathrm{E}_{1i} < H_{E_1}$, a shift in the scale parameter is indicated.

(iv) If $\mathrm{E}_{2i} < H_{E_{2L}}$ and $0 < \mathrm{E}_{1i} < H_{E_1}$, a shift in the scale parameter is indicated

(v) If $\mathrm{E}_{1i} > H_{E_1}$ and $\mathrm{E}_{2i} > H_{E_{2U}}$, a shift in both the location and scale parameters is indicated.

(vi) If $\mathrm{E}_{1i} < 0$ and $\mathrm{E}_{2i} > H_{E_{2U}}$, a shift in both the location and scale parameters is indicated.

(vii) If $\mathrm{E}_{1i} > H_{E_1}$ and $\mathrm{E}_{2i} < H_{E_{2L}}$, a shift in both the location and scale parameters is indicated.

(viii) If $\mathrm{E}_{1i} < 0$ and $\mathrm{E}_{2i} < H_{E_{2L}}$, a shift in both the location and scale parameters is indicated.

4.7.2 Distribution of the Plotting Statistics for the SEMLE-2 scheme

The SEMLE-2 control scheme consists of two charts. The process is declared *OOC* whenever a signal occurs on either chart, that is, any time $\mathrm{E}_1 < 0$, $\mathrm{E}_1 > H_{E_1}$, $\mathrm{E}_2 > H_{E_{2U}}$, or $\mathrm{E}_2 < H_{E_{2L}}$ where the control limits H_{E_1}, $H_{E_{2U}}$, and $H_{E_{2L}}$ are obtained so that the *IC ARL* is some given nominal value. E_1 and E_2 are independent because $\hat{\theta}_2$ and $\bar{V} - \hat{\theta}_2$ are, and as mentioned previously, both have the chi-square distribution (with 2 and $2n - 2$ degrees of freedom, respectively) when the process is *IC*. The joint cumulative distribution function of the two plotting statistics E_1 and E_2 is given by

$$P[(0 < \mathrm{E}_1 \leq g_1) \,\&\, (g_2 \leq \mathrm{E}_2 \leq g_3)] = P(0 < \mathrm{E}_1 \leq g_1)P(g_2 \leq \mathrm{E}_2 \leq g_3)$$

$$= \left\{G\left[\frac{\lambda_0}{\lambda_2}(g_1) + \frac{2n(\theta_0 - \theta_2)}{\lambda_2}, 2\right] - G\left[\frac{2n(\theta_0 - \theta_2)}{\lambda_2}, 2\right]\right\}$$

$$\times \left\{G\left\{\frac{\lambda_0}{\lambda_2}(g_3), 2n - 2\right\} - G\left\{\frac{\lambda_0}{\lambda_2}(g_2), 2n - 2\right\}\right\}.$$

When the process is *IC*, the joint cumulative distribution function of the plotting statistics E_1 and E_2 simplifies to $P[(0 < \mathrm{E}_1 \leq g_1) \,\&\, (g_2 \leq \mathrm{E}_2 \leq g_3)] = \{G(g_1, 2)\}\{G(g_3, 2n - 2) - G(g_2, 2n - 2)\}$.

4.8 Implementation

In order to use the proposed charts, one must select the appropriate control limits for each corresponding to the desired nominal *IC ARL*. For several of the charts, this can be accomplished using the analytical expressions for the *IC ARL* given in the earlier sections. For the remaining charts, we use can obtain the control limits through simulation. Here, we used simulations in R to compute all of the control limits, and where possible we used the analytical expressions to verify the results. As expected, we find that higher nominal *ARL*s require higher *UCL*s and lower *LCL*s.

Table 4.1: Appropriate control limits for the shifted exponential charts when θ and λ are known and $n = 5$, for various *IC ARL*s

IC ARL	SEMLE-Max Chart *UCL*	SEMVUE-Max Chart *UCL*	SEMLE-ChiMax Chart *UCL*	SE-LR Chart *LCL*	SEMLE-2 Scheme (Location Chart *UCL*/ Scale Chart *UCL*/ Scale Chart *LCL*)
125	2.88	2.82	11.04	0.000899	11.04/ 24.35/1.04
250	3.09	3.02	12.43	0.000365	12.43/ 26.12/0.86
500	3.29	3.20	13.82	0.000154	13.82/ 27.87/0.71
750	3.40	3.29	14.63	0.0000929	14.63/ 28.88/0.64
1000	3.48	3.35	15.20	0.0000659	15.20/ 29.59/0.59

4.9 Performance Comparisons

The performance of the four one-chart schemes and the two-chart SEMLE-2 scheme for various location and scale shifts is evaluated in a simulation study so that they can easily be compared. Tables 4.2, 4.3, and 4.4 provide the ARL, run length standard deviation, and specified quantiles of the run length distribution when $n = 5$. We use $\theta = 0$ and $\lambda = 1$ for our *IC* shifted exponential distribution.

Table 4.2: Run length characteristics for the SEMLE-Max and SEMVUE-Max charts for various values of θ_2 and λ_2 when $\theta_0 = 0$, $\lambda_0 = 1$, and $n = 5$

		SEMLE-Max Chart			***SEMVUE-Max Chart***		
θ_2	λ_2	*ARL*	*SDRL*	*5%, 25%, 50%, 75%, 95%*	*ARL*	*SDRL*	*5%, 25%, 50%, 75%, 95%*
0	*1*	**498.67**	498.85	26, 142, 346, 696, 1492	**500.81**	502.66	27, 144, 347, 692, 1514
0.1	*1*	**539.96**	539.34	26, 155, 374, 748, 1603	**546.42**	536.07	28, 163, 387, 758, 1627
0.25	*1*	**359.83**	355.74	20, 106, 251, 501, 1062	**420.43**	421.85	23, 122, 288, 582,1274
0.5	*1*	**141.72**	140.99	8, 41, 98, 198, 420	**205.33**	204.97	10, 59, 143, 285, 614
0.75	*1*	**44.50**	43.45	3, 13, 31, 61, 132	**73.96**	73.65	4, 22, 52, 102, 223
1	*1*	**13.23**	12.53	1, 4, 9, 18, 38	**22.74**	22.08	2, 7, 16, 31, 66
1.25	*1*	**3.77**	3.28	1, 1, 3, 5, 10	**6.68**	6.27	1, 2, 5, 9, 19
1.5	*1*	**1.10**	0.33	1, 1, 1, 1, 2	**1.93**	1.34	1, 1, 1, 2, 5
0	*1.25*	**136.85**	135.79	8, 40, 96, 191, 398	**115.85**	117.50	6, 33, 79, 158, 357
0.1	*1.25*	**126.36**	125.17	7, 37, 88, 176, 373	**132.52**	131.14	8, 39, 92, 183, 390
0.25	*1.25*	**91.62**	91.17	5, 27, 64, 125, 274	**109.23**	108.99	6, 32, 76, 150, 327
0.5	*1.25*	**46.44**	45.49	3, 14, 32, 65, 138	**67.51**	66.81	4, 18, 47, 94, 200
0.75	*1.25*	**19.91**	19.79	1, 6, 14, 27, 58	**32.10**	31.60	2, 10, 23, 44, 95
1	*1.25*	**7.78**	7.26	1, 3, 6, 11, 22	**13.58**	13.11	1, 4, 10, 19, 39
1.25	*1.25*	**2.91**	2.38	1, 1, 2, 4, 8	**5.29**	4.73	1, 2, 4, 7, 15
1.5	*1.25*	**1.09**	0.30	1, 1, 1, 1, 2	**2.00**	1.42	1, 1, 1, 3, 5
0	*1.5*	**41.88**	41.04	3, 12, 29, 58, 122	**36.63**	36.16	2, 11, 25, 51, 107
0.1	*1.5*	**39.08**	37.44	3, 12, 28, 55, 115	**39.03**	39.10	3, 11, 27, 54. 116
0.25	*1.5*	**31.76**	31.54	2, 9, 22, 44, 94	**35.10**	34.74	2, 10, 24, 49, 105
0.5	*1.5*	**19.78**	19.22	1, 6, 14, 28, 59	**26.26**	25.65	2, 8, 19, 36, 76
0.75	*1.5*	**10.91**	10.33	1, 4, 8, 15, 32	**16.69**	16.19	1, 5, 11, 23, 49
1	*1.5*	**5.26**	4.67	1, 2, 4, 7, 14	**8.88**	8.38	1, 3, 6, 12, 26
1.25	*1.5*	**2.37**	1.79	1, 1, 2, 3, 6	**4.37**	3.86	1, 2, 3, 6, 12
1.5	*1.5*	**1.06**	0.26	1, 1, 1, 1, 2	**2.01**	1.43	1, 1, 2, 3, 5
0	*1.75*	**17.83**	17.43	1, 5, 12, 24, 53	**16.15**	15.58	1, 5, 11, 22, 47
0.1	*1.75*	**16.58**	16.00	1, 5, 12, 23, 48	**16.87**	16.37	1, 5, 12, 23, 49
0.25	*1.75*	**14.44**	13.92	1, 5, 10, 20, 42	**15.57**	14.90	1, 5, 11 , 22, 46
0.5	*1.75*	**10.31**	9.73	1, 3, 7, 14, 30	**12.89**	12.31	1, 4, 9, 18, 37
0.75	*1.75*	**6.76**	6.30	1, 2, 5, 9, 19	**9.57**	9.08	1, 3, 7, 13, 27
1	*1.75*	**3.85**	3.28	1, 1, 3, 5, 10	**6.27**	5.74	1, 2, 4, 9, 18
1.25	*1.75*	**2.10**	1.52	1, 1, 2, 3, 5	**3.60**	3.04	1, 1, 3, 5, 10
1.5	*1.75*	**1.05**	0.24	1, 1, 1, 1, 2	**1.95**	1.37	1 , 1, 1, 2, 5
0	*2*	**9.75**	9.26	1, 3, 7, 13, 28	**8.92**	8.34	1, 3, 6, 12, 25
0.1	*2*	**9.16**	8.60	1, 3, 7, 12, 27	**9.28**	8.76	1, 3, 7, 13, 27
0.25	*2*	**8.15**	7.71	1, 3, 6, 11, 24	**8.73**	8.14	1, 3, 6, 12, 25
0.5	*2*	**6.47**	5.97	1, 2, 5, 9, 18	**7.66**	7.08	1, 3, 5, 10, 22
0.75	*2*	**4.62**	4.04	1, 2, 3, 6, 13	**6.13**	5.55	1, 2, 4, 8, 17
1	*2*	**3.00**	2.44	1, 1, 2, 4, 8	**4.50**	3.96	1, 2, 3, 6, 12
1.25	*2*	**1.81**	1.20	1, 1, 1, 2, 4	**2.97**	2.46	1, 1, 2, 4, 8
1.5	*2*	**1.05**	0.22	1, 1, 1, 1, 1	**1.85**	1.25	1, 1, 1, 2, 4

Table 4.3: Run length characteristics for the SE-LR and SEMLE-ChiMax charts for various values of θ_2 and λ_2 when $\theta_0 = 0$, $\lambda_0 = 1$, and $n = 5$

		SE-LR Chart			*SEMLE-ChiMax Chart*		
θ_2	λ_2	*ARL*	*SDRL*	*5%, 25%, 50%, 75%, 95%*	*ARL*	*SDRL*	*5%, 25%, 50%, 75%, 95%*
0	*1*	**506.65**	512.37	27, 143, 350, 697, 1519	**499.21**	500.19	26, 141, 346, 696, 1505
0.1	*1*	**339.11**	332.76	19, 101, 235 , 473, 1009	**380.14**	381.13	20, 110, 263, 528, 1144
0.25	*1*	**193.34**	192.78	10, 57, 134, 267, 579	**223.61**	222.46	12, 66, 156, 310, 668
0.5	*1*	**71.55**	71.35	4, 21, 49, 99, 213	**75.61**	74.73	4, 22, 53, 105, 223
0.75	*1*	**27.25**	26.18	2, 8, 19, 38, 80	**22.83**	22.45	2, 7, 16, 31, 68
1	*1*	**10.70**	10.15	1, 3, 8, 15, 31	**6.79**	6.23	1, 2, 5, 9, 19
1.25	*1*	**4.35**	3.74	1, 2, 3, 6, 12	**1.93**	1.34	1, 1, 1, 2, 5
1.5	*1*	**1.84**	1.26	1, 1, 1, 2, 4	**1**	0	1, 1, 1, 1, 1
0	*1.25*	**323.75**	322.02	18, 94, 224, 451, 974	**87.35**	86.78	5, 26, 61, 121, 260
0.1	*1.25*	**222.41**	219.80	11, 65, 156, 311, 666	**74.33**	74.41	4, 21, 52, 102, 225
0.25	*1.25*	**127.88**	126.77	7, 37, 90, 177, 380	**55.23**	55.15	3, 16 , 38, 77, 165
0.5	*1.25*	**51.51**	50.91	3, 15, 36, 71, 153	**27.10**	26.63	2, 8, 19, 37, 81
0.75	*1.25*	**20.79**	20.07	2, 6, 15, 29, 61	**11.60**	11.07	1, 4, 8, 16, 34
1	*1.25*	**8.76**	8.18	1, 3, 6, 12, 25	**4.49**	3.96	1, 2, 3, 6, 12
1.25	*1.25*	**3.81**	3.27	1, 1, 3, 5, 10	**1.68**	1.07	1, ,1, 1, 2, 4
1.5	*1.25*	**1.74**	1.16	1, 1, 1, 2, 4	**1**	0	1, 1, 1, 1, 1
0	*1.5*	**120.79**	119.82	7, 36, 84, 168, 362	**27.76**	27.20	2, 8, 19, 38, 82
0.1	*1.5*	**88.77**	87.67	5, 25, 62, 124, 264	**25.54**	24.97	2, 8, 18, 35, 75
0.25	*1.5*	**54.74**	54.61	3, 16, 37, 76, 166	**20.78**	20.35	2, 6, 14, 29, 62
0.5	*1.5*	**26.50**	26.16	2, 8, 18, 36, 78	**12.90**	12.44	1, 4, 9, 18, 37
0.75	*1.5*	**12.63**	12.20	1, 4, 9, 17, 37	**6.89**	6.33	1, 2, 5, 9, 20
1	*1.5*	**6.01**	5.50	1, 2, 4, 8, 17	**3.34**	2.75	1, 1, 2, 4, 9
1.25	*1.5*	**2.96**	2.44	1, 1, 2, 4, 8	**1.53**	0.91	1, 1, 1, 2, 3
1.5	*1.5*	**1.56**	0.93	1, 1, 1, 2, 3	**1**	0	1, 1, 1, 1, 1
0	*1.75*	**47.55**	46.74	3, 14, 34, 65, 139	**12.65**	12.09	1, 4, 9, 17, 37
0.1	*1.75*	**36.34**	35.58	2, 11, 26, 50, 106	**11.79**	11.23	1, 4, 8, 16, 34
0.25	*1.75*	**25.08**	25.28	2, 7, 17, 34, 76	**10.19**	9.67	1, 3, 7, 14, 29
0.5	*1.75*	**13.28**	12.54	1, 4, 9, 18, 39	**7.36**	6.87	1, 2, 5, 10, 21
0.75	*1.75*	**7.29**	6.85	1, 2, 5, 10, 21	**4.70**	4.15	1, 2, 3, 6, 13
1	*1.75*	**4.14**	3.62	1, 2, 3, 5, 11	**2.68**	2.15	1, 1, 2, 3, 7
1.25	*1.75*	**2.36**	1.78	1, 1, 2, 3, 6	**1.43**	0.78	1, 1, 1, 2, 3
1.5	*1.75*	**1.42**	0.78	1, 1, 1, 2, 3	**1**	0	1, 1, 1, 1, 1
0	*2*	**22.57**	21.97	2, 7, 16, 31, 66	**7.24**	6.78	1, 2, 5, 10, 21
0.1	*2*	**17.85**	17.24	1, 6, 12, 25, 52	**6.85**	6.38	1, 2, 5, 9, 19
0.25	*2*	**13.14**	12.64	1, 4, 9, 18, 38	**6.16**	5.60	1, 2, 4, 8, 17
0.5	*2*	**7.94**	7.51	1, 3, 6, 11, 23	**4.81**	4.27	1, 2, 3, 6, 13
0.75	*2*	**4.86**	4.31	1, 2, 4, 7, 13	**3.45**	2.90	1, 1, 3, 5, 9
1	*2*	**3.01**	2.47	1, 1, 2, 4, 8	**2.22**	1.64	1, 1, 2, 3, 6
1.25	*2*	**1.93**	1.34	1, 1, 1, 2, 5	**1.33**	0.67	1, 1, 1, 1, 3
1.5	*2*	**1.31**	0.64	1, 1, 1, 1, 3	**1**	0	1, 1, 1, 1, 1

Table 4.4: Run length characteristics for the SEMLE-2 scheme for various values of θ_2 and λ_2 when $\theta_0 = 0$, $\lambda_0 = 1$, and $n = 5$

		SEMLE-2 Scheme		
θ_2	*λ_2*	*ARL*	*SDRL*	*5%, 25%, 50%, 75%, 95%*
0	*1*	**503.12**	503.82	26, 145, 350, 696, 1510
0.1	*1*	**380.19**	380.06	20, 109, 264, 526, 1135
0.25	*1*	**222.28**	221.88	12, 64, 154, 308, 667
0.5	*1*	**76.28**	75.72	4, 22, 53, 105, 228
0.75	*1*	**23.09**	22.62	2, 7, 16, 32, 68
1	*1*	**6.71**	6.21	1, 2, 5, 9, 19
1.25	*1*	**1.93**	1.33	1, 1, 1, 2, 5
1.5	*1*	**1**	0	1, 1, 1, 1, 1
0	*1.25*	**116.35**	115.47	7, 34, 81, 161, 347
0.1	*1.25*	**95.83**	95.58	6, 28, 66, 132, 286
0.25	*1.25*	**65.14**	64.95	4, 19, 45, 90, 194
0.5	*1.25*	**29.49**	29.02	2, 9, 21, 41, 87
0.75	*1.25*	**11.88**	11.37	1, 4, 8, 16, 35
1	*1.25*	**4.54**	4.03	1, 2, 3, 6, 13
1.25	*1.25*	**1.69**	1.08	1, 1, 1, 2, 4
1.5	*1.25*	**1**	0	1, 1, 1, 1, 1
0	*1.5*	**36.70**	36.26	2, 11, 25, 51, 109
0.1	*1.5*	**32.23**	31.69	2, 10, 23, 44, 96
0.25	*1.5*	**24.99**	24.49	2, 8, 17, 34, 74
0.5	*1.5*	**14.44**	13.92	1, 5, 10, 20, 42
0.75	*1.5*	**7.31**	6.79	1, 2, 5, 10, 21
1	*1.5*	**3.41**	2.85	1, 1, 3, 5, 9
1.25	*1.5*	**1.54**	0.91	1, 1, 1, 2, 3
1.5	*1.5*	**1**	0	1, 1, 1, 1, 1
0	*1.75*	**16.12**	15.60	1, 5, 11, 22, 47
0.1	*1.75*	**14.65**	14.07	1, 5, 10, 20, 43
0.25	*1.75*	**12.27**	11.70	1, 4, 9, 17, 36
0.5	*1.75*	**8.29**	7.76	1, 3, 6, 11, 24
0.75	*1.75*	**4.99**	4.46	1, 2, 4, 7, 14
1	*1.75*	**2.74**	2.19	1, 1, 2, 4, 7
1.25	*1.75*	**1.43**	0.78	1, 1, 1, 2, 3
1.5	*1.75*	**1**	0	1, 1, 1, 1, 1
0	*2*	**8.90**	8.42	1, 3, 6, 12, 26
0.1	*2*	**8.25**	7.71	1, 3, 6, 11, 24
0.25	*2*	**7.32**	6.77	1, 2, 5, 10, 21
0.5	*2*	**5.40**	4.89	1, 2, 4, 7, 15
0.75	*2*	**3.68**	3.12	1, 1, 3, 5, 10
1	*2*	**2.29**	1.71	1, 1, 2, 3, 6
1.25	*2*	**1.35**	0.68	1, 1, 1, 2, 3
1.5	*2*	**1**	0	1, 1, 1, 1, 1

From the Table 4.2, it is seen that the SEMLE-Max chart exhibits reasonably good performance for detecting shifts in parameters of processes with shifted exponential distributions. There is one noticeable defect in the performance of the SEMLE-Max chart, however. In the second line of the table, we see that when $n = 5$ and there is a location shift of 0.1 but no variance shift, the resulting *ARL* is approximately 539.96, a value larger than the *IC ARL* of 500. This suggests than when a very small location shift occurs and is not accompanied by a variance shift, the chart is unable to detect it and that the *OOC ARL* may actually be higher than the *IC ARL*. To see this mathematically, note that when $n = 5$, $\theta_2 = 0.1$, and $\lambda_2 = 1$, the probability of exceeding the *UCL* $H_{\mathcal{M}} = 3.29$ is $P(\mathcal{M} > 3.29) = 1 - P(\mathcal{M} \leq 3.29) = 0.00182695$. The *OOC ARL* is simply is $\frac{1}{P(\mathcal{M}>3.29)} = 547.36$.

To investigate this issue more carefully, we took a closer look at the relationship between the sample size (n), location shift, and *OOC ARL* for the SEMLE-Max chart. Table 4.5 provides the run length characteristics for several very small locations shifts (0.01 to 0.20) at various sample sizes (5, 10, and 30). From this table, we see that the larger the sample size, the smaller the shift size that the chart can correctly detect. For example, when $n = 5$, the chart is unable to detect shifts of size 0.1; however, shifts of this size can be detected when $n = 10$ or 30. Moreover, when $n = 10$, the chart is unable to detect shift of size 0.07 or smaller, though the chart can detect shifts as small as 0.03 when $n = 30$.

The bias can be investigated mathematically as well. From section C.5 in the Appendix, it can be seen that when $\theta_0 = 0$ and $\lambda_0 = 1$ and there has been a shift in the location parameter but not in the scale parameter, bias occurs when $0 < \theta_2 < \frac{G^{-1}(\Phi(g),2) - G^{-1}\{\Phi(g) - \Phi(-g),2\}}{2n}$.

Table 4.5: Run length characteristics for the SEMLE-Max chart for small location shifts not accompanied by scale shifts for various values n

		$n = 5$			$n = 10$			$n = 30$		
μ_2	σ_2	*ARL*	*SDRL*	*5%, 25%, 50%, 75%, 95%*	*ARL*	*SDRL*	*5%, 25%, 50%, 75%, 95%*	*ARL*	*SDRL*	*5%, 25%, 50%, 75%, 95%*
0	*1*	**501.37**	494.70	27, 144, 350, 697, 1470	**500.53**	498.97	26, 141, 350, 696, 1507	**500.36**	511.14	26, 140, 338, 683, 1522
0.01	*1*	**648.37**	644.33	33, 188, 452, 890, 1960	**636.76**	627.98	32, 183, 445, 879, 1907	**590.84**	588.61	30, 173, 410, 821, 1745
0.02	*1*	**644.45**	636.15	33, 191, 454, 895, 1925	**618.29**	619.69	31, 180, 421, 861, 1890	**513.70**	507.97	28, 154, 355, 711, 1543
0.03	*1*	**632.52**	633.83	32, 181, 436, 879, 1923	**604.33**	600.88	31, 177, 417, 836, 1838	**448.09**	453.89	23, 126, 310, 624, 1342
0.04	*1*	**621.79**	613.15	32, 177, 433, 865, 1853	**581.69**	585.36	31, 168, 400, 806, 1745	**376.58**	371.10	20, 110, 267, 523, 1113
0.05	*1*	**600.82**	597.19	33, 174, 422, 824, 1794	**544.19**	541.55	32, 159, 379, 762, 1612	**309.70**	307.00	17, 89, 215, 428, 926
0.06	*1*	**598.68**	593.15	31, 173, 425, 823, 1765	**518.57**	519.68	28, 148, 364, 721, 1538	**249.18**	246.86	12, 71, 173, 347, 741
0.07	*1*	**585.90**	579.16	32, 175, 409, 814, 1742	**501.03**	496.67	26, 145, 352, 697, 1498	**198.89**	192.90	11, 60, 141, 275, 582
0.08	*1*	**580.14**	584.88	31, 165, 401, 812, 1688	**477.05**	482.54	23, 133, 325, 668, 1450	**151.56**	152.43	9, 45, 104, 207, 463
0.09	*1*	**564.78**	560.18	29, 167, 399, 781, 1688	**447.53**	446.84	22, 127, 308, 620, 1367	**120.69**	119.44	6, 36, 84, 167, 362
0.10	*1*	**562.28**	558.75	30, 165, 396, 772, 1679	**426.39**	426.90	21, 118, 295, 596, 1273	**90.15**	90.19	5, 26, 62, 125, 266
0.11	*1*	**540.47**	545.22	27, 155, 367, 750, 1619	**399.56**	398.30	21, 117, 275, 561, 1184	**69.26**	68.69	4, 20, 48, 97, 206
0.12	*1*	**520.79**	522.69	27, 151, 361, 722, 1556	**374.68**	369.67	20, 111, 261, 517, 1105	**52.25**	51.72	3, 15, 36, 72, 155
0.13	*1*	**504.78**	497.85	26, 147, 348, 705, 1511	**349.48**	353.88	19, 97, 240, 480, 1052	**38.64**	38.37	2, 12, 27, 53, 117
0.14	*1*	**495.53**	494.49	26, 144, 346, 686, 1475	**334.09**	336.77	17, 95, 232, 460, 989	**29.42**	2903	2, 9, 21, 40, 88
0.15	*1*	**486.74**	486.70	26, 139, 339, 675, 1454	**310.04**	306.24	16, 91, 216, 430, 922	**21.70**	21.66	2, 6, 15, 30, 64
0.16	*1*	**479.55**	481.31	24, 138, 328, 668, 1455	**289.49**	287.69	16, 83, 200, 406, 876	**16.06**	15.64	1, 5, 11, 22, 47
0.17	*1*	**464.77**	464.45	23, 133, 329, 646, 1391	**269.29**	268.08	14, 80, 188, 373, 795	**11.85**	11.46	1, 4, 8, 16, 34
0.18	*1*	**443.43**	443.37	22, 127, 304, 617, 1336	**247.75**	247.94	14, 72, 169, 346, 749	**8.97**	8.50	1, 3, 6, 12, 26
0.19	*1*	**432.65**	429.44	22, 128, 302, 600, 1270	**228.35**	223.49	12, 67, 164, 318, 670	**6.63**	6.08	1, 2, 5, 9, 19
0.20	*1*	**425.15**	423.35	23, 123, 298, 597, 1270	**211.88**	211.27	10, 60, 145, 296, 646	**4.89**	4.35	1, 2, 3, 7, 14

As noted by Acosta-Meija (1998), “a desired feature is to have all of [the control chart’s] out-of-control *ARL* values smaller than the in-control *ARL*.” Charts which have this property are called *ARL*-unbiased. Charts like the SEMLE-Max Chart, in which the *OOC ARL* is larger than the *IC ARL* for certain shift sizes, are called *ARL*-biased.

The presence of this undesirable quality might lead us to question whether it was caused by the use of biased estimators for the location and scale parameters. However, Table 4.2 shows us that the SEMVUE-Max chart, which is composed of unbiased estimators, is also *ARL*-biased. Furthermore, the SEMVUE-Max chart typically performs more poorly than the SEMLE-Max chart. Given its generally poor performance, the SEMVUE-Max will not be considered further in this paper.

The SEMLE-ChiMax chart, on the other hand, is not *ARL*-biased for detecting changes in the location parameter and increases in the scale parameter, and it substantially out-performs the other charts except when there is a small location shift (≤ 0.5) which is not accompanied by a mean shift. It seems likely, then, that the bias is a result of using the probability integral transform to put the location and scale estimates on the normal scale.

The SE-LR chart is also *ARL*-unbiased, but it has worse performance for nearly every shift size than does the SEMLE-ChiMax chart. It also performs worse than the SEMLE-Max chart whenever a shift in variance occurs. In many cases, its performance is also worse than that of the SEMVUE-Max chart.

The SEMLE-ChiMax chart has the best overall performance among the one-chart schemes, in addition to its favorable quality of *ARL*-unbiasedness. Note, however, that unlike the other charts discussed, this chart is not suitable for detecting decreases in the scale parameter.[15] If detection of this type of change is desirable, the practitioner should use another chart. The SEMLE-2 scheme is a promising alternative. In general, it has the second-best performance among the charts considered and can detect both increases and decreases in both parameters. The SEMLE-2 scheme is also *ARL*-unbiased for increases in the parameters; however, note that it exhibits bias for small decreases in the scale parameter which are accompanied by small or no changes in the location parameter.

4.10 Performance Comparisons versus Normal Theory Charts

It is of interest to determine whether the proposed charts perform better for process data from a shifted exponential distribution than would normal theory charts. Here, we consider the

[15] It is not uncommon for control charts to be ineffective for detecting decreases in scale parameters. For example, a number of normal theory charts are useful only for detecting increases in the variance.

performance of two normal theory charts for various location and scale shifts and sample sizes. The *UCL*s for the normal theory charts must be selected so that they have a specified nominal *IC ARL*. For $n = 5$, the appropriate *UCL* for the normal theory max chart is 3.29. Table 4.6 provides the *ARL*, run length standard deviation, and specified quantiles of the run length distribution. Note that the underlying distribution of the process data is shifted exponential. We again use $\theta = 0$ and $\lambda = 1$ for our *IC* shifted exponential distribution. The mean of the distribution is $\theta + \lambda$, and its variance is λ^2 (Johnson and Kotz, 1970). In other words, the mean and variance of our I*C* distribution are both 1, and these are values to which the normal theory max and distance charts will compare the sample means and variances.

At first glance, one might note that Chen and Cheng's (1998) normal theory Max chart and Ramzy's (2005) Distance chart have shorter *ARL*s than the shifted exponential charts explored above and conclude that they are preferable. However, note that the *IC ARL*s for the normal theory charts are far lower than the nominal value of 500. This means that the charts will have an unacceptably high number of false alarms, rendering them virtually useless for monitoring this type of process.

Table 4.6: Run length characteristics for normal theory charts applied to shifted exponential data for various values of θ_2 and λ_2 when $\theta_1 = 0$, $\lambda_1 = 1$, and $n = 5$

		Normal Theory Max Chart			Normal Theory Distance Chart		
θ_2	λ_2	ARL	SDRL	5%, 25%, 50%, 75%, 95%	ARL	SDRL	5%, 25%, 50%, 75%, 95%
0	1	**37.38**	37.15	2, 11, 26, 51, 110	**20.43**	19.74	2, 7, 14, 28, 59
0.1	1	**35.17**	34.92	2, 10, 25, 49, 105	**19.51**	19.11	1, 6, 14, 27, 57
0.25	1	**30.88**	30.50	2, 9, 22, 43, 92	**17.07**	16.30	1, 5, 12, 24, 49
0.5	1	**21.78**	21.19	2, 7, 15, 30, 63	**12.97**	12.21	1, 4, 9, 18, 37
0.75	1	**12.55**	12.17	1, 4, 9, 17, 37	**8.27**	7.57	1, 3, 6, 11, 24
1	1	**6.72**	6.15	1, 2, 5, 9, 19	**5.19**	4.67	1, 2, 4, 7, 14
1.25	1	**3.58**	3.09	1, 1, 3, 5, 10	**2.99**	2.48	1, 1, 2, 4, 8
1.5	1	**2.12**	1.51	1, 1, 2, 3, 5	**1.77**	1.18	1, 1, 1, 2, 4
0	1.25	**14.20**	13.59	1, 5, 10, 20, 41	**9.18**	8.60	1, 3, 6, 13, 27
0.1	1.25	**13.19**	12.56	1, 4, 9, 18, 38	**8.31**	7.71	1, 3, 6, 11, 23
0.25	1.25	**11.32**	10.88	1, 4, 8, 15, 34	**7.14**	6.47	1, 2, 5, 10, 20
0.5	1.25	**7.88**	7.41	1, 3, 6, 11, 22	**5.41**	4.88	1, 2, 4, 7, 15
0.75	1.25	**5.15**	4.59	1, 2, 4, 7, 14	**3.91**	3.42	1, 1, 3, 5, 11
1	1.25	**3.32**	2.76	1, 1, 2, 4, 9	**2.80**	2.26	1, 1, 2, 4, 7
1.25	1.25	**2.17**	1.58	1, 1, 2, 3, 5	**1.97**	1.39	1, 1, 1, 2, 5
1.5	1.25	**1.52**	0.89	1, 1, 1, 2, 3	**1.40**	0.76	1, 1, 1, 2, 3
0	1. 5	**7.00**	6.50	1, 2, 5, 9, 20	**4.92**	4.43	1, 2, 4, 7, 14
0.1	1.5	**6.43**	6.02	1, 2, 5, 9, 18	**4.55**	4.04	1, 2, 3, 6, 13
0.25	1.5	**5.52**	4.97	1, 2, 4, 7, 16	**3.94**	3.36	1, 1, 3, 5, 11
0.5	1.5	**4.18**	3.64	1, 2, 3, 6, 11	**3.16**	2.60	1, 1, 2, 4, 8
0.75	1.5	**3.02**	2.50	1, 1, 2, 4, 8	**2.53**	1.95	1, 1, 2, 3, 6
1	1.5	**2.16**	1.60	1, 1, 2, 3, 5	**1.92**	1.34	1, 1, 1, 2, 5
1.25	1.5	**1.61**	1.00	1, 1, 1, 2, 4	**1.54**	0.91	1, 1, 1, 2, 3
1.5	1.5	**1.30**	0.64	1, 1, 1, 1, 3	**1.22**	0.51	1, 1, 1, 1, 2
0	1.75	**4.23**	3.63	1, 2, 3, 6, 12	**3.18**	2.63	1, 1, 2, 4, 8
0.1	1.75	**3.96**	3.48	1, 1, 3, 5, 11	**3.02**	2.44	1, 1, 2, 4, 8
0.25	1.75	**3.52**	2.94	1, 1, 3, 5, 10	**2.68**	2.14	1, 1, 2, 3, 7
0.5	1.75	**2.80**	2.23	1, 1, 2, 4, 7	**2.25**	1.67	1, 1, 2, 3, 6
0.75	1.75	**2.17**	1.58	1, 1, 2, 3, 5	**1.85**	1.24	1, 1, 1, 2, 4
1	1.75	**1.67**	1.05	1, 1, 1, 2, 4	**1.55**	0.93	1, 1, 1, 2, 3
1.25	1.75	**1.38**	0.72	1, 1, 1, 2, 3	**1.32**	0.65	1, 1, 1, 1, 3
1.5	1.75	**1.18**	0.46	1, 1, 1, 1, 2	**1.14**	0.39	1, 1, 1, 1, 2
0	2	**2.99**	2.46	1, 1, 2, 4, 8	**2.36**	1.79	1, 1, 2, 3, 6
0.1	2	**2.76**	2.19	1, 1, 2, 4, 7	**2.24**	1.67	1, 1, 2, 3, 6
0.25	2	**2.53**	1.98	1, 1, 2, 3, 7	**2.07**	1.49	1, 1, 2, 3, 5
0.5	2	**2.11**	1.52	1, 1, 2, 3, 5	**1.79**	1.19	1, 1, 1, 2, 4
0.75	2	**1.72**	1.13	1, 1, 1, 2, 3	**1.56**	0.92	1, 1, 1, 2, 3
1	2	**1.43**	0.78	1, 1, 1, 2, 3	**1.35**	0.69	1, 1, 1, 2, 3
1.25	2	**1.25**	0.57	1, 1, 1, 1, 2	**1.20**	0.49	1, 1, 1, 1, 2
1.5	2	**1.11**	0.36	1, 1, 1, 1, 2	**1.09**	0.31	1, 1, 1, 1, 2

4.11 Summary and Conclusions

Monitoring the location and scale parameters of a shifted exponential distribution is an important problem in statistical process control. This chapter provides some possibilities for monitoring data from a known shifted exponential distribution, of which the SEMLE-ChiMax chart and the SEMLE-2 scheme appear to be the most promising. However, much more work in this area is needed. In particular, these charts are only suitable for sample sizes larger than 1, since they rely on statistics which are functions of order statistics. Additionally, these charts are suitable only for Case K, and their performance may be degraded significantly if the parameters are estimated from a Phase I sample. Finally, the adaptation of these charts for Case U is not straightforward.

CHAPTER 5

CONTROL CHARTS FOR SIMULTANEOUS MONITORING OF KNOWN LOCATION AND SCALE PARAMETERS OF PROCESSES FOLLOWING A LAPLACE DISTRIBUTION

5.1 Introduction

The Laplace, or double exponential, distribution is the appropriate statistical model in a variety of circumstances. Suppose, for example, that some process arises as the difference between two exponential distributions with a common scale, such as flood levels at different points along a river. Then the difference follows a Laplace distribution (Puig and Stephens, 2000; Bain and Engelhardt, 1973). This distribution also has applications for modeling measurement error and financial data (Kotz, Kozubowski, and Podgórski, 2001).

The Laplace distribution has pdf $\frac{1}{2b}e^{-|x-a|/b}$, for $-\infty < \mathrm{x} < \infty, -\infty < \mathrm{a} < \infty$, and $\mathrm{b} > 0.$ It is similar to the normal distribution in the sense that it is symmetric, yet the distributions also differ greatly. In Chapter 3, it was demonstrated that case U charts for the normal distribution do not perform well when the underlying data actually have a Laplace distribution. The Laplace distribution is heavier-tailed than the normal, and it has a sharp peak rather than a gentle curve in the center. The difference in its tails, in particular, makes the development of charts for Laplace data essential.

There are a number of possible approaches to monitoring processes which follow a Laplace distribution, including exploiting the distribution's relationship to the exponential and chi-square distributions and monitoring the location and scale parameters directly using a max-type chart designed specifically for the Laplace. Here, we discuss and compare several possibilities for one-chart schemes for jointly monitoring the parameters of this distribution. First, we propose a joint monitoring scheme similar to the max charts we have discussed for the normal and shifted exponential distributions. This scheme, known as the Laplace MLE Max (LapMLE-Max) chart, transforms the estimators for each parameter so that they each have the standard normal distribution and then combines them together using a max function. Next, we consider a chart known as the Laplace/Chi-square (LapChi) chart which utilizes the relationship between the Laplace and chi-square distributions. Third, we consider a likelihood ratio-type chart, which we will refer to as the Laplace Likelihood Ratio (Lap-LR) chart. Finally, we suggest transforming data so that the Shifted Exponential ChiMax Chart discussed in the previous chapter can be used to monitor it.

Additionally, we consider a two-chart joint monitoring scheme made up of a control chart for monitoring the location and a separate control chart for monitoring the scale. Each of these charts utilizes the MLE of the parameter that it monitors, and the control limits for the two charts are selected so that the overall *IC ARL* of the two-chart scheme is a specified value. We refer to this as the LapMLE-2 joint monitoring scheme.

5.2 Statistical Framework and Preliminaries

Let us consider the case where the *IC* parameters, a_0 and b_0, are known or specified. Let $V_1, V_2, \dots, V_n$ be a random sample of size n from the Laplace distribution, with location parameter a_2 and scale parameter $b_2 > 0$. In the interest of simplicity, let n be an odd number; in other words, $n = 2k + 1$ where k is some positive integer. The parameters a_2 and b_2 are unknown;

however, when the process is *IC*, $a_2 = a_0$ and $b_2 = b_0$. When the process is *OOC*, one or both of these equalities is violated; in other words, either the location parameter, the scale parameter, or both differ from the *IC* parameters, a_0 and b_0. However, at the outset, it is unclear whether or not the distributions are the same.

5.3 The LapMLE-Max Chart

Now, let $\hat{a}_2$ be the sample median. This is the MLE for the location parameter, and it is unbiased (Johnson and Kotz, 1970). Also, let $\hat{b}_2 = \frac{\sum_{i=1}^{n}|V_i - \hat{a}_2|}{n}$. This is the maximum likelihood estimator of the scale parameter (Johnson and Kotz, 1970). When n is odd, $n = 2k + 1$ where k is some positive integer. Then $\hat{a}_2 = V_{(k+1)}$, the $(k + 1)$th order statistic of the sample, and $\hat{b}_2 = \frac{\left[\sum_{i=k+2}^{n} V_{(i)}\right]}{n} - \frac{\left[\sum_{i=1}^{k} V_{(i)}\right]}{n}$. It is clear that $\hat{a}_2$ and $\hat{b}_2$ are independent in this case, since the V_i's are mutually independent and $V_{(k+1)}$ is not used in computing $\hat{b}_2$.

Since $\hat{a}_2$ is the $(k + 1)$th order statistic of the sample, its pdf is $f_{\hat{a}_2}(y_1) = \frac{n!}{(k!)^2}\left(\frac{1}{2}\right)^n \frac{1}{b_2} e^{-(k+1)|y_1 - a_2|/b_2}\left(2 - e^{-|y_1 - a_2|/b_2}\right)^k$ (Kotz, Kozubowski, & Podgorski, 2001; Karst and Polowy, 1963). When $a = 0$ and $b = 1$, the cdf of $\hat{a}_2$ is $F_{\hat{a}_2}(y_1) = \left(\frac{1}{2}\right)^n \sum_{i=k+1}^{n}\binom{n}{i} e^{iy_1}(2 - e^{y_1})^{n-i} I_{(-\infty,0)}(y_1) + \left(\frac{1}{2}\right)^n \sum_{i=k+1}^{n}\binom{n}{i} e^{-(n-i)y_1}(2 - e^{-y_1})^i I_{[0,\infty)}(y_1)$. When $n = 5$, this further simplifies to $F_{\hat{a}_2}(y_1) = \frac{e^{3y_1}}{32}\{10(2 - e^{y_1})^2 + 5e^{y_1}(2 - e^{y_1}) + e^{2y_1}\} I_{(-\infty,0)}(y_1) + \frac{(2-e^{-y_1})^3}{32}\{10e^{-2y_1} + 5e^{-y_1}(2 - e^{-y_1}) + (2 - e^{-y_1})^2\} I_{[0,\infty)}(y_1)$.

The distribution of $\hat{b}_2$ is more complicated to obtain. However, Karst and Polowy (1963) derived the pdf of $s = \frac{n\hat{b}_2}{b_2}$. They demonstrated that when $n = 5$, its pdf is $f_s(y_2) = \left[\left(-\frac{173}{18} + \right.\right.$

$\left.\frac{29y_2}{6} - \frac{5y_2^2}{4} + \frac{15y_2^3}{48}\right) e^{-y_2} + \frac{48e^{-\frac{3y_2}{2}}}{5} + \frac{e^{-4y_2}}{90}\Bigg] I_{[0,\infty)}(y_2)$. By integrating, it is easy to show that its cdf in this case is $F_s(y_2) = \Big[-\frac{15}{48}y_2^3e^{-y_2} + \frac{5}{16}y_2^2e^{-y_2} - \frac{202}{48}y_2e^{-y_2} + \frac{389}{72}e^{-y_2} - \frac{32}{5}e^{-\frac{3y_2}{2}} - \frac{1}{360}e^{-4y_2} + 1\Big] I_{[0,\infty)}(y_2)$.

Now, let $R_1 = \Phi^{-1}\{\daleth(\hat{a}_2, a_0, b_0)\}$ where $\daleth(., a, b)$ is the cdf of the $(k+1)$th order statistic of a Laplace distribution with location parameter a and scale parameter b. Also, let $R_2 = \Phi^{-1}\left\{\mathrm{M}\left(\frac{n\hat{b}_2}{b_0}, a_0, b_0\right)\right\}$ where $\mathrm{M}(., a, b)$ is the cdf of s. Note that both R_1 and R_2 have a standard normal distribution when the process is *IC*. We will use these two statistics to construct the LapMLE-Max chart.

5.3.1 Proposed Charting Procedure for the LapMLE-Max chart

We propose the following method for constructing LapMLE-Max charts when the location and scale parameters, a_0 and b_0, are known or specified:

Step 1. Let $Y_{i,n} = (Y_{i1}, Y_{i2}, \dots, Y_{in})$ be the ith Phase II sample of size $n, i = 1,2, \dots$

Step 2. Identify the $V's$ with the $Y's$. Calculate the statistics R_{1i} and R_{2i} for the ith test sample, for $i = 1,2, \dots$

Step 3: Calculate the plotting statistic $\Upsilon_i = \max\{|R_{1i}|, |R_{2i}|\}$.

Step 4. Plot Υ_i against a *UCL* H_Υ. Note that $\Upsilon_i \geq 0$ by definition so that the *LCL* is 0 and that larger values of Υ_i suggest an *OOC* process.

Step 5. If Υ_i exceeds H_Υ, the process is declared *OOC* at the ith test sample. If not, the process is considered to be *IC*, and testing continues to the next sample.

Step 6. Follow up: When the process is declared *OOC* at the *i*th test sample, compare each of $|R_{1i}|$ and $|R_{2i}|$ with H_Υ.

(i) If $|R_{2i}| < H_\Upsilon < |R_{1i}|$, a shift in the location parameter is indicated.

(ii) If $|R_{1i}| < H_\Upsilon < |R_{2i}|$, a shift in the scale parameter is indicated.

(iii) If $|R_{1i}|$ and $|R_{2i}|$ both exceed H_Υ, a shift in both the location and scale parameters is indicated.

5.3.2 Distribution of the Plotting Statistic for the LapMLE-Max chart

For the LapMLE-Max chart, the process is declared *OOC* when $\Upsilon > H_\Upsilon$ where the *UCL* H_Υ is obtained so that the *IC ARL* is some given nominal value. R_1 and R_2 are independent because $\hat{a}_2$ and $\hat{b}_2$ are, and as mentioned previously, both have the standard normal distribution when the process is *IC*. The cdf of the plotting statistic Υ is given by

$P(\Upsilon \le g) = P(\max\{|R_{1i}|, |R_{2i}|\} \le g) = P\{(|R_{1i}| \le g) \,\&(|R_{2i}| \le g)\}$

$= \{(\daleth[\daleth^{-1}(\Phi(g), a_0, b_0), a_2, b_2]) - (\daleth[\daleth^{-1}(\Phi(-g), a_0, b_0), a_2, b_2])\}$

$\times \left\{M\left(\frac{b_0}{b_2} M^{-1}(\Phi(g), a_0, b_0), a_2, b_2\right) - M\left(\frac{b_0}{b_2} M^{-1}(\Phi(-g), a_0, b_0), a_2, b_2\right)\right\}$.[16] When the process is *IC*, the cdf of the plotting statistic Υ simplifies to $P(\Upsilon \le g|IC) = \{\Phi(g) - \Phi(-g)\}^2$. The *IC ARL* is $\frac{1}{P(\Upsilon > g)} = \frac{1}{1-\{\Phi(g)-\Phi(-g)\}^2} = \frac{1}{1-\{2\Phi(g)-1\}^2}$. Thus, the *UCL* is $H_\Upsilon = \Phi^{-1}\left(\frac{1+\sqrt{1-\frac{1}{IC\,ARL}}}{2}\right)$.

[16] Details of the derivation are given in D.1 in the Appendix.

5.4 The LapChi Chart

Next, note that $\frac{2\sum_{i=1}^{n}|V_i - a_2|}{b_2}$ has a chi-square distribution with $2n$ degrees of freedom. Now, define a statistic $X = \frac{2\sum_{i=1}^{n}|V_i - a_0|}{b_0}$. When the process is *IC*, X always has a chi-square distribution with $2n$ degrees of freedom. This will be a plotting statistic used to define the LapChi chart.

5.4.1 Proposed Charting Procedure for the Lap-Chi chart

We propose the following method for constructing LapChi charts when the location and scale parameters, a_0 and b_0, are known or specified:

Step 1. Let $Y_{i,n} = (Y_{i1}, Y_{i2}, \dots, Y_{in})$ be the *i*th Phase II sample of size $n, i = 1,2, \dots$.

Step 2. Identify the $V's$ with the $Y's$. Calculate the statistics X_i for the ith test sample, for $i = 1,2, \dots$.

Step 3: Step 3. Plot X_i against a *UCL* H_X. Note that $X_i \geq 0$ by definition so that the *LCL* is 0 and that larger values of X_i suggest an *OOC* process.

Step 4. If X_i is larger than H_X, the process is declared *OOC* at the *i*th test sample. If not, the process is considered to be *IC*, and testing continues to the next sample.

Step 5. Follow up: When the process is declared *OOC* at the *i*th test sample, calculate $\hat{a}_2$ and $\widehat{b}_2$. Let $p_1 = P[a_2 > \hat{a}_2 \mid IC]$ and $p_2 = P[b_2 > \hat{b}_2 \mid IC]$. These values can be determined via Monte Carlo simulation.

(i) If both $p_1, p_2 < 0.005$ or both $p_1, p_2 > 0.995$, a shift in both the location and scale parameters is indicated.

(ii) If both $p_1, p_2 > 0.025$ or both $p_1, p_2 < 0.9975$, a false alarm is indicated.

(iii) If $p_1 < 0.005$ and $p_2 > 0.025$, a shift in the location parameter is indicated.

(iv) If $p_1 > 0.995$ and $p_2 < 0.975$, a shift in the location parameter is indicated.

(v) If $p_2 < 0.005$ and $p_1 > 0.025$, a shift in the scale parameter is indicated.

(vi) If $p_2 > 0.995$ and $p_1 < 0.975$, a shift in the scale parameter is indicated.

(vii) If $p_1 < 0.005$ and $0.005 \leq p_2 \leq 0.025$ or $0.975 \leq p_2 \leq 0.995$, a major shift in the location parameter with possible associated shift in the scale parameter is indicated.

(viii) If $p_1 > 0.995$ and $0.005 \leq p_2 \leq 0.025$ or $0.975 \leq p_2 \leq 0.995$, a major shift in the location parameter with possible associated shift in the scale parameter is indicated.

(ix) If $p_2 < 0.005$ and $0.005 \leq p_1 \leq 0.025$ or $0.975 \leq p_1 \leq 0.995$, a major shift in the scale parameter with possible associated shift in the location parameter is indicated.

(x) If $p_2 > 0.995$ and $0.005 \leq p_1 \leq 0.025$ or $0.975 \leq p_1 \leq 0.995$, a major shift in the scale parameter with possible associated shift in the location parameter is indicated.

5.4.2 Distribution of the Plotting Statistic for the LapChi chart

For the LapChi chart, the process is declared *OOC* when $\mathrm{X} > H_{\mathrm{X}}$ where the *UCL* H_{X} is obtained so that the *IC ARL* is some given nominal value. The cdf of the plotting statistic *X* is given by $P(\mathrm{X} \leq g) = P\left(\frac{2\sum_{i=1}^{n}|V_i - a_0|}{b_0} \leq g\right)$. When the process is *IC*, the cdf of the plotting statistic X simplifies to $P(\mathrm{X} \leq g|IC) = G(g, 2n)$. The *IC ARL* is $\frac{1}{P(\mathrm{X}>g)} = \frac{1}{1-G(g,2n)}$. Thus, the *UCL* is $H_{\mathrm{X}} = \mathrm{X}^{-1}\left(1 - \frac{1}{IC\ ARL}, 2n\right)$.

5.5 The SEMLE-ChiMax Chart for Laplace Data

Now, note that $|V_i - a_2|$ has a shifted exponential distribution with location parameter $\theta = 0$ and scale parameter $\lambda = b_2$. Define a statistic $V_i^* = |V_i - a_0|$. When the process is *IC*, V_i^* has a shifted exponential distribution with location parameter $\theta = 0$ and scale parameter $\lambda = b_0$. Thus, $\hat{\theta}_2 = V_{(1)}{}^*$, the first order statistics of the transformed sample, is the MLE for θ and $\hat{\lambda}_2 = \frac{\sum_{i=1}^{n}(V_i{}^* - \hat{\theta}_2)}{n} = \frac{\sum_{i=1}^{n} V_i{}^*}{n} - \hat{\theta}_2 = \bar{V}^* - \hat{\theta}_2$ is the MLE of the scale parameter. Let $D_1 = \frac{2n(\hat{\theta}_2 - 0)}{b_0}$ and $D_2 = \mathrm{G}^{-1}\left\{\mathrm{G}\left(\frac{2n\hat{\lambda}_2}{b_0}, 2n-2\right), 2\right\}$. Note that both D_1 and D_2 have a chi-square distribution with two degrees of freedom when the process is *IC*. We will use these two statistics to construct the SEMLE-ChiMax chart for Laplace-distributed data.

5.5.1 Proposed Charting Procedure for the SEMLE-ChiMax chart for Laplace data

We propose the following method for transforming Laplace data for use with the SEMLE-ChiMax chart when the location and scale parameters, a_0 and b_0, are known or specified:

Step 1. Let $Y_{i,n} = (Y_{i1}, Y_{i2}, \dots, Y_{in})$ be the *i*th Phase II sample of size $n, i = 1,2, \dots$

Step 2. Identify the $V's$ with the $Y's$. Calculate $Y_{i,n}{}^* = |Y_{i1} - a_0|$ for $= 1,2, \dots, n$. Calculate the statistics D_{1i} and D_{2i} for the ith test sample, for $i = 1,2, \dots$. Note that if the process is *IC*, both of these quantities should be positive. If $D_{1i} \leq 0$, the process is declared *OOC* at the *i*th test sample. If $D_{1i} > 0$, continue to step 3.

Step 3: Calculate the plotting statistic $\mathrm{T}_i = \max\{D_{1i}, D_{2i}\}$.

Step 4. Plot T_i against a *UCL* H_T. Note that $\mathrm{T}_i \geq 0$ so that the *LCL* is 0 and that large values of T_i suggest an *OOC* process.

Step 5. If T_i is greater than H_T or less than 0, the process is declared *OOC* at the *i*th test sample. If not, the process is considered to be *IC*, and testing continues to the next sample.

Step 6. Follow up: When the process is declared *OOC* at the *i*th test sample, use the follow-up procedure described above for the LapChi chart.

5.5.2 Distribution of the Plotting Statistic for the SEMLE-ChiMax chart for Laplace data

When the SEMLE-ChiMax chart is used with Laplace data, the process is declared *OOC* when $\mathrm{T} \leq 0$ or $\mathrm{T} > H_{\mathrm{T}}$ where the *UCL* H_{T} is obtained so that the *IC ARL* is some given nominal value. As mentioned previously, D_1 and D_2 are independent because $\hat{\theta}_2$ and $\bar{V} - \hat{\theta}_2$ are, and both have the chi-square distribution with two degrees of freedom when the process is *IC*. The cdf of the plotting statistic T is given by $P(T \leq g \;\&\; D_1 > 0) = P(\max\{ D_1, D_2\} \leq g \;\&\; D_1 > 0) = P\left(0 < \frac{2n(\hat{\theta}_2 - 0)}{\lambda_0} \leq g\right) P\left(\mathrm{G}^{-1}\left\{\mathrm{G}\left(\frac{2n\hat{\lambda}_2}{\lambda_0}, 2n-2\right), 2n-2\right\} \leq g\right)$. When the process is *IC*, the cdf of the plotting statistic T simplifies to $P(\mathrm{T} \leq g \;\&\; D_1 > 0 | IC) = \{G(g,2)\}\{G(g,2)\} = \{G(g,2)\}^2$. The *IC ARL* is $\frac{1}{P(\mathrm{T} > g \text{ or } D_1 \leq 0)} = \frac{1}{1 - \{G(g,2)\}^2}$. Thus, the *UCL* is

$$H_{\mathrm{T}} = G^{-1}\left(\sqrt{1 - \frac{1}{IC\ ARL}}, 2\right).$$

5.6 The Lap-LR Chart

Since joint monitoring of the location and scale is analogous to repeatedly testing the null hypothesis that the sample at hand comes from a completely specified Laplace population (a simple null hypothesis) versus all alternatives (a composite alternative hypothesis), we once again wish to consider a chart based upon the perspective of a likelihood ratio statistic. It can be shown that the likelihood ratio statistic for the Laplace distribution is given by

$\mathrm{L} = \left(\frac{b}{\hat{b}}\right)^n e^{[\sum_{i=1}^{n}|V_i - a|/b] - [\sum_{i=1}^{n}|V_i - \hat{a}|/\hat{b}]}$. This will be a plotting statistic used to define the Lap-LR chart.

5.6.1 Proposed Charting Procedure for the Lap-LR chart

We propose the following method for constructing Lap-LR charts when the location and scale parameters, a_0 and b_0, are known or specified:

Step 1. Let $Y_{i,n} = (Y_{i1}, Y_{i2}, \dots, Y_{in})$ be the *i*th Phase II sample of size $n, i = 1,2, \dots$

Step 2. Identify the $V's$ with the $Y's$. Calculate the statistics L_i for the ith test sample, for $i = 1,2, \dots$

Step 3: Step 3. Plot L_i against a *LCL* H_{L}. Note that $\mathrm{L}_i \leq 1$ by definition so that the *UCL* is 1 and that smaller values of L_i suggest an *OOC* process.

Step 4. If L_i is lower than H_{L}, the process is declared *OOC* at the *i*th test sample. If not, the process is considered to be *IC*, and testing continues to the next sample.

Step 5. Follow up: When the process is declared *OOC* at the *i*th test sample, use the follow-up procedure described above for the LapChi chart.

5.6.2 Distribution of the Plotting Statistic for the Lap-LR chart

For the Lap-LR chart, the process is declared *OOC* when $\mathrm{L} < H_{\mathrm{L}}$, where the *LCL* H_{L} is obtained so that the *IC ARL* is equal to some given nominal value. However, the distribution is rather intractable.

When m and n are large, it is useful to consider the asymptotic properties of L. Consider a function of L, $-2\ln \mathrm{L} = -2 \ln\left\{\left(\frac{b}{\hat{b}}\right)^n e^{[\sum_{i=1}^{n}|V_i - a|/b] - [\sum_{i=1}^{n}|V_i - \hat{a}|/\hat{b}]}\right\}$. As mentioned previously, it can be shown (see for example Hogg, McKean and Craig, 2005) that $-2\ln \mathrm{L}$ converges in distribution to a chi-square random variable with 2 degree of freedom. Using this property, it is simple to obtain H_{L} as long as m and n are appropriately large. However, when m and n are small or moderate, H_{L} can easily be obtained through Monte Carlo simulation.

5.7 The LapMLE-2 Scheme

Let $\beth_1 = \hat{a}_2$ and $\beth_2 = s = \frac{n\hat{b}_2}{b_0}$. Note that when the process is *IC*, the distribution of $\beth_1$ is $f_{\hat{a}_2}(y_1) = \frac{n!}{(k!)^2}\left(\frac{1}{2}\right)^n \frac{1}{b_0} e^{-(k+1)|y_1-a_0|/b_0}\left(2 - e^{-|y_1-a_0|/b_0}\right)^k$ and the distribution of $\beth_2$ is $f_s(y_2) = \left[\left(-\frac{173}{18} + \frac{29y_2}{6} - \frac{5y_2^2}{4} + \frac{15y_2^3}{48}\right)e^{-y_2} + \frac{48e^{-\frac{3y_2}{2}}}{5} + \frac{e^{-4y_2}}{90}\right] I_{[0,\infty)}(y_2)$ when $n = 5$. These are the two statistics that we will use to construct the charts which make up the LapMLE-2 scheme. Note that as before we will use $\daleth(.,a,b)$ to denote the cdf of $\hat{a}_2$, the $(k+1)$th order statistic of a Laplace distribution with location parameter a and scale parameter b and $\mathrm{M}(.,a,b)$ to denote the cdf of s.

5.7.1 Proposed Charting Procedure for the LapMLE-2 scheme

We propose the following method for constructing LapMLE-2 schemes when the location and scale parameters, a_0 and b_0, are known or specified:

Step 1. Let $Y_{i,n} = (Y_{i1}, Y_{i2}, \dots, Y_{in})$ be the ith Phase II sample of size $n, i = 1,2, \dots$

Step 2. Identify the $V's$ with the $Y's$. Calculate the plotting statistics $\beth_{1i}$ and $\beth_{2i}$ for the ith test sample, for $i = 1,2, \dots$.

Step 3. Plot $\beth_{1i}$ against a *UCL* $H_{\beth_{1U}}$ and an *LCL* $H_{\beth_{1L}}$.

Step 4. On a separate chart, plot $\beth_{2i}$ against a *UCL* $H_{\beth_{2U}}$ and an *LCL* $H_{\beth_{2L}}$.

Step 5. If $\beth_{1i}$ is greater than $H_{\beth_{1U}}$ or less than $H_{\beth_{1L}}$ and/or $\beth_{2i}$ is greater than $H_{\beth_{2U}}$ or less than $H_{\beth_{2L}}$, the process is declared *OOC* at the *i*th test sample. If not, the process is considered to be *IC*, and testing continues to the next sample.

Step 6. Follow up: When the process is declared *OOC* at the *i*th test sample, compare $\beth_{1i}$ with $H_{\beth_{1U}}$ and $H_{\beth_{1L}}$ and $\beth_{2i}$ with $H_{\beth_{2U}}$ and *LCL* $H_{\beth_{2L}}$.

(i) If $\beth_{1i} > H_{\beth_{1U}}$ and $H_{\beth_{2L}} < \beth_{2i} < H_{\beth_{2U}}$, a shift in the location parameter is indicated.

(ii) If $\beth_{1i} < H_{\beth_{1L}}$ and $H_{\beth_{2L}} < \beth_{2i} < H_{\beth_{2U}}$, a shift in the location parameter is indicated.

(iii) If $\beth_{2i} > H_{\beth_{2U}}$ and $H_{\beth_{1L}} < \beth_{1i} < H_{\beth_{1U}}$, a shift in the scale parameter is indicated.

(iv) If $\beth_{2i} < H_{\beth_{2L}}$ and $H_{\beth_{1L}} < \beth_{1i} < H_{\beth_{1U}}$, a shift in the scale parameter is indicated

(v) If $\beth_{1i} > H_{\beth_{1U}}$ and $\beth_{2i} > H_{\beth_{2U}}$, a shift in both the location and scale parameters is indicated.

(vi) If $\beth_{1i} < H_{\beth_{1L}}$ and $\beth_{2i} > H_{\beth_{2U}}$, a shift in both the location and scale parameters is indicated.

(vii) If $\beth_{1i} > H_{\beth_{1U}}$ and $\beth_{2i} < H_{\beth_{2L}}$, a shift in both the location and scale parameters is indicated.

(viii) If $\beth_{1i} < H_{\beth_{1L}}$ and $\beth_{2i} < H_{\beth_{2L}}$, a shift in both the location and scale parameters is indicated.

5.7.2 Distribution of the Plotting Statistics for the LapMLE-2 scheme

The LapMLE-2 control scheme consists of two charts. The process is declared *OOC* whenever a signal occurs on either chart, that is, any time $\beth_1 < H_{\beth_{1L}}$, $\beth_1 > H_{\beth_{1U}}$, $\beth_2 < H_{\beth_{2L}}$, or $\beth_2 > H_{\beth_{2U}}$,where the control limits $H_{\beth_{1L}}$, $H_{\beth_{1U}}$, $H_{\beth_{2L}}$, and $H_{\beth_{2U}}$ are obtained so that the *IC ARL* is some given nominal value. $\beth_1$ and $\beth_2$ are independent and have the distributions specified above. The joint cdf of the two plotting statistics $\beth_1$ and $\beth_2$ is given by

$P[(g_1 < \beth_1 \leq g_2)\ \&\ (g_3 \leq \beth_2 \leq g_4)] = [\daleth(g_2, a_2, b_2) - \daleth(g_1, a_2, b_2)] \times \left[\mathrm{M}\left(\frac{b_0}{b_2} g_4, a_2, b_2\right) - \mathrm{M}\left(\frac{b_0}{b_2} g_3, a_2, b_2\right)\right]$. When the process is *IC*, the joint cdf of the plotting statistics $\beth_1$ and $\beth_2$ simplifies to $[(g_1 < \beth_1 \leq g_2)\ \&(g_3 \leq \beth_2 \leq g_4)|IC] = [\daleth(g_2, a_2, b_2) - \daleth(g_1, a_2, b_2)] \times [\mathrm{M}(g_4, a_2, b_2) - \mathrm{M}(g_3, a_2, b_2)]$.

5.8 Implementation

In order to use the proposed charts, one must select the appropriate control limits for each corresponding to the desired nominal *IC ARL*. This can be accomplished using the analytical expressions for the *IC ARL* given in the earlier sections, though doing so is rather tedious. Instead we use 100,000 simulations in R to calculate the control limits. As expected, we find that higher nominal *ARL*s require higher *UCL*s and lower *LCL*s.

Table 5.1: Appropriate control limits for the Laplace charts when a and b are known and $n = 5$, for various *IC ARL*s

IC ARL	LapMLE-Max Chart *UCL*	SEMLE-ChiMax Chart *UCL*	Lap-LR Chart *LCL*	Lap-Chi Chart *UCL*	LapMLE-2 Scheme (Location Chart *UCL* & *LCL*/ Scale Chart *UCL*/ Scale Chart *LCL*)[17]
125	2.88	11.04	.00263	23.85	±2.83/15.26/0.36
250	3.09	12.43	.00113	25.81	±2.72/14.92/0.39
500	3.29	13.82	.000475	27.72	±2.58/14.45/0.43
750	3.40	14.63	.000285	28.82	±2.35/13.54/0.52
1000	3.48	15.20	.000195	29.59	±2.11/12.65/0.62

[17] We selected the control limits for the LapMLE-2 Scheme so that both of the underlying charts have the same ARL.

5.9 Performance Comparisons

The performance of the three charts for various location and scale shifts is evaluated in a simulation study so that they can easily be compared. Tables 5.2, 5.3, and 5.4 provide the ARL, run length standard deviation, and specified quantiles of the run length distribution when $n = 5$. We use $a = 0$ and $b = 1$ for our IC Laplace distribution.

From the tables, it is seen that the Lap-LR chart performs best among the four charts when there is a shift in only the location parameter. However, when there is a scale shift, it is always outperformed by the LapChi chart and usually outperformed by one of the other charts as well.

The SEMLE-ChiMax chart performs surprisingly well for this data. For most of the shifts considered, its performance was second-best among the charts. However, this chart is not ideal, since it is unable to detect decreases in the scale parameter.

Table 5.2: Run length characteristics for the SEMLE-ChiMax chart for Laplace data and the Lap-LR chart for various values of a_2 and b_2 when $a_0 = 0, b_0 = 1$, and $n = 5$

		SEMLE-ChiMax Chart			Lap-LR Chart		
a_2	b_2	*ARL*	*SDRL*	*5%, 25%, 50%, 75%, 95%*	*ARL*	*SDRL*	*5%, 25%, 50%, 75%, 95%*
0	*1*	**502.44**	507.55	25, 142, 348, 689, 1511	**499.11**	496.82	26, 146, 350, 691, 1471
0.1	*1*	**490.58**	478.23	26, 145, 345, 689, 1459	**455.95**	451.69	25, 138, 319, 634, 1341
0.25	*1*	**452.25**	451.87	24, 127, 317, 626, 1349	**324.25**	330.47	16, 89, 221, 449, 991
0.5	*1*	**326.16**	325.96	18, 93, 225, 449, 988	**137.50**	135.27	8, 41, 98, 191, 404
0.75	*1*	**195.97**	193.84	11, 57, 136, 272, 583	**56.99**	56.48	3, 17, 40, 78, 168
1	*1*	**93.95**	93.85	5, 26, 65, 132, 281	**24.17**	23.75	2, 7, 17, 33, 72
1.25	*1*	**37.16**	36.82	2, 11, 26, 51, 109	**11.48**	10.86	1, 4, 8, 16, 33
1.5	*1*	**13.79**	13.39	1, 4, 10, 19, 41	**6.05**	5.50	1, 2, 4, 8, 17
0	*1.25*	**88.82**	87.50	5, 26, 63, 125, 260	**298.27**	296.01	15, 87, 208, 416, 889
0.1	*1.25*	**88.08**	87.93	5, 26, 60, 123, 263	**280.16**	276.99	16, 82, 194, 391, 823
0.25	*1.25*	**85.02**	85.68	5, 24, 58, 116, 258	**221.89**	221.53	12, 65, 156, 308, 653
0.5	*1.25*	**71.97**	71.16	4, 21, 50, 100, 213	**115.03**	115.10	7, 34, 80 159 347
0.75	*1.25*	**53.68**	53.84	3, 15, 37, 74, 165	**53.99**	53.16	3, 16, 38, 74, 157
1	*1.25*	**35.69**	35.18	2, 11, 25, 49, 105	**25.62**	25.29	2, 8, 18, 36, 75
1.25	*1.25*	**20.44**	19.79	2, 6, 14, 28, 59	**12.76**	12.48	1, 4, 9, 17, 37
1.5	*1.25*	**10.84**	10.20	1, 3, 8, 15, 31	**7.05**	6.48	1, 2, 5, 10, 20
0	*1. 5*	**28.19**	27.80	2, 8, 20, 39, 83	**99.63**	98.50	6, 29, 69, 138, 297
0.1	*1.5*	**27.93**	27.40	2, 8, 20, 38, 82	**96.69**	95.56	6, 28, 67, 135, 285
0.25	*1.5*	**27.35**	26.92	2, 8, 19, 38, 81	**86.15**	87.54	5, 25, 59, 119, 260
0.5	*1.5*	**24.72**	24.05	2, 7, 17, 34, 73	**58.22**	58.10	3, 17, 40, 80, 177
0.75	*1.5*	**20.68**	20.45	1, 6, 14, 28, 62	**34.66**	34.46	2, 11, 24, 48, 103
1	*1.5*	**16.39**	16.13	1, 5, 11, 22, 49	**20.11**	19.58	2, 6, 14, 27, 60
1.25	*1.5*	**11.67**	11.16	1, 4, 8, 16, 34	**11.45**	10.91	1, 4, 8, 16, 33
1.5	*1.5*	**7.69**	7.19	1, 3, 5, 10, 22	**6.87**	6.44	1, 2, 5, 9, 20
0	*1.75*	**12.77**	12.18	1, 4, 9, 17, 37	**37.73**	37.55	2, 11, 26, 52, 112
0.1	*1.75*	**12.44**	11.72	1, 4, 9, 17, 36	**37.18**	35.90	2, 11, 26, 52, 110
0.25	*1.75*	**12.28**	11.87	1, 4, 9, 17, 36	**35.42**	35.08	2, 10, 24, 49, 106
0.5	*1.75*	**11.63**	11.15	1, 4, 8, 16, 34	**27.77**	27.37	2, 8, 19, 38, 83
0.75	*1.75*	**10.91**	10.35	1, 4, 8, 15, 31	**19.94**	19.34	1, 6, 14, 27, 58
1	*1.75*	**9.01**	8.54	1, 3, 6, 12, 26	**13.69**	13.17	1, 4, 10, 19, 40
1.25	*1.75*	**7.16**	6.54	1, 2, 5, 10, 20	**8.95**	8.44	1, 3, 6, 12, 26
1.5	*1.75*	**5.41**	4.93	1, 2, 4, 7, 15	**6.02**	5.54	1, 2, 4, 8, 17
0	*2*	**7.23**	6.71	1, 2, 5, 10, 21	**18.13**	17.70	1, 6, 13, 25, 53
0.1	*2*	**7.25**	6.72	1, 2, 5, 10, 21	**17.72**	17.21	1, 5, 12, 24, 52
0.25	*2*	**7.14**	6.56	1, 2, 5, 10, 20	**17.18**	16.76	1, 5, 12, 24, 50
0.5	*2*	**6.91**	6.43	1, 2, 5, 9, 20	**14.96**	14.45	1, 5, 10, 21, 44
0.75	*2*	**6.40**	5.79	1, 2, 5, 9, 18	**11.72**	11.20	1, 4, 8, 16, 34
1	*2*	**5.69**	5.18	1, 2, 4, 8, 16	**9.04**	8.55	1, 3, 6, 12, 26
1.25	*2*	**4.96**	4.39	1, 2, 4, 7, 14	**6.66**	6.14	1, 2, 5, 9, 19
1.5	*2*	**4.01**	3.46	1, 2, 3, 5, 11	**4.92**	4.37	1, 2, 4, 7, 14

Table 5.3: Run length characteristics for the LapMLE-Max and LapChi charts for various values of a_2 and b_2 when $a_0 = 0, b_0 = 1$, and $n = 5$

		LapMLE-Max Chart			LapChi Chart		
a_2	b_2	*ARL*	*SDRL*	*5%, 25%, 50%, 75%, 95%*	*ARL*	*SDRL*	*5%, 25%, 50%, 75%, 95%*
0	*1*	**499.87**	497.96	26, 143, 347, 694, 1495	**502.11**	507.23	26, 143, 345, 695, 1508
0.1	*1*	**489.67**	488.18	26, 142, 340, 680, 1465	**491.78**	487.77	26, 140, 338, 689, 1466
0.25	*1*	**438.49**	436.48	23, 128, 305, 607, 1307	**448.78**	449.14	23, 129, 310, 621, 1345
0.5	*1*	**306.82**	306.56	16, 89, 212, 425, 924	**324.26**	318.22	17, 95, 225, 453, 964
0.75	*1*	**180.41**	180.24	10, 52, 125, 249, 539	**205.05**	204.70	11, 59, 142, 284, 609
1	*1*	**99.90**	99.32	5, 29, 69, 139, 297	**116.84**	116.24	6, 34, 81, 162, 349
1.25	*1*	**51.50**	51.27	3, 15, 36, 71, 155	**59.41**	59.02	4, 17, 41, 83, 176
1.5	*1*	**26.66**	26.07	2, 8, 19, 37, 79	**30.61**	30.25	2, 9, 21, 42, 91
0	*1.25*	**108.35**	107.94	6, 31, 75, 150, 324	**69.98**	70.00	4, 21, 48, 97, 211
0.1	*1.25*	**106.09**	105.43	6, 31, 74, 146, 318	**69.42**	67.77	4, 20, 48, 97, 207
0.25	*1.25*	**100.47**	100.72	6, 29, 70, 139, 300	**65.25**	64.89	4, 19, 46, 90, 193
0.5	*1.25*	**79.74**	79.07	5, 23, 56, 111, 238	**54.69**	54.16	3, 16, 38, 75, 162
0.75	*1.25*	**56.70**	56.14	3, 17, 40, 79, 169	**41.09**	40.93	2, 12, 29, 57, 124
1	*1.25*	**37.19**	36.79	2, 11, 26, 51, 110	**28.78**	28.39	2, 8, 20, 40, 85
1.25	*1.25*	**23.34**	22.82	2, 7, 16, 32, 69	**18.85**	18.14	1, 6, 14, 26, 55
1.5	*1.25*	**14.37**	13.95	1, 4, 10, 20, 42	**12.23**	11.90	1, 4, 9, 17, 36
0	*1. 5*	**33.26**	32.67	2, 10, 23, 46, 98	**21.19**	20.92	2, 6, 15, 29, 62
0.1	*1.5*	**33.04**	32.81	2, 10, 23, 46, 98	**20.81**	20.52	2, 6, 14, 29, 61
0.25	*1.5*	**32.09**	31.56	2, 10, 22, 44, 95	**20.26**	19.79	2, 6, 14, 28, 59
0.5	*1.5*	**28.13**	27.70	2, 8, 20, 39, 83	**17.92**	16.86	1, 6, 13, 25, 51
0.75	*1.5*	**22.91**	22.47	2, 7, 16, 32, 68	**14.77**	14.10	1, 5, 11, 20, 43
1	*1.5*	**17.41**	16.84	1, 5, 12, 24, 51	**11.85**	11.29	1, 4, 8, 16, 34
1.25	*1.5*	**12.76**	12.25	1, 4, 9, 18, 37	**9.04**	8.63	1, 3, 6, 12, 26
1.5	*1.5*	**8.95**	8.43	1, 3, 6, 12, 26	**6.60**	6.12	1, 2, 5, 9, 19
0	*1.75*	**14.56**	14.05	1, 4, 10, 20, 43	**9.59**	9.12	1, 3, 7, 13, 28
0.1	*1.75*	**14.43**	13.97	1, 5, 10, 20, 42	**9.50**	8.98	1, 3, 7, 13, 28
0.25	*1.75*	**14.14**	13.54	1, 4, 10, 20, 41	**9.29**	8.80	1, 3, 7, 13, 27
0.5	*1.75*	**13.11**	12.54	1, 4, 9, 18, 38	**8.56**	7.96	1, 3, 6, 12, 25
0.75	*1.75*	**11.52**	11.00	1, 4, 8, 16, 34	**7.58**	7.05	1, 3, 5, 10, 22
1	*1.75*	**9.70**	9.20	1, 3, 7, 13, 28	**6.47**	5.91	1, 2, 5, 9, 19
1.25	*1.75*	**7.83**	7.30	1, 3, 6, 11, 22	**5.31**	4.83	1, 2, 4, 7, 15
1.5	*1.75*	**6.14**	5.63	1, 2, 4, 8, 17	**4.27**	3.75	1, 2, 3, 6, 12
0	*2*	**8.09**	7.58	1, 3, 6, 11, 23	**5.55**	5.01	1, 2, 4, 7, 16
0.1	*2*	**8.06**	7.52	1, 3, 6, 11, 23	**5.52**	4.99	1, 2, 4, 7, 15
0.25	*2*	**7.89**	7.33	1, 3, 6, 11, 23	**5.42**	4.94	1, 2, 4, 7, 15
0.5	*2*	**7.51**	6.98	1, 3, 5, 10, 22	**5.20**	4.71	1, 2, 4, 7, 15
0.75	*2*	**6.92**	6.40	1, 2, 5, 9, 20	**4.65**	4.07	1, 2, 3, 6, 13
1	*2*	**6.13**	5.62	1, 2, 4, 8, 17	**4.16**	3.55	1, 2, 3, 6, 11
1.25	*2*	**5.31**	4.78	1, 2, 4, 7, 15	**3.66**	3.10	1, 1, 3, 5, 10
1.5	*2*	**4.45**	3.91	1, 2, 3, 6, 12	**3.18**	2.59	1, 1, 2, 4, 8

Table 5.4: Run length characteristics for the LapMLE-2 scheme for various values of a_2 and b_2 when $a_0 = 0, b_0 = 1$, and $n = 5$

		LapMLE-2 Scheme		
a_2	b_2	*ARL*	*SDRL*	*5%, 25%, 50%, 75%, 95%*
0	*1*	**503.17**	504.90	26, 145, 348, 697, 1509
0.1	*1*	**490.78**	489.29	26, 142, 341, 679, 1458
0.25	*1*	**437.65**	435.72	23, 126, 304, 607, 1312
0.5	*1*	**302.64**	303.01	16, 87, 210, 419, 904
0.75	*1*	**178.53**	177.32	10, 52, 124, 247, 534
1	*1*	**97.29**	96.59	6, 28, 68, 134, 291
1.25	*1*	**50.80**	50.14	3, 15, 35, 70, 152
1.5	*1*	**26.13**	25.71	2, 8, 18, 36, 77
0	*1.25*	**107.83**	107.28	6, 31, 75, 149, 321
0.1	*1.25*	**107.28**	107.24	6, 31, 74, 148, 322
0.25	*1.25*	**99.81**	98.77	6, 29, 69, 139, 298
0.5	*1.25*	**79.43**	79.03	5, 23, 55, 110, 238
0.75	*1.25*	**55.93**	55.43	3, 17, 39, 77, 166
1	*1.25*	**36.69**	36.25	2, 11, 26, 51, 109
1.25	*1.25*	**22.98**	22.44	2, 7, 16, 32, 68
1.5	*1.25*	**14.08**	13.59	1, 4, 10, 19, 41
0	*1. 5*	**33.30**	32.76	2, 10, 23, 46, 99
0.1	*1.5*	**33.19**	32.89	2, 10, 23, 46, 99
0.25	*1.5*	**31.90**	31.45	2, 9, 22, 44, 95
0.5	*1.5*	**27.97**	27.39	2, 8, 20, 39, 83
0.75	*1.5*	**22.80**	22.30	2, 7, 16, 32, 67
1	*1.5*	**17.35**	16.82	1, 5, 12, 24, 51
1.25	*1.5*	**12.57**	12.04	1, 4, 9, 17, 37
1.5	*1.5*	**8.89**	8.39	1, 3, 6, 12, 26
0	*1.75*	**14.70**	14.21	1, 5, 10, 20, 43
0.1	*1.75*	**14.57**	14.03	1, 5, 10, 20, 43
0.25	*1.75*	**14.20**	13.68	1, 4, 10, 19, 42
0.5	*1.75*	**13.05**	12.57	1, 4, 9, 18, 38
0.75	*1.75*	**11.44**	10.96	1, 4, 8, 16, 33
1	*1.75*	**9.66**	9.10	1, 3, 7, 13, 28
1.25	*1.75*	**7.80**	7.30	1, 3, 6, 11, 22
1.5	*1.75*	**6.05**	5.49	1, 2, 4, 8, 17
0	*2*	**8.06**	7.55	1, 3, 6, 11, 23
0.1	*2*	**8.01**	7.54	1, 3, 6, 11, 23
0.25	*2*	**7.93**	7.40	1, 3, 6, 11, 23
0.5	*2*	**7.50**	7.00	1, 3, 5, 10, 21
0.75	*2*	**6.90**	6.36	1, 2, 5, 9, 20
1	*2*	**6.09**	5.59	1, 2, 4, 8, 17
1.25	*2*	**5.28**	4.78	1, 2, 4, 7, 15
1.5	*2*	**4.43**	3.89	1, 2, 3, 6, 12

The LapMLE-Max chart performs fairly poorly in comparison to the other charts, nearly always performing worse than the SEMLE-ChiMax and LapChi charts. Its best performance is seen where there is a small shift in location and no scale shift; however, the Lap-LR chart outperforms it in this case. The LapMLE-2 scheme performs analogously to the LapMLE-Max chart, because the two charts are equivalent.

The LapChi chart has the best performance among the charts studied, except when there is a location shift but no scale shift. As a result, this is the best joint monitoring scheme to use with processes that follow a Laplace distribution, unless it is expected that the most commonly occurring assignable causes will produce shifts only in the location.

5.10 Performance Comparisons versus Normal Theory Charts

It is again of interest to determine whether the proposed charts perform better for process data from a Laplace distribution than would normal theory charts. Here, we consider the performance of two normal theory charts for various location and scale shifts and sample sizes. The *UCL*s for the normal theory charts must be selected so that they have a specified nominal *IC ARL*. For $n = 5$, the appropriate *UCL* for the normal theory max chart is 3.29. Table 5.5 provides the *ARL*, run length standard deviation, and specified quantiles of the run length distribution. Note that the underlying distribution of the process data is Laplace. We again use $a = 0$ and $b = 1$ for our *IC* Laplace distribution. The mean of the distribution is a, and its variance is $2b^2$ (Johnson and Kotz, 1970). In other words, the mean of our I*C* distribution is 0, its variance is 2, and these are values to which the normal theory max and distance charts will compare the sample means and variances.

Table 5.5: Run length characteristics for normal theory charts applied to Laplace data for various values of a_2 and b_2 when $a_1 = 0, b_1 = 1$, and $n = 5$

		Normal Theory Max Chart			Normal Theory Distance Chart		
a_2	b_2	ARL	SDRL	5%, 25%, 50%, 75%, 95%	ARL	SDRL	5%, 25%, 50%, 75%, 95%
0	*1*	**66.97**	66.72	4, 20, 46, 93, 201	**39.13**	38.66	2, 12, 27, 54, 116
0.1	*1*	**66.41**	65.93	4, 19, 46, 92, 199	**38.65**	38.16	2, 12, 27, 53, 115
0.25	*1*	**62.22**	61.72	4, 18, 43, 86, 186	**36.00**	35.41	2, 11, 25, 50, 106
0.5	*1*	**48.65**	48.42	3, 14, 34, 67, 145	**27.92**	27.54	2, 8, 19, 38, 83
0.75	*1*	**32.04**	31.47	2, 10, 22, 44, 95	**18.67**	18.09	1, 6, 13, 26, 55
1	*1*	**18.42**	17.79	1, 6, 13, 25, 54	**11.30**	10.80	1, 4, 8, 15, 33
1.25	*1*	**10.19**	9.73	1, 3, 7, 14, 30	**6.45**	5.94	1, 2, 5, 9, 18
1.5	*1*	**5.70**	5.18	1, 2, 4, 8, 16	**3.86**	3.34	1, 1, 3, 5, 11
0	*1.25*	**19.46**	18.82	1, 6, 14, 27, 57	**12.68**	12.21	1, 4, 9, 17, 37
0.1	*1.25*	**19.25**	18.62	1, 6, 14, 27, 56	**12.56**	12.12	1, 4, 9, 17, 37
0.25	*1.25*	**18.51**	17.98	1, 6, 13, 25, 54	**12.06**	11.59	1, 4, 8, 17, 35
0.5	*1.25*	**15.78**	15.25	1, 5, 11, 22, 46	**10.39**	9.92	1, 3, 7, 14, 30
0.75	*1.25*	**12.28**	11.74	1, 4, 9, 17, 36	**8.21**	7.71	1, 3, 6, 11, 24
1	*1.25*	**8.79**	8.26	1, 3, 6, 12, 25	**6.11**	5.54	1, 2, 4, 8, 17
1.25	*1.25*	**5.99**	5.46	1, 2, 4, 8, 17	**4.36**	3.82	1, 2, 3, 6, 12
1.5	*1.25*	**4.08**	3.55	1, 2, 3, 5, 11	**3.10**	2.55	1, 1, 2, 4, 8
0	*1. 5*	**8.43**	7.91	1, 3, 6, 11, 24	**6.07**	5.56	1, 2, 4, 8, 17
0.1	*1.5*	**8.37**	7.88	1, 3, 6, 11, 24	**6.05**	5.52	1, 2, 4, 8, 17
0.25	*1.5*	**8.18**	7.66	1, 3, 6, 11, 23	**5.87**	5.33	1, 2, 4, 8, 17
0.5	*1.5*	**7.42**	6.88	1, 2, 5, 10, 21	**5.38**	4.86	1, 2, 4, 7, 15
0.75	*1.5*	**6.36**	5.84	1, 2, 5, 9, 18	**4.67**	4.16	1, 2, 3, 6, 13
1	*1.5*	**5.15**	4.65	1, 2, 4, 7, 14	**3.86**	3.32	1, 1, 3, 5, 10
1.25	*1.5*	**4.03**	3.51	1, 2, 3, 5, 11	**3.11**	2.57	1, 1, 2, 4, 8
1.5	*1.5*	**3.11**	2.57	1, 1, 2, 4, 8	**2.48**	1.92	1, 1, 2, 3, 6
0	*1.75*	**4.84**	4.31	1, 2, 3, 6, 13	**3.74**	3.22	1, 1, 3, 5, 10
0.1	*1.75*	**4.83**	4.31	1, 2, 3, 6, 13	**3.71**	3.17	1, 1, 3, 5, 10
0.25	*1.75*	**4.72**	4.20	1, 2, 3, 6, 13	**3.65**	3.11	1, 1, 3, 5, 10
0.5	*1.75*	**4.44**	3.92	1, 2, 3, 6, 12	**3.44**	2.89	1, 1, 3, 5, 9
0.75	*1.75*	**4.03**	3.49	1, 2, 3, 5, 11	**3.13**	2.59	1, 1, 2, 4, 8
1	*1.75*	**3.50**	2.95	1, 1, 3, 5, 9	**2.78**	2.22	1, 1, 2, 4, 7
1.25	*1.75*	**2.99**	2.44	1, 1, 2, 4, 8	**2.40**	1.83	1, 1, 2, 3, 6
1.5	*1.75*	**2.50**	1.93	1, 1, 2, 3, 6	**2.06**	1.48	1, 1, 2, 3, 5
0	*2*	**3.28**	2.72	1, 1, 2, 4, 9	**2.66**	2.11	1, 1, 2, 3, 7
0.1	*2*	**3.27**	2.73	1, 1, 2, 4, 9	**2.65**	2.09	1, 1, 2, 3, 7
0.25	*2*	**3.23**	2.70	1, 1, 2, 4, 9	**2.64**	2.07	1, 1, 2, 3, 7
0.5	*2*	**3.11**	2.57	1, 1, 2 , 4, 8	**2.54**	1.98	1, 1, 2, 3, 6
0.75	*2*	**2.88**	2.32	1, 1, 2, 4, 8	**2.37**	1.80	1, 1, 2, 3, 6
1	*2*	**2.64**	2.07	1, 1, 2, 3, 7	**2.19**	1.61	1, 1, 2, 3, 5
1.25	*2*	**2.38**	1.81	1, 1, 2, 3, 6	**1.98**	1.39	1, 1, 1, 2, 5
1.5	*2*	**2.10**	1.51	1, 1, 2, 3, 5	**1.79**	1.18	1, 1, 1, 2, 4

The results here are similar to those found for in the previous chapter. At first glance, one might note that Chen and Cheng's (1998) normal theory max chart and Ramzy's (2005) distance chart have shorter *ARL*s than the Laplace charts explored above and conclude that they are preferable. However, the *IC ARL*s for the normal theory charts are far lower than the nominal value of 500, indicating that the normal theory charts will have an unacceptably high number of false alarms and rendering them virtually useless for monitoring this type of process.

5.11 Summary and Conclusions

Monitoring the location and scale parameters of a Laplace distribution is an important problem in statistical process control. It is necessary, for example, for processes which arise as the difference between two exponential distributions with a common scale. This chapter provides some possibilities for monitoring data from a known Laplace distribution, among which the LapChi chart appears to be the most promising. However, much more work in this area is needed. In particular, these charts are only suitable for sample sizes larger than 1, since they rely on statistics which are functions of order statistics. Additionally, these charts are suitable only for case K, and their performance will be degraded significantly if the parameters are estimated from a Phase I sample. Finally, the adaptation of these charts for case U is not straightforward.

CHAPTER 6

CONCLUSIONS AND FUTURE RESEARCH

6.1 Summary

Two-parameter distributions constitute important problems for process monitoring. In general, it is desirable to utilize control schemes capable of identifying shifts in either or both of the parameters. This dissertation examined control schemes for jointly monitoring the two parameters of a shifted exponential or Laplace distribution with known *IC* parameters, as well as those for a normal distribution with unknown *IC* parameters. For the shifted exponential and Laplace distributions, a variety of new one- and two-chart schemes were introduced, studied, and compared. For the normal distribution, a pair of charts designed for the known parameter case were adapted to account for the additional variability introduced by parameter estimation.

In Chapter 3, Chen and Cheng's (1998) Max chart and Razmy's (2005) Distance chart were modified for monitoring normally distributed processes with unknown means and variances. The modified charts were shown to perform similarly, with the Modified Distance chart being slightly superior in most cases. Additionally, both charts were shown to have good performance for normally distributed data but far poorer performance for data from other distributions, whether they are skewed or symmetric.

In Chapter 4, we introduced and compared five schemes for jointly monitoring the location and scale parameters of a shifted exponential distribution with known parameters: the SEMLE-Max, SEMVUE-Max, SEMLE-ChiMax, and SE-LR charts, and the two-chart SEMLE-

2 scheme. The two max-type charts were shown to be *ARL*-biased for small mean shifts unaccompanied by variance shifts. The SEMLE-2 scheme was shown to have the best overall performance, followed closely by the SEMLE-ChiMax chart.

In Chapter 5, we introduced and compared the LapMLE-Max, LapChi, and Lap-LR charts and the two-chart LapMLE-2 scheme. We also considered transforming the data so that it could be monitored using the SEMLE-ChiMax chart introduced in the previous chapter. Overall, the LapChi chart was shown to be the best joint monitoring scheme to use with processes that follow a Laplace distribution, unless the most commonly occurring assignable causes are expected to produce shifts only in the location parameter. The Lap-LR chart was shown to perform best among the four charts when there is a shift in only the location parameter.

6.2 Future Research

In chapter 3, we considered the unconditional and conditional *IC ARL* of the normal theory charts when parameter estimates were used for the mean and standard deviation. The "unconditional" *IC ARL* was obtained by averaging over the distributions of the mean and the standard deviation, while the "conditional" *IC ARL*s were obtained by considering particular values of the estimators. It was seen that the conditional *IC ARL*s vary widely depending on whether low, medium, or high estimates of each parameter are used, and in most cases, the conditional *IC ARL*s deviate substantially from the nominal *IC ARL*. However, in practice, one would have no way of determining whether the parameter estimates being utilized were low or high since the true parameters are unknown. Therefore, it is desirable to create monitoring procedures which are less dependent on the quality of the parameter estimates. More research is needed to create charts for which both the unconditional *IC ARL* and the conditional *IC ARL*s resulting from particular parameter estimates are correctly maintained at a specified nominal value.

For the Laplace and shifted exponential distributions, only charts for monitoring known parameters are presented. Modifications are needed to produce one- and two-chart schemes suitable for monitoring unknown parameters. Doing so is not particularly straightforward, and much more work is needed to produce the charts.

Each of the charts presented in this dissertation is suitable for data from a particular parametric distribution: the normal, the Laplace, or the shifted exponential. However, in practice, it is not uncommon for a practitioner to be unsure of his data's underlying distribution. For this reason, it is imperative that more work be done in the area of nonparametric joint monitoring of location and scale parameters.

Finally, all of the charts considered in this dissertation are univariate. In practice, many monitoring problems are multivariate in nature, so these charts should be adapted for use with multivariate data.

REFERENCES

Acosta-Meija, C.A. (1998). "Monitoring Reduction in Variability with the Range," *IIE Transactions, 30*(6), 515-513.

Ahmadi, J. & MirMostafaee, S.M.T.K. (2009). "Prediction Intervals for Future Records and Order Statistics Coming From Two Parameter Exponential Distribution," *Statistics and Probability Letters, 79*(7)*,* 977-983.

Ahsanullah, M. (1980). "Linear Prediction of Record Values for the Two Parameter Exponential Distribution," *Annals of the Institute of Statistical Mathematics, 32*(1)*,* 363-368.

Basu, A.P. (1971). "On a Sequential Rule for Estimating the Location Parameter of an Exponential Distribution," *Naval Research Logistics Quarterly, 18*(3), 329-337.

Bain, L.J. & Engelhardt, M. (1973). "Interval Estimation for the Two-Parameter Double Exponential Distribution," *Technometrics, 15*(4), 875-887.

Baklizi, A. (2008). "Estimation of Pr(X < Y) Using Record Values in the One and Two Parameter Exponential Distributions," *Communications in Statistics - Theory and Methods, 37*(5), 692-698.

Balakrishnan, N. & Sandhu, R.A. (1996). "Best Linear Unbiased and Maximum Likelihood Estimation for Exponential Distributions under General Progressive Type-II Censored Samples," *Sankhyā: The Indian Journal of Statistics, Series B (1960-2002), 58*(1), 1-9.

Beg, M.A. (1980). "On the Estimation of Pr{Y<X} for the Two-Parameter Exponential Distribution," *Metrika, 27*(1), 29-34.

Chakraborti, S., Human, S. W., & Graham, M. A. (2011). "Nonparametric (Distribution-free) Control Charts," Chapter 26 in *Methods and Applications of Statistics in Engineering, Quality and the Physical Sciences*, N. Balakrishnan ed., John Wiley, New York.

Chakraborti, S., Human, S.W., & Graham, M.A. (2009). "Phase I Statistical Process Control Charts: An Overview and Some Results," *Quality Engineering, 21*(1), 52-62.

Chao, M.T. & Cheng, S.W. (1996). "Semicircle Control Chart for Variables Data," *Quality Engineering, 8*(3), 441-446.

Chao, M.T. & Cheng, S.W. (2008). "On 2-D Control Charts," *Quality Technology & Quantitative Management, 5*(3), 243-261.

Chen, G. & Cheng S.W. (1998). "Max Chart: Combining X-bar Chart and S Chart," *Statistica Sinica*, *8*(1998), 263-271.

Chen, G., Cheng, S.W., & Xie H. (2001). "Monitoring Process Mean and Variability with One EWMA Chart," *Journal of Quality Technology, 33*(2), 223-233.

Chen, G. Cheng, S.W., & Xie H. (2004). "A New EWMA Control Chart for Monitoring Both Location and Dispersion," *Quality Technology & Quantitative Management, 1*(2), 217-231.

Cheng, S.W. & Thaga, K. (2006). "Single Variables Control Charts: An Overview," *Quality and Reliability Engineering International, 22*(7), 811-820.

Chengalur, I.N., Arnold, J.C., & Reynolds, M.R., Jr. (1989). Variable Sampling Intervals for Multiparameter Shewhart Charts, *Communications in Statistics - Theory and Methods, 18*(5), 1769-1792.

Cohen, A.C., & Helm, F.R. (1973). "Estimators in the Exponential Distribution," *Technometrics, 15*(2), 415-418.

Costa, A.B.F. & De Magalhães, M.S. (2007), "An Adaptive Chart for Monitoring the Process Mean and Variance," *Quality and Reliability Engineering International, 23*, 821-831.

Costa, A.B.F. & Rahim, M.A. (2004). "Monitoring Process Mean and Variability with One Non-central Chisquare Chart." *Journal of Applied Statistics, 31*(10), 1171-1183.

Costa, A.B.F. & Rahim, M.A. (2006). "A Single EWMA Chart for Monitoring Process Mean and Process Variance," *Quality Technology & Quantitative Management, 3*(3), 295-305.

Domangue, R. & Patch, S.C. (1991) Some Omnibus Exponentially Weighted Moving Average Statistical Process Monitoring Schemes, *Technometrics, 33*(3), 299-313.

Epstein, B. (1960). "Estimation of the Parameters of Two Parameter Exponential Distributions from Censored Samples," *Technometrics, 2*(3), 403-406.

Gan, F.F. (1995). "Joint Monitoring of Process Mean and Variance using Exponentially Weighted Moving Average Control Charts," *Technometrics, 37*(4), 446-453.

Gan, F.F. (1997). "Joint Monitoring of Process Mean and Variance," *Nonlinear Analysis, Proceedings of the 2nd World Congress of Nonlinear Analysis*, USA. 30, 4017-4024.

Gan, F.F., Ting, K.W., & Chang, T.C. (2004). "Interval Charting Schemes for Joint Monitoring of Process Mean and Variance," *Quality and Reliability Engineering International, 20*(4), 291-303.

Govindarajulu, Z. (1966). “Characterization of the Exponential and Power Distributions,” *Scandinavian Actuarial Journal, 1966*(3-4), 132-136.

Hawkins, D.M. (1987). “Self-starting CUSUM charts for Location and Scale,” *The Statistician, 36*(4), 299-315.

Hawkins, D.M. & Deng, Q. (2009). “Combined Charts for Mean and Variance Information,” *Journal of Quality Technology, 41*(4), 415-425.

Hawkins, D. M. & Zamba, K.D. (2005). “Statistical Process Control for Shifts in Mean or Variance Using a Changepoint Formulation,” *Technometrics, 47*, 164-173.

Hogg, R.V., McKean, J.W., and Craig, A.T. (2005). *Introduction to Mathematical Statistics, 6th Edition.* Englewood Cliffs, NJ: Prentice Hall.

Huang, C.C. & Chen F.L. (2010). “Economic Design of Max Charts,” *Communications in Statistics - Theory and Methods, 39*(16), 2961-2976.

Jensen, W., Jones-Farmer, L.A., Champ, C.W., & Woodall, W.H. (2006). “Effects of Parameter Estimation on Control Chart Properties,” *Journal of Quality Technology, 38*(4), 349-364.

Johnson, N.L., & Kotz, S. (1970). *Distributions in Statistics, Volume 1: Continuous Univariate Distributions*, Boston: Houghton Mifflin.

Johnson, N.L., Kotz, S., & Balakrishnan, N. (1994). *Distributions in Statistics, Volume 1: Continuous Univariate Distributions, 2nd Edition.* Boston: Houghton Mifflin.

Kao, S.C. (2010). “Normalization of the Origin-shifted Exponential Distribution for Control Chart Construction,” *Journal of Applied Statistics, 37*(7), 1067-1087.

Karst, O.J. & Polowy, H. (1963). “Sampling Properties of the Median of a Laplace Distribution,” *The American Mathematical Monthly, 70*(6), 628-636.

Kececioglu, D. & Li, D. (1985). “Optimum Two-Sided Confidence Interval for the Location Parameter of the Exponential Distribution,” *Relibility Engineering, 13*(1), 1-10.

Khoo, M. B. C. (2004). “A New Bivariate Control Chart to Monitor the Multivariate Process Mean and Variance Simultaneously,” *Quality Engineering, 17*(1), 109-118.

Khoo, M.B.C., Wu, Z., Chen, C.-H., & Yeong, K.W. (2010a). “Using One EWMA Chart to Jointly Monitor the Process Mean and Variance,” *Computational Statistics, 25*(2), 299–316.

Khoo, M.B.C., Teh, S.Y., & Wu, Y. (2010b). "Monitoring Process Mean and Variability with One Double EWMA Chart," *Communications in Statistics - Theory and Methods, 39*(20), 3678 -3694.

Kotz, S., Kozubowski, T.J., & Podgórski, K. (2001). *The Laplace Distribution and Generalizations: A Revisit with Applications to Communications, Economics, Engineering, and Finance.* Boston: Birkhauser.

Lam, K., Sinha, B.K., & Wu, Z. (1994). "Estimation of Parameters in a Two-Parameter Exponential Distribution Using Ranked Set Sample," *Annals of the Institute of Statistical Mathematics, 46*(4), 723-736.

Li, Z., Zhang, J., & Wang, Z. (2010). "Self-starting Control Chart for Simultaneously Monitoring Process Mean and Variance," *International Journal of Production Research, 48*(15), 4537-4553.

Lu, C.-W. & Reynolds, M.R., Jr (1999). "Control Charts for Monitoring the Mean and Variance of Autocorrelated Processes," *Journal of Quality Technology*, *31*(3), 259-274.

Maboudou-Tchao, E. & Hawkins, D. (2011). "Self-Starting Multivariate Control Charts for Location and Scale," *Journal of Quality Technology, 43*(2), 113-126.

Mahmoud, M.A., Henderson, G.R., Epprecht, E.K., & Woodall, W.H. (2010). "Estimating the Standard Deviation in Quality Control Applications," *Journal of Quality Technology, 42*(4), 348-357.

Memar, A.O.M. & Niaki, S.T.A. (2011). "The Max EWMAMS Control Chart for Joint Monitoring of Process Mean and Variance with Individual Observations," *Quality and Reliability Engineering International, 27*(4), 499-514.

Mukherjee, A. & Chakraborti, S. (2012). "A Distribution-Free Control Chart for Joint Monitoring of Location and Scale," *Quality and Reliability Engineering International, 28*(3), 335-352.

Puig, P. & Stephens, M.A. (2000). "Tests of Fit for the Laplace Distribution, with Applications," *Technometrics, 42*(4), 417-424.

Quesenberry, C.P. (1991). "SPC Q Charts for Start-Up Processes and Short or Long Runs," *Journal of Quality Technology, 23*(3), 213-224.

Rahim, M.A. & Costa, A.B.F. (2000). "Joint Economic Design of Xbar and R Charts under Weibull Shock Models," *International Journal of Production Research, 38*(13), 2871–2889.

Ramalhoto, M.F. & Morais, M. (1999). "Shewhart Control Charts for the Scale Parameter of a Weibull Control Variable with Fixed and Variable Sampling Intervals," *Journal of Applied Statistics, 26*(1), 129-160.

Razmy, A. M. (2005), "Schemes for Joint Monitoring of Process Mean and Process Variance," Masters Thesis, Department of Statistics and Applied Probability, NUS. Singapore.

Reynolds, M.R., Jr. & Cho, G. Y. (2006). "Multivariate Control Charts for Monitoring the Mean Vector and Covariance Matrix," *Journal of Quality Technology*, *38*(3), 230-253.

Reynolds, M.R., Jr. & Cho, G.Y. (2011). "Multivariate Monitoring of the Process Mean and Variability With Variable Sampling Intervals," *Sequential Analysis, 30*(1), 1-40.

Reynolds, M.R., Jr. & Kim, K. (2007). "Multivariate Control Charts for Monitoring the Process Mean and Variability Using Sequential Sampling," *Sequential Analysis, 26*(3), 283-315.

Reynolds, M.R., Jr. & Stoumbos, Z.G. (2001a). "Individuals Control Schemes for Monitoring the Mean and Variance of Processes Subject to Drifts," *Stochastic Analysis and Applications*, *19*(5), 863-892.

Reynolds, M.R., Jr. & Stoumbos, Z.G. (2001b). "Monitoring the Process Mean and Variance Using Individual Observations and Variable Sampling Intervals," *Journal of Quality Technology*, *33*(2), 181-205.

Reynolds, M.R., Jr. & Stoumbos, Z.G. (2004). "Control Charts and the Optimal Allocation of Sampling Resources," *Technometrics*, *46*(2), 200-214.

Reynolds, M.R., Jr. & Stoumbos, Z.G. (2005). "Should Exponentially Weighted Moving Average and Cumulative Sum Charts be used with Shewhart Limits?" *Technometrics, 47*(4), 409-424.

Reynolds, M.R., Jr. & Stoumbos, Z.G. (2006). "Comparisons of Some Exponentially Weighted Moving Average Control Charts for Monitoring the Process Mean and Variance," *Technometrics, 48*(4), 550-567.

Reynolds, M.R., Jr. & Stoumbos, Z.G. (2008). "Combinations of Multivariate Shewhart and MEMWA Control Charts for Monitoring the Mean Vector and Covariance Matrix," *Journal of Quality Technology*, *40*(4), 381-393.

Reynolds, M.R., Jr. & Stoumbos, Z.G. (2010). "Robustness to Non-Normality of CUSUM Control Charts for Monitoring the Process Mean and Variance," *Quality and Reliability Engineering International*, *26*(5), 453-473.

Serel, D. & Moskowitz, H. (2008). "Joint Economic Design of EWMA Control Charts for Mean and Variance," *European Journal of Operational Research, 184*(1), 157-168.

Stoumbos, Z.G. & Reynolds, M.R., Jr. (2005). "Economic Statistical Design of Adaptive Control Schemes for Monitoring the Process Mean and Variance: An Application to Analyzers," *Nonlinear Analysis: Real World Applications*, *6*(5), 817-844.

Sürücü, B. & Sazak, H. S. (2009). "Monitoring Reliability for a Three-Parameter Weibull Distribution," *Reliability Engineering and System Safety, 94*(2), 503-508.

Takahashi, T. (1989). "Simultaneous Control Charts Based on $(\bar{x}, s)$ and $(\bar{x}, R)$ for Multiple Decision on Process Change," *Reports of Statistical Application Research, Union of Japanese Scientists and Engineers, 36*(2), 1-20.

Tanis, E.A. (1964). "Linear Forms in the Order Statistics from an Exponential Distribution," *The Annals of Mathematical Statistics, 35*(1), 270-276.

Thiagarajah, K. & Paul, S.R. (1997). "Interval Estimation for the Scale Parameterof the Two-Parameter Exponential Dsitribution Based on Time-Censored Data," *Journal of Statistical Planning and Inference, 59*(2), 279-289.

Varde, S.D. (1969). "Life Testing and Reliability Estimation for the Two Parameter Exponential Distribution," *Journal of the American Statistical Association, 64*(326), 621-631.

Viveros, R., & Balakrishnan, N. (1994). "Interval Estimation of Parameters of Life from Progressively Censored Data," *Technometrics, 36*(1), 84-91.

Wright, F.T., Engelhardt, M., & Bain, L.J. (1978). "Inferences for the Two-Parameter Exponential Distribution Under Type I Censored Sampling," *Journal of the American Statistical Association, 73*(363), 650-655.

Wu, Z. & Tian, Y. (2005). "Weighted-loss-function CUSUM Chart for Monitoring Mean and Variance of a Production Process," *International Journal of Production Research, 43*(14), 3027-3044.

Wu, Z. & Wang, Q. (2007). "A Single CUSUM Chart Using a Single Observation to Monitor a Variable," *International Journal of Production Research, 45*(3), 719-741.

Wu, Z., Zhang, S., & Wang , P. (2007). "A CUSUM Scheme with Variable Sample Sizes and Sampling Intervals for Monitoring the Process Mean and Variance," *Quality and Reliability Engineering International, 23*(2), 157-170.

Yeh, A.B., Lin, D.K.J., & Venkataramani, C. (2004). "Unified CUSUM Charts for Monitoring Process Mean and Variability," *Quality Technology & Quantitative Management, 1*(1), 65-86.

Zhang J., Li Z., & Wang Z. (2010). "A Multivariate Control Chart for Simultaneously Monitoring Process Mean and Variability," *Computational Statistics & Data Analysis, 54*(10), 2244-2252.

Zhang, J., Zou, C., & Wang, Z. (2010). “A Control Chart Based on Likelihood Ratio Test for Monitoring Process Mean and Variability,” *Quality and Reliability Engineering International, 26*(1), 63-73.

Zhang, J., Zou, C., & Wang, Z. (2011). “A New Chart for Detecting the Process Mean and Variability,” *Communications in Statistics - Simulation and Computation, 40*(5), 728 - 743.

Zhou, Q., Luo, Y., & Wang, Z. (2010). “A Control Chart Based on Likelihood Ratio Test for Detecting Patterned Mean and Variance Shifts,” *Computational Statistics & Data Analysis, 54*(6), 1634-1645.

Zou, C. & Tsung, F. (2010). “Likelihood Ratio-based Distribution-free EWMA Control Charts,” *Journal of Quality Technology*, *42*(2), 174-196.

APPENDIX

A: SUPPLEMENTARY DERIVATIONS FOR CHAPTER 3

A.1 Distribution of W_1^* and W_2^*

Recall that $W_1^* = \Phi^{-1}\{\zeta_{m-1}(W_1)\}$ and $W_2^* = \Phi^{-1}\{F_{m-1,n-1}(W_2)\}$, where $W_1 = \sqrt{\frac{mn}{N}}\frac{(\bar{V}-\bar{U})}{S_U}$ and $W_2 = \frac{S_V^2}{S_U^2}$. First, consider the joint cdf of W_1^* and W_2^*:

$F_{W_1^*,W_2^*}(v_1, v_2) = P[W_1^* \le v_1, W_2^* \le v_2]$

$= P\{W_1 \le \zeta_{m-1}^{-1}(\Phi(\sqrt{v_1}, m-1)),\ W_2 \le F_{n-1,m-1}^{-1}(\Phi(\sqrt{v_2}, n-1, m-1))\}$

$= P[W_1 \le b, W_2 \le d]$, where $b = \zeta_{m-1}^{-1}\{\Phi(\sqrt{v_1})\}$, $d = F_{n-1,m-1}^{-1}\{\Phi(\sqrt{v_2})\}$. Note that since W_1 and W_2 are not independent, the calculation of the joint probability is not straightforward. However, this can be conveniently obtained by conditioning on $\bar{U}$ and S_U^2 or, equivalently, on $Z_U = \frac{\sqrt{m}(\bar{U}-\mu_1)}{\sigma_1}$, $Y_U = \frac{(n-1)S_U^2}{\sigma_1^2}$. To this end, first, conditionally on Z_U and Y_U we can write

$$F_{W_1^*,W_2^*}(v_1, v_2|Z_u, Y_u) = P\left[Z_V \le \sqrt{\frac{N}{n}}\, b\sqrt{\frac{Y_u}{m-1}} + \sqrt{\frac{n}{m}}Z_U + \Delta, T_V \le \frac{(n-1)}{(m-1)}d\tau Y_U\right]$$

where $Z_V = \frac{\sqrt{n}(\bar{V}-\mu_2)}{\sigma_2}$, $T_v = \frac{(n-1)S_V^2}{\sigma_2^2}$, $\tau = \frac{\sigma_1^2}{\sigma_2^2}$ and $\Delta = \frac{\sqrt{n}(\mu_1-\mu_2)}{\sigma_1}$.

Now since Z_V and T_V, have a standard normal and a chi-square distribution with $(n-1)$ degrees of freedom, respectively, and are mutually independent, we have,

$$F_{W_1^*,W_2^*}(v_1, v_2|Z_u, Y_u) = \Phi\left(\tau\left(\sqrt{\frac{N}{n}}\, b\sqrt{\frac{Y_U}{m-1}} + \sqrt{\frac{n}{m}}Z_U + \Delta\right)\right)\left(F_{\chi^2_{(n-1)}}\left(\frac{(n-1)}{(m-1)}d\tau Y_U\right)\right) \text{(*)}$$

Finally, the unconditional cdf of W_1^* and W_2^* can be obtained by calculating the expectation of the conditional cdf in (*) over the distributions of Z_U and Y_U, which are mutually independent and follow the standard normal distribution and the chi-square distribution with $(m-1)$ degrees of freedom, respectively. Thus the unconditional joint cdf of W_1^* and W_2^* is given by:

$$F_{W_1^*,W_2^*}(v_1, v_2)$$

$$= \int_0^\infty \int_{-\infty}^\infty \left\{ \Phi\left[\tau\left(\sqrt{\frac{N}{n}}\, b\sqrt{\frac{y}{m-1}} + \sqrt{\frac{n}{m}}z + \Delta\right)\right]\left[F_{\chi^2_{(n-1)}}\left[\frac{(n-1)}{(m-1)}d\tau y\right]\right]\right\} \phi(z) f_{\chi^2_{(m-1)}}(y)dzdy.$$

RESULT 1.1

Note that in the *IC* case, $\Delta = 0$ and $\tau = 1$, so that from (*) and Result 1.1 it is clear that neither the conditional nor the unconditional joint cdf depends on any nuisance parameters; in other words, the *IC* joint distributions do not depend on any unknown parameters. This result implies that the *IC* run length distributions of all control charts based on W_1^* and W_2^* are free from any nuisance parameters. Hence, for example, the false alarm rates and all *IC* run length distribution characteristics, such as the standard deviation and the percentiles, are all free from any unknown parameters.

A.2 Distribution of $\widehat{\Psi}$

The cdf of the Max chart plotting statistic $\widehat{\Psi}$ can be obtained directly from the above results. For example, for the unconditional cdf, using Result 1.1, we get for any $g > 0$,

$P(\widehat{\Psi} \le g) = P(\max\{|W_1^*|, |W_2^*|\} \le g) = P(h \le W_1^* \le k, c \le W_2^* \le d)$

where $h = \zeta_{m-1}^{-1}\{\Phi(-g)\}$, $k = \zeta_{m-1}^{-1}\{\Phi(g)\}$ $c = F_{n-1,m-1}^{-1}\{\Phi(-g)\}$ and $d = F_{n-1,m-1}^{-1}\{\Phi(g)\}$.

This probability can then be easily found by first noting that $P(h \leq W_1^* \leq k, c \leq W_2^* \leq d) = F(k,d) - F(h,d) - F(k,c) + F(h,c)$ where $F(.,.)$ denotes the cdf of W_1^* and W_2^* given in Result 1.1. Alternatively, a direct calculation can be used to show that the unconditional cdf is given by $P(\widehat{\Psi} \leq g)$

$$= \int_0^\infty \int_{-\infty}^\infty \left\{\Phi\left[\tau\left(\sqrt{\frac{N}{n}}\, k\sqrt{\frac{y}{m-1}} + \sqrt{\frac{n}{m}}z + \Delta\right)\right] - \Phi\left[\tau\left(-\sqrt{\frac{N}{n}}\, h\sqrt{\frac{y}{m-1}} + \sqrt{\frac{n}{m}}z + \Delta\right)\right]\right\}$$

$$\times \left\{F_{\chi^2_{(n-1)}}\left[\frac{(n-1)}{(m-1)}d\tau y\right] - F_{\chi^2_{(n-1)}}\left[\frac{(n-1)}{(m-1)}c\tau y\right]\right\}\phi(z) f_{\chi^2_{(m-1)}}(y)dzdy.$$

RESULT 1.2

A.3 Distribution of $\widehat{\Delta}$

Next consider the distribution of $\widehat{\Delta}$. This can also be obtained in a similar manner using the joint cdf of W_1^* and W_2^*. For example, for the unconditional cdf, for some $g > 0$,

$$P(\widehat{\Delta} \leq g) = P(W_1^{*2} + W_2^{*2} \leq g^2) = \int_{-\infty}^{\infty} \int_{-\sqrt{g^2-v_2}}^{\sqrt{g^2-v_2}} f_{W_1^*,W_2^*}(v_1,v_2) dv_1\, dv_2$$

where $f_{W_1^*,W_2^*}(v_1,v_2)$ is the unconditional joint pdf of (W_1^*, W_2^*) which can be obtained by differentiating the unconditional joint cdf $F_{W_1^*,W_2^*}(v_1,v_2)$ given in Result 1.1.

Alternatively, we can write $P(\widehat{\Delta} \leq g) = \int_0^\infty \int_{-\infty}^\infty P(W_1^{*2} + W_2^{*2} \leq g^2 | Z_U, Y_U)\, dZ_U dY_U$.

Now since $P(W_1^{*2} + W_2^{*2} \leq g^2 | Z_U, Y_U) = \int_{-\infty}^{\infty} \int_{-\sqrt{g^2-v_2}}^{\sqrt{g^2-v_2}} f_{W_1^*,W_2^*}(v_1, v_2 | Z_U, Y_U)\, dv_1 dv_2$, an equivalent expression for the unconditional cdf can be then obtained in terms of the conditional joint pdf of W_1^* and W_2^*

$$P(\widehat{\Delta} \leq g) = \int_0^{\infty} \int_{-\infty}^{\infty} \int_{-\infty}^{\infty} \int_{-\sqrt{g^2-v_2}}^{\sqrt{g^2-v_2}} f_{W_1^*,W_2^*}(v_1, v_2|z_U, y_U)\, dv_1 dv_2\, \phi(z_U) f_{\chi^2_{(m-1)}}(y_U) dz_U dy_U$$

RESULT 1.3

A.4 The $(\bar{X}/S)$ scheme

Consider a two-chart control scheme consisting of an $\bar{X}$ chart and an S chart, in which a signal on either chart is taken as an indication that the process is *OOC*.

The $\bar{X}$ and S charts recommended by Montgomery (2005) are based on 3-sigma control limits, rather than probability limits. Because $\bar{X}$ and S have different statistical distributions, the standards known $\bar{X}$ and S charts with 3-sigma control limits have different *IC ARL*s. The $\bar{X}$ chart has an *IC ARL* of 370.40 regardless of the sample size n, while the *IC ARL* of the S chart depends on n. For Montgomery's S chart, the *IC ARL* is $\frac{1}{P(signal)} = \frac{1}{1-P(LCL<S_i<UCL)} = \frac{1}{1-P(B_5\sigma_0<S_i<B_6\sigma_0)} = \frac{1}{1-\left[F_{\chi^2_{(n-1)}}\left(\frac{(n-1)(B_6\sigma_0)^2}{\sigma_0^2}\right)-F_{\chi^2_{(n-1)}}\left(\frac{(n-1)(B_5\sigma_0)^2}{\sigma_0^2}\right)\right]}$ where S_i is the standard deviation of the *i*th sample, n is the sample size, $B_5 = c_4 - 3\sqrt{1-c_4^2}$ and $B_6 = c_4 + 3\sqrt{1-c_4^2}$ are the sample size-dependent charting constants, and $c_4 = \sqrt{\frac{2}{n-1}}\frac{\Gamma\left(\frac{n}{2}\right)}{\Gamma\left(\frac{n-1}{2}\right)}$. For $n = 5$, Montgomery's S chart has an *IC ARL* of 257.13. The FAR for the combined $(\bar{X}/S)$ scheme is $1 - \left(1 - \frac{1}{(IC\ ARL)_{\bar{X}\text{ chart}}}\right)\left(1 - \frac{1}{(IC\ ARL)_{S\text{ chart}}}\right)$, and the corresponding *IC ARL* is $\frac{1}{FAR}$. The table below shows the *IC ARL* of the charts and the resulting two-chart scheme for various values of n. These values were calculated using Mathcad and confirmed using simulations in R. From the table, it is clear that the FAR of the combined $(\bar{X}, S)$ scheme depends upon n.

Table A.1: *IC ARL* for the $(\bar{X}/S)$ scheme and its component charts when the mean and the standard deviation are known

n	$\bar{X}$ Chart *IC ARL*	S Chart *IC ARL*	$(\bar{X}, S)$ Scheme *IC ARL*
5	370.40	257.13	151.77
15	370.40	350.99	180.22
25	370.40	359.28	182.38

Montgomery's standards unknown $\bar{X}$ and S charts also have 3-sigma control limits. However, because these control limits incorporate parameter estimates obtained from a Phase I data set, their *IC ARL*s depend upon the number of samples *r* in the Phase I data set.[18]

For the $\bar{X}$ chart, the control limits are $\bar{\bar{x}} \pm A_3\bar{s}$ where $\bar{\bar{x}}$ is the grand mean of the Phase I data set, $\bar{s}$ is the mean of the standard deviations of the *r* Phase I samples, and $A_3 = 3/\left(c_4\sqrt{n}\right)$ is the sample size-dependent charting constant. For this chart, a signal occurs anytime a Phase II sample has a sample mean greater than $\bar{\bar{x}} + A_3\bar{s}$ or less than $\bar{\bar{x}} - A_3\bar{s}$.

Likewise, for the S chart, the control limits are $B_3\bar{s}$ and $B_4\bar{s}$, where $B_3 = 1 - \frac{3}{c_4}\sqrt{1 - c_4^2}$ and $B_4 = 1 + \frac{3}{c_4}\sqrt{1 - c_4^2}$ are sample size-dependent charting constants. For this chart, a signal occurs anytime a Phase II sample has a sample standard deviation greater than $B_4\bar{s}$ or less than $B_3\bar{s}$.

It is worth noting that the standards unknown $\bar{X}$ and S charts and the two-chart scheme they comprise do not necessarily have the same *IC ARL* as their standards known counterparts, since the parameter estimation introduces addition variability. Through simulation in R, it is easy to see that a large number of Phase I samples must be used for the parameter estimation in order

[18] Each of the r samples has sample size n, resulting in a total Phase I data set of size $m = rn$.

for the standards unknown *IC ARL*s to be roughly equal to their standards known counterparts.[19] As r increases, the observed *IC ARL* for the standards unknown scheme approaches that of the standards known scheme.

Table A.2: Observed *IC ARL* for the $\left(\frac{\bar{X}}{S}\right)$ scheme and its component charts when the mean and the standard deviation of a Phase I sample are used to estimate μ and σ

n	r	$\bar{X}$ Chart Observed *IC ARL*	S Chart Observed *IC ARL*	$(\bar{X}, S)$ Scheme Observed *IC ARL*
5	10	607.67	1634.11	382.34
5	20	440.15	571.15	233.86
5	50	390.19	339.18	177.97
5	500	370.65	262.80	153.99
15	10	336.75	410.57	174.63
15	20	341.63	401.62	180.07
15	50	356.58	379.00	182.22
15	500	369.65	354.93	181.82
25	10	307.15	340.21	153.58
25	20	327.22	358.26	166.78
25	50	343.98	362.55	176.29
25	500	366.51	360.09	182.35

In order to directly compare a two-chart $(\bar{X}/S)$ scheme to the Modified Max and Distance charts, it is necessary to make some modifications to the $\bar{X}$ and S charts recommended by Montgomery. First, in case K, probability limits should be selected so that $\bar{X}$ and S charts

[19] The precise number r of samples needed is dependent upon the sample size *n*, but in many cases, $r = 50$ is not large enough.

have the same *IC ARL* and the overall *IC ARL* for the scheme is 500. The appropriate control limits for the $\bar{X}$ chart are $\mu_0 \pm \frac{\Phi(1-p_0/2)\sigma_0}{\sqrt{n}}$ while the appropriate control limits for the S chart are $\sqrt{\frac{\sigma_0^2 F_{\chi^2_{(n-1)}}(p_0/2)}{\mathrm{n}-1}}$ and $\sqrt{\frac{\sigma_0^2 F_{\chi^2_{(n-1)}}(1-p_0/2)}{\mathrm{n}-1}}$ where p_0=$\left(1-\sqrt{1-\frac{1}{IC\ ARL}}\right)$.

Next, in case U, we need to select the control limits in a way which accounts for the additional variability caused by the parameter estimation. As for the Max and Distance charts, we accomplish this using the conditioning technique described in section 3.4.

Recall that $U_1, U_2, \ldots, U_m$ is a random sample of size m from normal distribution with unknown mean μ_1 and variance σ_1^2, that $V_1, V_2, \ldots, V_n$ is a random sample of size n, likewise from the normal distribution, with unknown mean μ_2 and variance and σ_2^2, and that the U's and the V's are mutually independent. Next, recall that the sample means $\bar{U}$ and $\bar{V}$ are normally distributed with mean and variance μ_1 and $\frac{\sigma_1^2}{m}$ and μ_2 and $\frac{\sigma_2^2}{n}$, respectively, that $\frac{(m-1)S_U^2}{\sigma_1^2}$ is distributed as a chi-square with $(m-1)$ degrees of freedom, that $\frac{(n-1)S_V^2}{\sigma_2^2}$ is distributed as a chi-square with $(n-1)$ degrees of freedom, and that $\bar{U}$, $\bar{V}$, S_U^2, and S_V^2 are mutually independent.

Recall that for the case K $\bar{X}$ chart, plotting statistic is $\bar{V}$ and the control limits are $\mu_0 \pm \frac{\Phi(1-p_0/2)\sigma_0}{\sqrt{n}}$. In case U, the plotting statistic is still $\bar{V}$, but since μ_0 and σ_0 are unknown, the new control limits $\bar{U} \pm \frac{\Phi\left(1-\frac{p_0}{2}\right)S_U}{\sqrt{n}}$ are obtained by plugging in $\bar{U}$ and S_U for μ_0 and σ_0. Likewise, for the case U S chart, S_V is the plotting statistic, and the control limits are $\sqrt{\frac{S_U^2 F_{\chi^2_{(n-1)}}\left(\frac{p_0}{2}\right)}{n-1}}$ and $\sqrt{\frac{S_U^2 F_{\chi^2_{(n-1)}}\left(1-\frac{p_0}{2}\right)}{n-1}}$.

Now, in order for the scheme to have a particular *IC ARL*, the appropriate percentile p_0 must be obtained by considering the joint distribution of the two plotting statistics. For each sample, $P(no\ signal) = P(LCL_{\bar{X}\text{ chart}} \leq \bar{V} \leq UCL_{\bar{X}\text{ chart}}, LCL_{S\text{ chart}} \leq S_V \leq UCL_{S\text{ chart}}) =$

$$P\left(\bar{U} - \frac{\Phi\left(1-\frac{p_0}{2}\right)S_U}{\sqrt{n}} \leq \bar{V} \leq \bar{U} + \frac{\Phi\left(1-\frac{p_0}{2}\right)S_U}{\sqrt{n}}, \sqrt{\frac{S_U^2 F_{\chi^2_{(n-1)}}\left(1-\frac{p_0}{2}\right)}{n-1}} \leq S_V \leq \sqrt{\frac{S_U^2 F_{\chi^2_{(n-1)}}\left(\frac{p_0}{2}\right)}{n-1}}\right) =$$

$\int_0^\infty \int_{-\infty}^\infty p'(z_U, y_U)\phi(z) f_{\chi^2_{(m-1)}} dzdy$ where $p'(z_U, y_U) = \left[\Phi\left(\frac{\sqrt{n}}{\sqrt{m}}\frac{\sigma_1}{\sigma_2}z_U + \left(\frac{\sigma_1}{\sigma_2}\frac{\sqrt{y_U}}{\sqrt{m-1}}\Phi^{-1}\left(1 - \frac{p_0}{2}\right) + \frac{\sqrt{n}(\mu_1-\mu_2)}{\sigma_2}\right)\right) - \Phi\left(\frac{\sqrt{n}}{\sqrt{m}}\frac{\sigma_1}{\sigma_2}z_U - \left(\frac{\sigma_1}{\sigma_2}\frac{\sqrt{y_U}}{\sqrt{m-1}}\Phi^{-1}\left(1 - \frac{p_0}{2}\right) + \frac{\sqrt{n}(\mu_1-\mu_2)}{\sigma_2}\right)\right)\right] \times$

$\left[F_{\chi^2_{(n-1)}}\left(\frac{\sigma_1^2}{\sigma_2^2}\frac{F^{-1}_{\chi^2_{(n-1)}}\left(1-\frac{p_0}{2}\right)}{m-1}y_U\right) - F_{\chi^2_{(n-1)}}\left(\frac{\sigma_1^2}{\sigma_2^2}\frac{F^{-1}_{\chi^2_{(n-1)}}\left(\frac{p_0}{2}\right)}{m-1}y_U\right)\right]$. The conditional *IC ARL* of the $(\bar{X}, S)$ scheme equals $[1 - p(Z_U, Y_U)]^{-1}$ and the unconditional *IC ARL* is given by

$\int_0^\infty \int_{-\infty}^\infty [1 - p(z_U, y_U)]^{-1}\phi(z_U) f_{\chi^2_{(m-1)}}(y_U) dz_U dy_U$. Using Mathcad, one can evaluate this equation and obtain the value of p_0 which results in the specified *IC ARL*.

B: ADDITIONAL TABLES AND FIGURES FOR CHAPTER 3

Table B.1: Run length characteristics for the modified normal theory schemes for various values of μ_2 and σ_2 when $\mu_1 = 0, \sigma_1 = 1, m = 100$, and $n = 5$

		MODIFIED MAX CHART (H=3.20)			MODIFIED DISTANCE CHART (H=3.43)			MODIFIED $(\bar{X}, S)$ SCHEME (p_0=0.000912)		
μ_2	σ_2	*ARL*	*SDRL*	*5%, 25%, 50%, 75%, 95%*	*ARL*	*SDRL*	*5%, 25%, 50%, 75%, 95%*	*ARL*	*SDRL*	*5%, 25%, 50%, 75%, 95%*
0	*1*	**499.48**	585.21	20, 117, 299, 662, 1660	**497.03**	602.45	19, 110, 294, 650, 1677	**501.06**	629.24	17, 104, 282, 650, 1731
0.1	*1*	**461.62**	547.08	18, 104, 272, 608, 1558	**454.98**	563.96	17, 97, 259, 594, 1564	**456.46**	585.99	16, 92, 252, 586, 1599
0.25	*1*	**310.58**	408.36	10, 62, 168, 393, 1093	**299.50**	404.29	10, 59, 157, 376, 1087	**298.27**	422.03	9, 54, 149, 366, 1098
0.5	*1*	**101.59**	152.50	4, 19, 51, 120, 368	**99.06**	150.93	3, 18, 49, 118, 363	**91.27**	150.44	3, 16, 43, 104, 333
0.75	*1*	**28.84**	45.52	1, 6, 15, 34, 102	**28.96**	42.33	1, 6, 15, 35, 100	**25.20**	38.88	1, 5, 13, 30, 89
1	*1*	**9.55**	12.99	1, 2, 5, 12, 31	**10.16**	13.45	1, 3, 6, 13, 33	**8.51**	11.29	1, 2, 5, 10, 28
1.25	*1*	**3.96**	4.29	1, 1, 3, 5, 12	**4.44**	5.11	1, 1, 3, 5, 14	**3.69**	3.97	1, 1, 2, 5, 11
1.5	*1*	**2.17**	1.86	1, 1, 2, 3, 6	**2.38**	2.14	1, 1, 2, 3, 6	**2.06**	1.72	1, 1, 1, 2, 5
2	*1*	**1.17**	0.44	1, 1, 1, 1, 2	**1.22**	0.55	1, 1, 1, 1, 2	**1.16**	0.46	1, 1, 1, 1, 2
3	*1*	**1.00**	0.02	1, 1, 1, 1, 1	**1.00**	0.04	1, 1, 1, 1, 1	**1.00**	0.03	1, 1, 1, 1, 1
0	*1.25*	**73.87**	110.32	3, 15, 38, 88, 260	**65.12**	101.1	2, 12, 33, 77, 233	**59.86**	89.34	2, 12, 31, 72, 210
0.1	*1.25*	**70.92**	106.82	3, 14, 37, 85, 253	**61.48**	94.86	2, 12, 31, 73, 221	**58.05**	86.24	2, 12, 30, 70, 204
0.25	*1.25*	**53.97**	79.65	2, 11, 29, 66, 185	**46.46**	69.77	2, 9, 24, 56, 163	**45.25**	67.06	2, 10, 24, 54, 158
0.5	*1.25*	**26.59**	36.88	1, 6, 15, 33, 91	**23.19**	33.51	1, 5, 13, 28, 80	**22.86**	31.00	1, 5, 13, 28, 77
0.75	*1.25*	**11.96**	14.80	1, 3, 7, 15, 38	**10.98**	13.97	1, 3, 6, 14, 36	**10.70**	13.19	1, 3, 6, 13, 34
1	*1.25*	**5.79**	6.35	1, 2, 4, 7, 18	**5.53**	6.27	1, 2, 4, 7, 17	**5.34**	5.84	1, 2, 3, 7, 16
1.25	*1.25*	**3.26**	3.10	1, 1, 2, 4, 9	**3.19**	3.06	1, 1, 2, 4, 9	**3.04**	2.84	1, 1, 2, 4, 8
1.5	*1.25*	**2.11**	1.69	1, 1, 2, 3, 5	**2.09**	1.70	1, 1, 1, 3, 5	**2.00**	1.56	1, 1, 1, 2, 5
2	*1.25*	**1.24**	0.55	1, 1, 1, 1, 2	**1.26**	0.61	1, 1, 1, 1, 2	**1.23**	0.56	1, 1, 1, 1, 2
3	*1.25*	**1.00**	0.07	1, 1, 1, 1, 1	**1.01**	0.07	1, 1, 1, 1, 1	**1.00**	0.06	1, 1, 1, 1, 1
0	*1. 5*	**14.94**	19.05	1, 4, 9, 19, 48	**12.53**	15.70	1, 3, 7, 16, 41	**12.63**	15.58	1, 3, 8, 16, 41
0.1	*1.5*	**14.56**	18.20	1, 4, 9, 19, 47	**12.26**	15.39	1, 3, 7, 15, 39	**12.45**	15.27	1, 3, 8, 16, 40
0.25	*1.5*	**13.1**	16.06	1, 4, 8, 17, 42	**10.89**	13.17	1, 3, 7, 14, 35	**11.30**	13.62	1, 3, 7, 14, 36
0.5	*1.5*	**9.40**	11.03	1, 3, 6, 12, 29	**7.92**	9.17	1, 2, 5, 10, 25	**8.33**	9.44	1, 2, 4, 7, 17
0.75	*1.5*	**6.14**	6.74	1, 2, 4, 8, 19	**5.17**	5.60	1, 2, 3, 7, 15	**5.53**	5.85	1, 2, 4, 7, 17
1	*1.5*	**3.97**	3.98	1, 1, 3, 5, 11	**3.45**	3.30	1, 1, 2, 4, 10	**3.69**	3.57	1, 1, 3, 5, 10
1.25	*1.5*	**2.71**	2.37	1, 1, 2, 3, 7	**2.46**	2.10	1, 1, 2, 3, 7	**2.56**	2.19	1, 1, 2, 3, 7
1.5	*1.5*	**1.97**	1.48	1, 1, 1, 2, 5	**1.82**	1.29	1, 1, 1, 2, 4	**1.89**	1.39	1, 1, 1, 2, 5
2	*1.5*	**1.29**	0.61	1, 1, 1, 1, 3	**1.26**	0.60	1, 1, 1, 1, 2	**1.28**	0.62	1, 1, 1, 1, 2
3	*1.5*	**1.01**	0.12	1, 1, 1, 1, 1	**1.01**	0.12	1, 1, 1, 1, 1	**1.01**	0.12	1, 1, 1, 1, 1
0	*1.75*	**5.63**	5.85	1, 2, 4, 7, 17	**4.92**	5.07	1, 2, 3, 6, 15	**5.09**	5.26	1, 2, 3, 7, 15
0.1	*1.75*	**5.65**	5.97	1, 2, 4, 7, 17	**4.85**	5.08	1, 2, 3, 6, 15	**5.01**	5.16	1, 2, 3, 6, 15
0.25	*1.75*	**5.36**	5.59	1, 2, 4, 7, 16	**4.60**	4.78	1, 2, 3, 6, 13	**4.81**	4.88	1, 2, 3, 6, 14
0.5	*1.75*	**4.60**	4.65	1, 2, 3, 6, 13	**3.84**	3.71	1, 1, 3, 5, 11	**4.14**	4.09	1, 1, 3, 5, 12
0.75	*1.75*	**3.65**	3.43	1, 1, 3, 5, 10	**3.13**	2.89	1, 1, 2, 4, 9	**3.36**	3.13	1, 1, 2, 4, 9
1	*1.75*	**2.86**	2.51	1, 1, 2, 4, 8	**2.46**	2.07	1, 1, 2, 3, 6	**2.67**	2.30	1, 1, 2, 3, 7
1.25	*1.75*	**2.23**	1.76	1, 1, 2, 3, 6	**1.97**	1.46	1, 1, 1, 2, 5	**2.13**	1.66	1, 1, 2, 3, 5
1.5	*1.75*	**1.80**	1.28	1, 1, 1, 2, 4	**1.64**	1.08	1, 1, 1, 2, 4	**1.73**	1.18	1, 1, 1, 2, 4
2	*1.75*	**1.30**	0.62	1, 1, 1, 1, 3	**1.25**	0.58	1, 1, 1, 1, 2	**1.28**	0.62	1, 1, 1, 1, 2
3	*1.75*	**1.03**	0.16	1, 1, 1, 1, 1	**1.02**	0.15	1, 1, 1, 1, 1	**1.02**	0.16	1, 1, 1, 1, 1
0	*2*	**3.15**	2.91	1, 1, 2, 4, 9	**2.81**	2.47	1, 1, 2, 4, 8	**2.94**	2.59	1, 1, 2, 4, 8
0.1	*2*	**3.16**	2.88	1, 1, 2, 4, 9	**2.81**	2.47	1, 1, 2, 4, 8	**2.92**	2.58	1, 1, 2, 4, 8
0.25	*2*	**3.08**	2.79	1, 1, 2, 4, 8	**2.75**	2.36	1, 1, 2, 3, 7	**2.85**	2.48	1, 1, 2, 4, 8
0.5	*2*	**2.84**	2.48	1, 1, 2, 4, 8	**2.50**	2.12	1, 1, 2, 3, 7	**2.63**	2.22	1, 1, 2, 3, 7
0.75	*2*	**2.50**	2.08	1, 1, 2, 3, 7	**2.22**	1.77	1, 1, 2, 3, 6	**2.34**	1.91	1, 1, 2, 3, 6
1	*2*	**2.16**	1.68	1, 1, 2, 3, 5	**1.91**	1.39	1, 1, 1, 2, 5	**2.06**	1.56	1, 1, 1, 3, 5
1.25	*2*	**1.86**	1.33	1, 1, 1, 2, 4	**1.68**	1.12	1, 1, 1, 2, 4	**1.78**	1.24	1, 1, 1, 2, 4
1.5	*2*	**1.61**	1.04	1, 1, 1, 2, 4	**1.48**	0.88	1, 1, 1, 2, 3	**1.56**	0.97	1, 1, 1, 2, 3
2	*2*	**1.27**	0.59	1, 1, 1, 1, 2	**1.22**	0.53	1, 1, 1, 1, 1	**1.26**	0.58	1, 1, 1, 1, 2
3	*2*	**1.04**	0.20	1, 1, 1, 1, 1	**1.03**	0.18	1, 1, 1, 1, 1	**1.04**	0.20	1, 1, 1, 1, 1

Table B.2: Run length characteristics for the modified normal theory schemes for various values of μ_2 and σ_2 when $\mu_1 = 0, \sigma_1 = 1, m = 75$, and $n = 5$

		MAX CHART (H=3.18)			DISTANCE CHART (3.41)			$(\bar{X}, S)$ SCHEME (p_0=0.000886)		
μ_2	σ_2	ARL	SDRL	5%, 25%, 50%, 75%, 95%	ARL	SDRL	5%, 25%, 50%, 75%, 95%	ARL	SDRL	5%, 25%, 50%, 75%, 95%
0	1	**503.99**	603.43	19, 111, 296, 665, 1681	**491.25**	594.13	17, 104, 282, 658, 1685	**499.58**	655.94	16, 95, 267, 640, 1784
0.1	1	**461.88**	551.51	16, 100, 271, 612, 1575	**462.46**	574.37	15, 94, 258, 605, 1626	**464.04**	621.32	14, 85, 242, 588, 1675
0.25	1	**324.88**	430.83	10, 61, 170, 413, 1176	**316.19**	438.47	9, 56, 158, 392, 1166	**312.01**	465.18	8, 51, 146, 373, 1185
0.5	1	**118.29**	195.28	3, 18, 52, 134, 458	**109.16**	174.43	3, 18, 50, 126, 407	**101.89**	181.25	3, 15, 43, 110, 393
0.75	1	**33.61**	56.24	1, 6, 16, 38, 124	**33.07**	52.84	1, 6, 16, 38, 121	**27.99**	48.26	1, 5, 13, 31, 101
1	1	**10.83**	16.62	1, 3, 6, 13, 37	**11.41**	16.67	1, 3, 6, 14, 39	**9.16**	13.47	1, 2, 5, 11, 31
1.25	1	**4.44**	5.37	1, 1, 3, 5, 14	**4.79**	5.86	1, 1, 3, 6, 15	**3.90**	4.60	1, 1, 2, 5, 12
1.5	1	**2.31**	2.25	1, 1, 2, 3, 6	**2.49**	2.38	1, 1, 2, 3, 7	**2.12**	1.88	1, 1, 1, 3, 6
2	1	**1.19**	0.49	1, 1, 1, 1, 2	**1.26**	0.63	1, 1, 1, 1, 2	**1.17**	0.49	1, 1, 1, 1, 2
3	1	**1.00**	0.03	1, 1, 1, 1, 1	**1.00**	0.04	1, 1, 1, 1, 1	**1.00**	0.03	1, 1, 1, 1, 1
0	1.25	**85.13**	135.49	3, 15, 41, 99, 310	**75.80**	129.69	3, 13, 35, 85, 278	**65.14**	109.56	2, 12, 31, 75, 237
0.1	1.25	**80.80**	131.16	3, 14, 38, 93, 302	**70.48**	117.14	2, 12, 32, 81, 260	**62.36**	103.26	2, 11, 30, 71, 228
0.25	1.25	**62.65**	103.21	2, 11, 30, 72, 229	**54.93**	95.41	2, 10, 25, 62, 201	**48.79**	81.12	2, 9, 24, 56, 177
0.5	1.25	**30.58**	47.03	1, 6, 16, 36, 110	**26.33**	42.58	1, 5, 13, 31, 92	**24.63**	37.75	1, 5, 13, 29, 85
0.75	1.25	**13.22**	18.38	1, 3, 7, 16, 44	**11.99**	16.94	1, 3, 7, 15, 40	**11.27**	15.17	1, 3, 6, 14, 37
1	1.25	**6.39**	7.68	1, 2, 4, 8, 20	**6.07**	7.43	1, 2, 4, 8, 19	**5.55**	6.53	1, 2, 3, 7, 17
1.25	1.25	**3.47**	3.66	1, 1, 2, 4, 10	**3.43**	3.69	1, 1, 2, 4, 10	**3.14**	3.12	1, 1, 2, 4, 9
1.5	1.25	**2.16**	1.83	1, 1, 2, 3, 6	**2.21**	1.90	1, 1, 2, 3, 6	**2.04**	1.65	1, 1, 1, 2, 5
2	1.25	**1.26**	0.56	1, 1, 1, 1, 2	**1.29**	0.67	1, 1, 1, 1, 3	**1.24**	0.58	1, 1, 1, 1, 2
3	1.25	**1.01**	0.07	1, 1, 1, 1, 1	**1.01**	0.09	1, 1, 1, 1, 1	**1.00**	0.07	1, 1, 1, 1, 1
0	1. 5	**16.73**	23.26	1, 4, 9, 20, 56	**13.74**	18.60	1, 3, 8, 17, 46	**13.41**	18.23	1, 3, 8, 16, 44
0.1	1.5	**16.33**	21.98	1, 4, 9, 20, 55	**13.62**	19.43	1, 3, 7, 17, 45	**13.12**	17.65	1, 3, 7, 16, 44
0.25	1.5	**14.46**	19.93	1, 4, 8, 18, 48	**12.11**	16.26	1, 3, 7, 15, 40	**11.83**	15.76	1, 3, 7, 15, 39
0.5	1.5	**10.36**	13.38	1, 3, 6, 13, 34	**8.59**	10.97	1, 2, 5, 11, 28	**8.70**	10.66	1, 2, 5, 11, 28
0.75	1.5	**6.65**	7.68	1, 2, 4, 8, 21	**5.57**	6.49	1, 2, 3, 7, 17	**5.77**	6.47	1, 2, 4, 7, 18
1	1.5	**4.25**	4.55	1, 1, 3, 5, 13	**3.64**	3.77	1, 1, 2, 5, 11	**3.79**	3.83	1, 1, 3, 5, 11
1.25	1.5	**2.83**	2.58	1, 1, 2, 4, 8	**2.54**	2.30	1, 1, 2, 3, 7	**2.60**	2.32	1, 1, 2, 3 , 7
1.5	1.5	**2.04**	1.59	1, 1, 1, 2, 5	**1.90**	1.45	1, 1, 1, 2, 5	**1.92**	1.47	1, 1, 1, 2, 5
2	1.5	**1.29**	0.62	1, 1, 1, 1, 3	**1.29**	0.65	1, 1, 1, 1, 3	**1.28**	0.64	1, 1, 1, 1, 3
3	1.5	**1.02**	0.13	1, 1, 1, 1, 1	**1.01**	0.12	1, 1, 1, 1, 1	**1.01**	0.12	1, 1, 1, 1, 1
0	1.75	**6.13**	6.91	1, 2, 4, 8, 19	**5.21**	5.83	1, 2, 3, 7, 16	**5.23**	5.65	1, 2, 3, 7, 16
0.1	1.75	**6.08**	6.86	1, 2, 4, 8, 19	**5.15**	5.66	1, 2, 3, 7, 16	**5.17**	5.64	1, 2, 3, 7, 16
0.25	1.75	**5.76**	6.48	1, 2, 4, 7, 18	**4.85**	5.18	1, 2, 3, 6, 14	**4.94**	5.29	1, 2, 3, 6, 15
0.5	1.75	**4.87**	5.22	1, 2, 3, 6, 14	**4.09**	4.23	1, 1, 3, 5, 12	**4.28**	4.45	1, 1, 3, 5, 13
0.75	1.75	**3.86**	3.96	1, 1, 3, 5, 11	**3.25**	3.13	1, 1, 2, 4, 9	**3.45**	3.38	1, 1, 2, 4, 10
1	1.75	**2.99**	2.80	1, 1, 2, 4, 8	**2.54**	2.22	1, 1, 2, 3, 7	**2.71**	2.41	1, 1, 2, 3, 7
1.25	1.75	**2.31**	1.95	1, 1, 2, 3, 6	**2.04**	1.60	1, 1, 1, 2, 5	**2.16**	1.73	1, 1, 2, 3, 5
1.5	1.75	**1.84**	1.35	1, 1, 1, 2, 4	**1.66**	1.12	1, 1, 1, 2, 4	**1.75**	1.23	1, 1, 1, 2, 4
2	1.75	**1.31**	0.64	1, 1, 1, 1, 3	**1.27**	0.61	1, 1, 1, 1, 2	**1.29**	0.63	1, 1, 1, 1, 3
3	1.75	**1.03**	0.17	1, 1, 1, 1, 1	**1.02**	0.16	1, 1, 1, 1, 1	**1.03**	0.16	1, 1, 1, 1, 1
0	2	**3.33**	3.20	1, 1, 2, 4, 9	**2.94**	2.75	1, 1, 2, 4, 8	**2.97**	2.74	1, 1, 2, 4, 8
0.1	2	**3.28**	3.11	1, 1, 2, 4, 9	**2.90**	2.62	1, 1, 2, 4, 8	**2.97**	2.72	1, 1, 2, 4, 8
0.25	2	**3.19**	2.96	1, 1, 2, 4, 9	**2.83**	2.53	1, 1, 2, 4, 8	**2.89**	2.63	1, 1, 2, 4, 8
0.5	2	**2.99**	2.72	1, 1, 2, 4, 8	**2.60**	2.25	1, 1, 2, 3, 7	**2.68**	2.35	1, 1, 2, 3, 7
0.75	2	**2.60**	2.25	1, 1, 2, 3, 7	**2.27**	1.84	1, 1, 2, 3, 6	**2.39**	1.99	1, 1, 2, 3, 6
1	2	**2.25**	1.83	1, 1, 2, 3, 6	**1.97**	1.49	1, 1, 1, 2, 5	**2.08**	1.63	1, 1, 2, 3, 5
1.25	2	**1.92**	1.44	1, 1, 1, 2, 5	**1.71**	1.20	1, 1, 1, 2, 4	**1.80**	1.28	1, 1, 1, 2, 4
1.5	2	**1.65**	1.09	1, 1, 1, 2, 4	**1.51**	0.93	1, 1, 1, 2, 3	**1.57**	1.01	1, 1, 1, 2, 4
2	2	**1.28**	0.60	1, 1, 1, 1, 2	**1.23**	0.56	1, 1, 1, 1, 2	**1.27**	0.60	1, 1, 1, 1, 2
3	2	**1.04**	0.21	1, 1, 1, 1, 1	**1.03**	0.18	1, 1, 1, 1, 1	**1.04**	0.20	1, 1, 1, 1, 1

Table B.3: Run length characteristics for the modified normal theory schemes for various values of μ_2 and σ_2 when $\mu_1 = 0, \sigma_1 = 1, m = 50$, and $n = 5$

		MAX CHART (H=3.15)			DISTANCE CHART (H=3.37)			$(\bar{X}, S)$ SCHEME (p_0=0.000839)		
μ_2	σ_2	*ARL*	*SDRL*	*5%, 25%, 50%, 75%, 95%*	*ARL*	*SDRL*	*5%, 25%, 50%, 75%, 95%*	*ARL*	*SDRL*	*5%, 25%, 50%, 75%, 95%*
0	*1*	**500.60**	591.78	17, 106, 296, 677, 1668	**501.75**	624.95	15, 97, 280, 668, 1736	**498.96**	689.19	12, 80, 243, 634, 1862
0.1	*1*	**471.16**	572.24	15, 96, 271, 633, 1607	**465.47**	589.63	13, 86, 255, 617, 1629	**466.31**	657.85	11, 72, 220, 585, 1756
0.25	*1*	**354.26**	479.14	9, 61, 181, 453, 1285	**337.83**	468.38	9, 56, 170, 429, 1242	**337.09**	538.68	7, 44, 141, 394, 1345
0.5	*1*	**151.59**	252.00	3, 20, 60, 170, 613	**135.11**	221.33	3, 19, 57, 155, 533	**121.94**	245.31	3, 14, 43, 120, 501
0.75	*1*	**48.16**	97.48	1, 6, 18, 48, 189	**44.02**	78.95	1, 7, 18, 48, 174	**34.70**	75.53	1, 5, 13, 34, 132
1	*1*	**15.14**	32.71	1, 3, 6, 15, 54	**14.94**	26.04	1, 3, 7, 16, 54	**10.92**	21.82	1, 2, 5, 12, 38
1.25	*1*	**5.62**	9.61	1, 1, 3, 6, 18	**5.95**	9.03	1, 1, 3, 7, 20	**4.34**	6.58	1, 1, 2, 5, 14
1.5	*1*	**2.66**	3.05	1, 1, 2, 3, 8	**2.89**	3.40	1, 1, 2, 3, 9	**2.27**	2.41	1, 1, 1, 3, 6
2	*1*	**1.23**	0.53	1, 1, 1, 1, 2	**1.33**	0.81	1, 1, 1, 1, 3	**1.20**	0.56	1, 1, 1, 1, 2
3	*1*	**1.00**	0.05	1, 1, 1, 1, 1	**1.00**	0.06	1, 1, 1, 1, 1	**1.00**	0.03	1, 1, 1, 1, 1
0	*1.25*	**114.75**	200.24	3, 17, 47, 125, 455	**100.63**	197.90	3, 14, 39, 104, 388	**75.23**	146.21	2, 11, 30, 78, 289
0.1	*1.25*	**110.73**	204.36	3, 15, 44, 118, 430	**93.41**	174.47	2, 12, 37, 99, 363	**72.32**	143.09	2, 10, 29, 75, 278
0.25	*1.25*	**85.04**	155.96	2, 12, 35, 91, 332	**73.31**	143.96	2, 10, 28, 75, 290	**57.15**	117.33	2, 9, 23, 59, 215
0.5	*1.25*	**41.20**	79.53	1, 7, 18, 43, 154	**36.09**	74.08	1, 6, 15, 37, 137	**28.39**	55.74	1, 5, 13, 30, 102
0.75	*1.25*	**17.38**	31.95	1, 3, 8, 19, 61	**15.45**	26.94	1, 3, 7, 17, 56	**12.82**	21.88	1, 3, 6, 14, 44
1	*1.25*	**7.72**	11.11	1, 2, 4, 9, 26	**7.32**	10.96	1, 2, 4, 8, 24	**6.04**	8.24	1, 2, 3, 7, 19
1.25	*1.25*	**3.94**	4.73	1, 1, 2, 5, 12	**3.88**	4.91	1, 1, 2, 5, 12	**3.34**	3.75	1, 1, 2, 4, 10
1.5	*1.25*	**2.43**	2.37	1, 1, 2, 3, 7	**2.40**	2.36	1, 1, 2, 3, 7	**2.13**	1.93	1, 1, 1, 3, 6
2	*1.25*	**1.29**	0.60	1, 1, 1, 1, 2	**1.34**	0.78	1, 1, 1, 1, 3	**1.26**	0.62	1, 1, 1, 1, 2
3	*1.25*	**1.01**	0.09	1, 1, 1, 1, 1	**1.01**	0.10	1, 1, 1, 1, 1	**1.01**	0.08	1, 1, 1, 1, 1
0	*1. 5*	**21.84**	37.12	1, 4, 10, 25, 78	**18.11**	33.54	1, 3, 9, 20, 64	**14.81**	23.88	1, 3, 8, 17, 52
0.1	*1.5*	**21.70**	36.46	1, 4, 11, 24, 77	**17.31**	29.54	1, 3, 8, 20, 62	**14.56**	23.74	1, 3, 7, 17, 51
0.25	*1.5*	**18.80**	31.04	1, 4, 9, 22, 67	**15.16**	25.66	1, 3, 8, 17, 53	**12.96**	19.49	1, 3, 7, 15, 44
0.5	*1.5*	**13.08**	20.65	1, 3, 7, 15, 45	**10.38**	16.68	1, 2, 5, 12, 35	**9.44**	13.99	1, 2, 5, 11, 31
0.75	*1.5*	**7.83**	10.69	1, 2, 4, 9, 26	**6.58**	9.21	1, 2, 4, 8, 21	**6.21**	8.12	1, 2, 4, 8, 20
1	*1.5*	**4.83**	5.95	1, 1, 3, 6, 15	**4.11**	4.89	1, 1, 3, 5, 12	**3.99**	4.52	1, 1, 3, 5, 12
1.25	*1.5*	**3.15**	3.17	1, 1, 2, 4, 9	**2.79**	2.92	1, 1, 2, 3, 8	**2.72**	2.64	1, 1, 2, 3, 8
1.5	*1.5*	**2.19**	1.86	1, 1, 2, 3, 6	**2.02**	1.71	1, 1, 1, 2, 5	**1.98**	1.61	1, 1, 1, 2, 5
2	*1.5*	**1.33**	0.67	1, 1, 1, 2, 3	**1.33**	0.72	1, 1, 1, 1, 3	**1.30**	0.67	1, 1, 1, 1, 3
3	*1.5*	**1.02**	0.15	1, 1, 1, 1, 1	**1.02**	0.14	1, 1, 1, 1, 1	**1.02**	0.13	1, 1, 1, 1, 1
0	*1.75*	**7.28**	10.63	1, 2, 4, 9, 23	**6.05**	7.77	1, 2, 4, 7, 19	**5.53**	6.79	1, 2, 3, 7, 17
0.1	*1.75*	**7.29**	10.03	1, 2, 4, 9, 24	**5.97**	7.87	1, 2, 4, 7, 19	**5.48**	6.66	1, 2, 3, 7, 17
0.25	*1.75*	**6.95**	9.41	1, 2, 4, 8, 22	**5.57**	6.94	1, 2, 3, 7, 17	**5.23**	6.30	1, 2, 3, 6, 16
0.5	*1.75*	**5.63**	6.74	1, 2, 3, 7, 18	**4.65**	5.54	1, 1, 3, 6, 14	**4.49**	5.17	1, 1, 3, 6, 14
0.75	*1.75*	**4.35**	4.95	1, 1, 3, 5, 13	**3.63**	4.19	1, 1, 2, 4, 11	**3.59**	3.79	1, 1, 2, 4, 11
1	*1.75*	**3.28**	3.36	1, 1, 2, 4, 9	**2.75**	2.66	1, 1, 2, 3, 8	**2.81**	2.70	1, 1, 2, 3, 8
1.25	*1.75*	**2.50**	2.27	1, 1, 2, 3, 7	**2.17**	1.85	1, 1, 2, 3, 6	**2.20**	1.86	1, 1, 2, 3, 6
1.5	*1.75*	**1.96**	1.57	1, 1, 1, 2, 5	**1.76**	1.33	1, 1, 1, 2, 4	**1.78**	1.33	1, 1, 1, 2, 4
2	*1.75*	**1.34**	0.68	1, 1, 1, 2, 3	**1.30**	0.66	1, 1, 1, 1, 3	**1.30**	0.67	1, 1, 1, 1, 3
3	*1.75*	**1.03**	0.19	1, 1, 1, 1, 1	**1.03**	0.18	1, 1, 1, 1, 1	**1.03**	0.17	1, 1, 1, 1, 1
0	*2*	**3.72**	3.96	1, 1, 2, 5, 11	**3.20**	3.21	1, 1, 2, 4, 9	**3.09**	3.05	1, 1, 2, 4, 9
0.1	*2*	**3.66**	3.79	1, 1, 2, 5, 10	**3.23**	3.40	1, 1, 2, 4, 9	**3.05**	3.00	1, 1, 2, 4, 9
0.25	*2*	**3.62**	3.93	1, 1, 2, 5, 10	**3.15**	3.14	1, 1, 2, 4, 9	**3.00**	2.94	1, 1, 2, 4, 8
0.5	*2*	**3.29**	3.38	1, 1, 2, 4, 10	**2.80**	2.70	1, 1, 2, 3, 8	**2.76**	2.59	1, 1, 2, 3, 8
0.75	*2*	**2.87**	2.73	1, 1, 2, 4, 8	**2.44**	2.18	1, 1, 2, 3, 7	**2.45**	2.18	1, 1, 2, 3, 7
1	*2*	**2.43**	2.73	1, 1, 2, 4, 8	**2.10**	1.72	1, 1, 1, 3, 5	**2.13**	1.78	1, 1, 1, 3, 5
1.25	*2*	**2.04**	1.64	1, 1, 1, 2, 5	**1.79**	1.31	1, 1, 1, 2, 4	**1.84**	1.39	1, 1, 1, 2, 4
1.5	*2*	**1.74**	1.28	1, 1, 1, 2, 4	**1.56**	1.01	1, 1, 1, 2, 3	**1.60**	1.06	1, 1, 1, 2, 4
2	*2*	**1.32**	0.65	1, 1, 1, 1, 3	**1.26**	0.60	1, 1, 1, 1, 2	**1.28**	0.63	1, 1, 1, 1, 3
3	*2*	**1.05**	0.22	1, 1, 1, 1, 1	**1.03**	0.19	1, 1, 1, 1, 1	**1.04**	0.21	1, 1, 1, 1, 1

Table B.4: Run length characteristics for the modified normal theory schemes for various values of μ_2 and σ_2 when $\mu_1 = 0, \sigma_1 = 1, m = 30$, and $n = 5$

		MAX CHART (H=3.15)			DISTANCE CHART (H=3.37)			$(\bar{X}, S)$ SCHEME (p_0=0.000763)		
μ_2	σ_2	*ARL*	*SDRL*	*5%, 25%, 50%, 75%, 95%*	*ARL*	*SDRL*	*5%, 25%, 50%, 75%, 95%*	*ARL*	*SDRL*	*5%, 25%, 50%, 75%, 95%*
0	*1*	**497.79**	591.70	15, 101, 289, 671, 1681	**494.29**	611.70	13, 90, 273, 669, 1730	**498.34**	750.80	8, 59, 209, 617, 1991
0.1	*1*	**479.93**	582.64	14, 92, 273, 644, 1666	**478.22**	607.48	12, 84, 260, 639, 1662	**477.30**	732.27	7, 54, 193, 587, 1914
0.25	*1*	**396.68**	521.43	9, 64, 202, 524, 1440	**381.12**	525.70	8, 57, 183, 491, 1435	**368.99**	619.63	5, 36, 131, 422, 1558
0.5	*1*	**204.95**	320.03	4, 23, 81, 248, 839	**180.86**	304.65	3, 21, 70, 210, 720	**159.52**	353.29	2, 12, 42, 142, 724
0.75	*1*	**83.01**	167.27	2, 8, 25, 81, 362	**69.98**	138.31	2, 7, 24, 72, 290	**51.49**	142.44	1, 5, 13, 40, 216
1	*1*	**28.62**	71.56	1, 3, 8, 24, 121	**23.93**	49.76	1, 3, 8, 24, 95	**15.81**	47.81	1, 2, 5, 13, 57
1.25	*1*	**9.68**	25.67	1, 2, 4, 8, 35	**9.16**	18.96	1, 2, 4, 9, 34	**5.57**	13.32	1, 1, 2, 5, 19
1.5	*1*	**3.92**	7.30	1, 1, 2, 4, 13	**4.15**	7.07	1, 1, 2, 4, 14	**2.65**	4.45	1, 1, 1, 3, 8
2	*1*	**1.32**	0.65	1, 1, 1, 1, 3	**1.51**	1.31	1, 1, 1, 2, 4	**1.25**	0.72	1, 1, 1, 1, 2
3	*1*	**1.01**	0.07	1, 1, 1, 1, 1	**1.01**	0.10	1, 1, 1, 1, 1	**1.00**	0.05	1, 1, 1, 1, 1
0	*1.25*	**191.30**	349.41	3, 20, 65, 204, 814	**156.17**	305.41	3, 15, 48, 154, 690	**96.71**	231.80	2, 9, 28, 85, 404
0.1	*1.25*	**179.23**	328.35	3, 18, 61, 189, 757	**151.26**	295.24	2, 14, 48, 151, 660	**92.00**	228.82	2, 9, 27, 80, 380
0.25	*1.25*	**146.92**	291.88	2, 14, 46, 146, 635	**123.08**	256.66	2, 11, 37, 117, 540	**74.30**	189.15	2, 7, 22, 65, 301
0.5	*1.25*	**76.17**	173.09	2, 8, 23, 69, 316	**63.74**	148.55	1, 6, 18, 57, 267	**38.38**	98.08	1, 4, 12, 34, 150
0.75	*1.25*	**30.41**	76.48	1, 4, 10, 28, 119	**26.91**	66.70	1, 3, 9, 25, 108	**16.51**	43.26	1, 3, 6, 16, 60
1	*1.25*	**12.54**	27.96	1, 2, 5, 12, 44	**11.77**	25.66	1, 2, 5, 12, 43	**7.38**	14.41	1, 2, 3, 8, 26
1.25	*1.25*	**5.79**	12.20	1, 1, 3, 6, 19	**5.65**	10.15	1, 1, 3, 6, 20	**3.82**	6.85	1, 1, 2, 4, 12
1.5	*1.25*	**3.15**	4.39	1, 1, 2, 3, 10	**3.14**	4.48	1, 1, 2, 3, 10	**2.30**	2.54	1, 1, 1, 3, 6
2	*1.25*	**1.39**	0.73	1, 1, 1, 2, 3	**1.52**	1.24	1, 1, 1, 2, 4	**1.30**	0.76	1, 1, 1, 1, 3
3	*1.25*	**1.02**	0.12	1, 1, 1, 1, 1	**1.02**	0.14	1, 1, 1, 1, 1	**1.01**	0.09	1, 1, 1, 1, 1
0	*1. 5*	**40.10**	95.14	1, 5, 14, 38, 156	**31.13**	75.91	1, 4, 11, 29, 121	**18.41**	41.87	1, 3, 7, 18, 67
0.1	*1.5*	**39.05**	90.41	1, 5, 14, 37, 156	**31.23**	82.49	1, 4, 10, 28, 122	**18.10**	43.45	1, 3, 7, 18, 66
0.25	*1.5*	**34.21**	79.33	1, 5, 12, 33, 132	**26.07**	61.45	1, 4, 10, 24, 100	**16.02**	36.26	1, 3, 7, 16, 58
0.5	*1.5*	**21.70**	46.41	1, 3, 9, 22, 82	**16.78**	37.22	1, 3, 7, 16, 61	**11.24**	21.87	1, 2, 5, 12, 40
0.75	*1.5*	**12.25**	23.63	1, 2, 5, 13, 43	**9.72**	22.19	1, 2, 4, 10, 34	**7.20**	14.64	1, 2, 4, 8, 24
1	*1.5*	**6.99**	13.52	1, 2, 4, 8, 23	**5.72**	10.58	1, 1, 3, 6, 19	**4.42**	6.28	1, 1, 3, 5, 14
1.25	*1.5*	**4.03**	5.56	1, 1, 2, 5, 13	**3.57**	5.09	1, 1, 2, 4, 11	**2.93**	3.37	1, 1, 2, 3, 9
1.5	*1.5*	**2.62**	2.79	1, 1, 2, 3, 7	**2.41**	2.69	1, 1, 2, 3, 7	**2.08**	1.95	1, 1, 1, 2, 6
2	*1.5*	**1.42**	0.77	1, 1, 1, 2, 3	**1.44**	0.96	1, 1, 1, 2, 3	**1.33**	0.77	1, 1, 1, 1, 3
3	*1.5*	**1.03**	0.17	1, 1, 1, 1, 1	**1.03**	0.20	1, 1, 1, 1, 1	**1.02**	0.14	1, 1, 1, 1, 1
0	*1.75*	**11.35**	21.04	1, 2, 5, 12, 40	**8.98**	16.77	1, 2, 4, 9, 31	**6.30**	10.07	1, 2, 3, 7, 21
0.1	*1.75*	**11.10**	22.21	1, 2, 5, 12, 39	**8.65**	15.83	1, 2, 4, 9, 30	**6.17**	9.63	1, 2, 3, 7, 20
0.25	*1.75*	**10.56**	20.75	1, 2, 5, 11, 37	**8.14**	15.33	1, 2, 4, 9, 27	**5.87**	9.17	1, 2, 3, 7, 19
0.5	*1.75*	**8.28**	13.70	1, 2, 4, 9, 28	**6.46**	10.52	1, 2, 3, 7, 22	**4.94**	6.81	1, 1, 3, 6, 16
0.75	*1.75*	**6.06**	9.70	1, 2, 3, 7, 20	**4.69**	6.94	1, 1, 3, 5, 15	**3.92**	5.07	1, 1, 2, 5, 12
1	*1.75*	**4.29**	5.87	1, 1, 2, 5, 14	**3.39**	4.45	1, 1, 2, 4, 10	**3.01**	3.44	1, 1, 2, 4, 9
1.25	*1.75*	**3.02**	3.46	1, 1, 2, 4, 9	**2.57**	2.81	1, 1, 2, 3, 7	**2.33**	2.30	1, 1, 2, 3, 6
1.5	*1.75*	**2.27**	2.22	1, 1, 2, 3, 6	**1.99**	1.84	1, 1, 1, 2, 5	**1.85**	1.52	1, 1, 1, 2, 5
2	*1.75*	**1.42**	0.78	1, 1, 1, 2, 3	**1.38**	0.84	1, 1, 1, 2, 3	**1.33**	0.75	1, 1, 1, 1, 3
3	*1.75*	**1.05**	0.23	1, 1, 1, 1, 1	**1.04**	0.21	1, 1, 1, 1, 1	**1.03**	0.18	1, 1, 1, 1, 1
0	*2*	**5.02**	7.30	1, 1, 3, 6, 16	**4.17**	5.56	1, 1, 2, 5, 13	**3.32**	3.94	1, 1, 2, 4, 10
0.1	*2*	**5.00**	6.79	1, 1, 3, 6, 16	**4.03**	5.42	1, 1, 2, 5, 12	**3.30**	3.80	1, 1, 2, 4, 10
0.25	*2*	**4.81**	6.59	1, 1, 3, 6, 16	**3.95**	5.18	1, 1, 2, 5, 12	**3.20**	3.77	1, 1, 2, 4, 9
0.5	*2*	**4.28**	5.93	1, 1, 3, 5, 13	**3.50**	4.25	1, 1, 2, 4, 14	**2.93**	3.28	1, 1, 2, 3, 8
0.75	*2*	**3.58**	4.18	1, 1, 2, 4, 11	**2.92**	3.22	1, 1, 2, 3, 8	**2.58**	2.68	1, 1, 2, 3, 7
1	*2*	**2.90**	3.21	1, 1, 2, 3, 8	**2.39**	2.34	1, 1, 2, 3, 7	**2.23**	2.08	1, 1, 1, 3, 6
1.25	*2*	**2.40**	2.32	1, 1, 2, 3, 7	**2.01**	1.76	1, 1, 1, 2, 5	**1.91**	1.58	1, 1, 1, 2, 5
1.5	*2*	**1.98**	1.72	1, 1, 1, 2, 5	**1.71**	1.32	1, 1, 1, 2, 4	**1.64**	1.20	1, 1, 1, 2, 4
2	*2*	**1.40**	0.74	1, 1, 1, 2, 3	**1.33**	0.76	1, 1, 1, 1, 3	**1.30**	0.68	1, 1, 1, 1, 3
3	*2*	**1.07**	0.27	1, 1, 1, 1, 2	**1.05**	0.24	1, 1, 1, 1, 1	**1.04**	0.22	1, 1, 1, 1, 1

Figure B.1: Region of Values of μ_2 and σ_2 (in red) for which the Modified Distance chart outperforms the Modified Max chart for various values of m when $\mu_1 = 0, \sigma_1 = 1$, and $n = 5$

$m = 100$

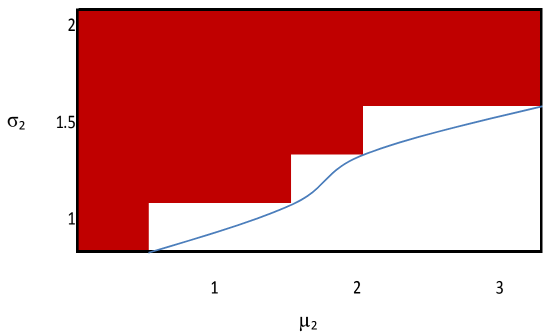

$m = 75$

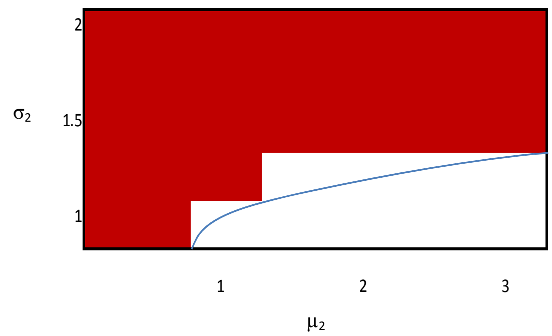

$m = 50$

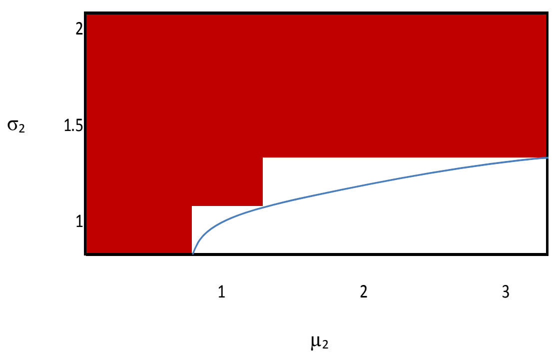

$m = 30$

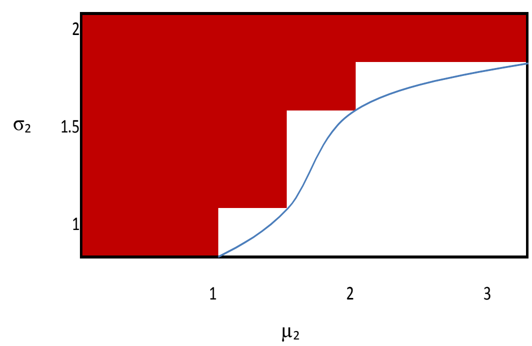

C: SUPPLEMENTARY DERIVATIONS FOR CHAPTER 4

C.1 The joint distribution of $\tilde{\theta}_2$ and $\tilde{\lambda}_2$

Recall that $\frac{2n\hat{\lambda}_2}{\lambda_2}$ has a chi-square distribution with $2n-2$ degrees of freedom and that $\hat{\theta}_2$ follows the shifted exponential distribution with location parameter θ_2 and scale parameter λ_2/n. Therefore, distribution of $\hat{\lambda}_2$ is $f_{\hat{\lambda}_2}(x_1) = \frac{\lambda_2}{2n}\left[\frac{1}{2^{n-1}\Gamma(n-1)}\right] x_1^{n-2} e^{-\frac{x_1}{2}}, x_1 > 0$ and the distribution of $\hat{\theta}_2$ is $f_{\hat{\theta}_2}(x_2) = \frac{n}{\lambda_2}\exp\left[\frac{-n(x_2-\theta_2)}{\lambda_2}\right], x_2 > \theta_2$. Since $\hat{\lambda}_2$ and $\hat{\theta}_2$ are independent, their joint distribution, $f_{\hat{\lambda}_2,\hat{\theta}_2}(x_1,x_2) = f_{\hat{\lambda}_2}(x_1) f_{\hat{\theta}_2}(x_2) =$ $\left\{\frac{\lambda_2}{2n}\left[\frac{1}{2^{n-1}\Gamma(n-1)}\right] x_1^{n-2} e^{-x_1/2}\right\}\left\{\frac{n}{\lambda_2}\exp\left[\frac{-n(x_2-\theta_2)}{\lambda_2}\right]\right\}, x_1 > 0, x_2 > \theta_2$. Now, note that $\tilde{\lambda}_2 = \frac{n(\bar{V}-V_{(1)})}{n-1} = \frac{n\hat{\lambda}_2}{n-1}$. Also, $\tilde{\theta}_2 = \frac{nV_{(1)}-\bar{V}}{n-1} = \frac{-\bar{V}+V_{(1)}+(n-1)V_{(1)}}{n-1} = \frac{-(\bar{V}-V_{(1)})}{n-1} + V_{(1)} = \frac{-\hat{\lambda}_2}{n-1} + \hat{\theta}_2$. In other words, both $\tilde{\lambda}_2$and $\tilde{\theta}_2$ can be written as one-to-one transformations of $\hat{\lambda}_2$ and $\hat{\theta}_2$. We can therefore use the Jacobian method to obtain the joint distribution of $\tilde{\lambda}_2$and $\tilde{\theta}_2$, $f_{\tilde{\theta}_2,\tilde{\lambda}_2}(y_1,y_2)$.

To use the Jacobian method, note that $\hat{\lambda}_2 = \frac{(n-1)\tilde{\lambda}_2}{n}$ and $\hat{\theta}_2 = \tilde{\theta}_2 + \frac{\tilde{\lambda}_2}{n}$. The resulting Jacobian is $\frac{-(n-1)}{n}$, a negative number. Hence, the joint pdf of of $\tilde{\lambda}_2$and $\tilde{\theta}_2$ is $f_{\tilde{\theta}_2,\tilde{\lambda}_2}(y_1,y_2) =$

$$\left\{\frac{\lambda_2}{2n}\left[\frac{1}{2^{n-1}\Gamma(n-1)}\right]\left[\frac{(n-1)y_2}{n}\right]^{n-2} e^{-\left[\frac{(n-1)y_2}{n}\right]/2}\right\}\left\{\frac{n}{\lambda_2}\exp\left[\frac{-n\left(y_1+\frac{y_2}{n}-\theta_2\right)}{\lambda_2}\right]\right\}\left|\frac{-(n-1)}{n}\right|$$

$$= \frac{n(n-1)^{n-1}}{\lambda_2^n\Gamma(n-1)} y_2^{n-2} e^{-\frac{n}{\lambda_2}(y_1+y_2-\theta_2)}, y_1 > \theta_2 - \frac{y_2}{n}, y_2 > 0.$$

Now, $\int_0^\infty \int_{\left[\theta_2-\frac{y_2}{n}\right]}^\infty f_{\tilde{\theta}_2,\tilde{\lambda}_2}(y_1,y_2)dy_1dy_2 = \int_0^\infty \int_{\left[\theta_2-\frac{y_2}{n}\right]}^\infty \frac{n(n-1)^{n-1}}{\lambda_2^n\Gamma(n-1)} y_2^{n-2} e^{-\frac{n}{\lambda_2}(y_1+y_2-\theta_2)} dy_1dy_2 =$

$$\int_0^\infty \frac{n(n-1)^{n-1}}{\lambda_2^n\Gamma(n-1)} y_2^{n-2} e^{-\frac{n}{\lambda_2}(y_2-\theta_2)} \int_{\left[\theta_2-\frac{y_2}{n}\right]}^\infty e^{-\frac{n}{\lambda_2}(y_1)} dy_1dy_2 =$$

$$\int_0^\infty \frac{n(n-1)^{n-1}}{\lambda_2^n\Gamma(n-1)} y_2^{n-2} e^{-\frac{n}{\lambda_2}(y_2-\theta_2)} \left[\frac{\lambda_2}{n} e^{-n\left[\theta_2-\frac{y_2}{n}\right]/\lambda_2}\right] dy_2 = \int_0^\infty \frac{(n-1)^{n-1}}{\lambda_2^{n-1}\Gamma(n-1)} y_2^{n-2} e^{\frac{-(n-1)y_2}{\lambda_2}} dy_2 = 1$$

since $\frac{(n-1)^{n-1}}{\lambda_2^{n-1}\Gamma(n-1)} y_2^{n-2} e^{\frac{-(n-1)y_2}{\lambda_2}}$ is the pdf of a Gamma$\left(n-1, \frac{\lambda_2}{n-1}\right)$ distribution.

C.2 The distribution of $\tilde{\theta}_2$

The marginal distribution of $\tilde{\theta}_2$ can be obtained by integrating the joint distribution of $\tilde{\lambda}_2$ and $\tilde{\theta}_2$over all possible values of $\tilde{\lambda}_2$. Notice that the joint distribution has the conditions $y_1 > \theta_2 - \frac{y_2}{n}$ and $y_2 > 0$. In other words, y_2 must be larger than both 0 and $n(\theta_2 - y_1)$. When y_1 is between -∞ and θ_2, $n(\theta_2 - y_1) > 0$, so $n(\theta_2 - y_1) < y_2 < \infty$. However, when y_1 is between $\theta_2$and ∞, $n(\theta_2 - y_1) < 0$, so $0 < y_2 < \infty$. Therefore, $f_{\tilde{\theta}_2}(y_1)$

$$= \int_0^\infty \frac{n(n-1)^{n-1}}{\lambda_2^n\Gamma(n-1)} y_2^{n-2} e^{\frac{-n(y_2+y_1-\theta_2)}{\lambda_2}} dy_2\, I_{(\theta_2,\infty)}(y_1)$$

$$+ \int_{n(\theta_2-y_1)}^\infty \frac{n(n-1)^{n-1}}{\lambda_2^n\Gamma(n-1)} y_2^{n-2} e^{\frac{-n(y_2+y_1-\theta_2)}{\lambda_2}} dy_2\, I_{(-\infty,\theta_2]}(y_1).$$

$$= \frac{(n-1)^{n-1}}{\lambda_2 n^{n-2}} e^{\frac{-n(y_1-\theta_2)}{\lambda_2}} I_{(\theta_2,\infty)}(y_1) + \int_{n(\theta_2-y_1)}^\infty \frac{n(n-1)^{n-1}}{\lambda_2^n\Gamma(n-1)} y_2^{n-2} e^{\frac{-n(y_2+y_1-\theta_2)}{\lambda_2}} dy_2\, I_{(-\infty,\theta_2]}(y_1).$$

Now, $\int_{-\infty}^\infty f_{\tilde{\theta}_2}(y_1)\, dy_1$

$$= \int_{\theta_2}^\infty \frac{(n-1)^{n-1}}{\lambda_2 n^{n-2}} e^{\frac{-n(y_1-\theta_2)}{\lambda_2}} dy_1 + \int_{-\infty}^{\theta_2}\int_{n(\theta_2-y_1)}^\infty \frac{n(n-1)^{n-1}}{\lambda_2^n\Gamma(n-1)} y_2^{n-2} e^{\frac{-n(y_2+y_1-\theta_2)}{\lambda_2}} dy_2 dy_1$$

$$= \frac{(n-1)^{n-1}}{n^{n-1}} + \int_{-\infty}^{\theta_2}\int_{n(\theta_2-y_1)}^\infty \frac{n(n-1)^{n-1}}{\lambda_2^n\Gamma(n-1)} y_2^{n-2} e^{\frac{-n(y_2+y_1-\theta_2)}{\lambda_2}} dy_2 dy_1$$

$$= \frac{(n-1)^{n-1}}{n^{n-1}} + \int_0^\infty \frac{n(n-1)^{n-1}}{\lambda_2^n\Gamma(n-1)} y_2^{n-2} e^{\frac{-n(y_2-\theta_2)}{\lambda_2}} \int_{\left(\theta_2-\frac{y_2}{n}\right)}^{\theta_2} e^{\frac{-ny_1}{\lambda_2}} dy_1 dy_2$$

$$= \frac{(n-1)^{n-1}}{n^{n-1}} + \int_0^\infty \frac{n(n-1)^{n-1}}{\lambda_2^n\Gamma(n-1)} y_2^{n-2} e^{\frac{-n(y_2-\theta_2)}{\lambda_2}} \left[\left(\frac{-\lambda_2}{n}\right)\left(e^{-n\theta_2/\lambda_2} - e^{-n\left(\theta_2-\frac{y_2}{n}\right)/\lambda_2}\right)\right] dy_2$$

$$= \frac{(n-1)^{n-1}}{n^{n-1}} + \frac{(n-1)^{n-1}}{\lambda_2^{n-1}\Gamma(n-1)} \int_0^\infty y_2^{n-2} e^{\frac{-n(y_2-\theta_2)}{\lambda_2}} \left[\left(-e^{-\frac{n\theta_2}{\lambda_2}} + e^{-n\left(\theta_2 - \frac{y_2}{n}\right)/\lambda_2}\right)\right] dy_2$$

$$= \frac{(n-1)^{n-1}}{n^{n-1}} + \frac{(n-1)^{n-1}}{\lambda_2^{n-1}\Gamma(n-1)} \left[- \int_0^\infty y_2^{n-2} e^{\frac{-ny_2}{\lambda_2}} dy_2 + \int_0^\infty y_2^{n-2} e^{\frac{-(n-1)y_2}{\lambda_2}} dy_2\right]$$

$$= \frac{(n-1)^{n-1}}{n^{n-1}} + \frac{(n-1)^{n-1}}{\lambda_2^{n-1}\Gamma(n-1)} \left[-\Gamma(n-1)\left(\frac{\lambda_2}{n}\right)^{n-1} \int_0^\infty \frac{1}{\Gamma(n-1)\left(\frac{\lambda_2}{n}\right)^{n-1}} y_2^{n-2} e^{\frac{-ny_2}{\lambda_2}} dy_2\right.$$

$$\left.+\Gamma(n-1)\left(\frac{\lambda_2}{n-1}\right)^{n-1} \int_0^\infty \frac{1}{\Gamma(n-1)\left(\frac{\lambda_2}{n-1}\right)^{n-1}} y_2^{n-2} e^{\frac{-(n-1)y_2}{\lambda_2}} dy_2\right]$$

$$= \frac{(n-1)^{n-1}}{n^{n-1}} + \frac{(n-1)^{n-1}}{\lambda_2^{n-1}\Gamma(n-1)} \left[-\Gamma(n-1)\left(\frac{\lambda_2}{n}\right)^{n-1} + \Gamma(n-1)\left(\frac{\lambda_2}{n-1}\right)^{n-1}\right]$$

$$= \frac{(n-1)^{n-1}}{n^{n-1}} + (n-1)^{n-1}\left[-\left(\frac{1}{n}\right)^{n-1} + \left(\frac{1}{n-1}\right)^{n-1}\right] = \frac{(n-1)^{n-1}}{n^{n-1}} - \left(\frac{(n-1)}{n}\right)^{n-1} + 1 = 1.$$

C.3 The distribution of $\mathcal{M}$

$$P(\mathcal{M} \le g) = P(\max\{|B_1|, |B_2|\} \le g) = P\{(|B_1| \le g)\,\&(|B_2| \le g)\}$$

$$= P(|B_1| \le g)P(|B_2| \le g) = P(-g \le B_1 \le g)P(-g \le B_2 \le g)$$

$$= P\left(-g \le \Phi^{-1}\left\{G\left(\frac{2n\left(\hat{\theta}_2-\theta_0\right)}{\lambda_0}, 2\right)\right\} \le g\right) \times P\left(-g \le \Phi^{-1}\left\{\mathrm{G}\left(\frac{2n\hat{\lambda}_2}{\lambda_0}, 2n-2\right)\right\} \le g\right)$$

$$= P\left(\frac{2n}{\lambda_2}\left(\frac{\lambda_0 G^{-1}(\Phi(-g),2)}{2n} + \theta_0 - \theta_2\right) \le \frac{2n\left(\hat{\theta}_2-\theta_2\right)}{\lambda_2} \le \frac{2n}{\lambda_2}\left(\frac{\lambda_0 G^{-1}(\Phi(g),2)}{2n} + \theta_0 - \theta_2\right)\right)$$

$$\times P\left(\frac{\lambda_0}{\lambda_2} G^{-1}(\Phi(-g), 2n-2) \le \frac{2n\hat{\lambda}_2}{\lambda_2} \le \frac{\lambda_0}{\lambda_2} G^{-1}(\Phi(-g), 2n-2)\right)$$

$$= P\left(\frac{2n}{\lambda_2}\left(\frac{\lambda_0 G^{-1}(\Phi(-g),2)}{2n} + \theta_0 - \theta_2\right) \le \chi_2^2 \le \frac{2n}{\lambda_2}\left(\frac{\lambda_0 G^{-1}(\Phi(g),2)}{2n} + \theta_0 - \theta_2\right)\right)$$

$$\times P\left(\frac{\lambda_0}{\lambda_2} G^{-1}(\Phi(-g), 2n-2) \le \chi^2_{2(n-1)} \le \frac{\lambda_0}{\lambda_2} G^{-1}(\Phi(g), 2n-2)\right)$$

$$= \left\{G\left(\frac{2n}{\lambda_2}\left(\frac{\lambda_0}{2n} G^{-1}(\Phi(g), 2) + \theta_0 - \theta_2\right), 2\right) - G\left(\frac{2n}{\lambda_2}\left(\frac{\lambda_0}{2n} G^{-1}(\Phi(-g), 2) + \theta_0 - \theta_2\right), 2\right)\right\}$$

$$\times\left\{G\left(\frac{\lambda_0}{\lambda_2}G^{-1}(\Phi(g),2n-2),2n-2\right)-G\left(\frac{\lambda_0}{\lambda_2}G^{-1}(\Phi(-g),2n-2),2n-2\right)\right\}.$$

C.4 The distribution of T

$P(T \leq g \,\&\, D_1 > 0) = P(\max\{D_1, D_2\} \leq g \,\&\, D_1 > 0) = P(D_1 \leq g \,\&\, D_2 \leq g \,\&\, D_1 > 0) =$

$P(0 < D_1 \leq g \,\&\, D_2 \leq g) = P(0 < D_1 \leq g)P(D_2 \leq g) =$

$$P\left(0<\frac{2n(\hat{\theta}_2-\theta_0)}{\lambda_0}\leq g\right)P\left(\mathrm{G}^{-1}\left\{\mathrm{G}\left(\frac{2n\hat{\lambda}_2}{\lambda_0},2n-2\right),2n-2\right\}\leq g\right)$$

$$=P\left(\frac{2n(\theta_0-\theta_2)}{\lambda_2}<\frac{2n(\hat{\theta}_2-\theta_2)}{\lambda_2}\leq\frac{2n}{\lambda_2}\left(\frac{\lambda_0 g}{2n}+\theta_0-\theta_2\right)\right)P\left(\frac{2n\hat{\lambda}_2}{\lambda_2}\leq\frac{\lambda_0}{\lambda_2}\mathrm{G}^{-1}\{\mathrm{G}(g,2),2n-2\}\right)$$

$$=P\left(\frac{2n(\theta_0-\theta_2)}{\lambda_2}<\chi_2^2\leq\frac{2n}{\lambda_2}\left(\frac{\lambda_0 g}{2n}+\theta_0-\theta_2\right)\right)P\left(\chi^2_{2(n-1)}\leq\frac{\lambda_0}{\lambda_2}\mathrm{G}^{-1}\{\mathrm{G}(g,2),2n-2\}\right)$$

$$=\left\{G\left[\frac{2n}{\lambda_2}\left(\frac{\lambda_0 g}{2n}+\theta_0-\theta_2\right),2\right]-G\left[\frac{2n}{\lambda_2}(\theta_0-\theta_2),2\right]\right\}\times\left\{G\left\{\frac{\lambda_0}{\lambda_2}G^{-1}[G(g,2),2n-2],2n-2\right\}\right\}$$

C.5 ARL Bias in the SEMLE-Max Chart

Suppose that some SEMLE-Max Chart has *UCL* $g > 0$. Note that *ARL* bias occurs when for some shift size, $P(\mathcal{M} \leq g|\theta_2, \lambda_2) > P(\mathcal{M} \leq g|\theta_0, \lambda_0)$. Recall that the cumulative distribution function of the statistic $\mathcal{M}$ which defines this chart is $P(\mathcal{M} \leq g) =$

$$\left\{G\left(\frac{2n}{\lambda_2}\left(\frac{\lambda_0}{2n}G^{-1}(\Phi(g),2)+\theta_0-\theta_2\right),2\right)-G\left(\frac{2n}{\lambda_2}\left(\frac{\lambda_0}{2n}G^{-1}(\Phi(-g),2)+\theta_0-\theta_2\right),2\right)\right\}\times$$

$\left\{G\left(\frac{\lambda_0}{\lambda_2}G^{-1}(\Phi(g),2n-2),2n-2\right)-G\left(\frac{\lambda_0}{\lambda_2}G^{-1}(\Phi(-g),2n-2),2n-2\right)\right\}$ and that it simplifies to $\{\Phi(g) - \Phi(-g)\}^2$ when the process is *IC*. Now, suppose that $\theta_0 = 0$ and $\lambda_0 = 1$ and that there has been a shift in the location parameter but not in the scale parameter. Then,

$$P(\mathcal{M}\leq g)=\left\{G\left(\frac{2n}{1}\left(\frac{1}{2n}G^{-1}(\Phi(g),2)-\theta_2\right),2\right)-G\left(\frac{2n}{1}\left(\frac{1}{2n}G^{-1}(\Phi(-g),2)-\theta_2\right),2\right)\right\}$$

$$\times\{G(G^{-1}(\Phi(g),2n-2),2n-2)-G(G^{-1}(\Phi(-g),2n-2),2n-2)\}$$

$= \left\{G\left((G^{-1}(\Phi(g),2) - 2n\theta_2),2\right) - G\left((G^{-1}(\Phi(-g),2) - 2n\theta_2),2\right)\right\} \times \{\Phi(g) - \Phi(-g)\}$.

We need to determine when $\left\{G\left((G^{-1}(\Phi(g),2) - 2n\theta_2),2\right) - G\left((G^{-1}(\Phi(-g),2) - 2n\theta_2),2\right)\right\}$ $\times \{\Phi(g) - \Phi(-g)\} > \{\Phi(g) - \Phi(-g)\}^2$.

Dividing both sides by $\{\Phi(g) - \Phi(-g)\}$ gives us $\left\{G\left((G^{-1}(\Phi(g),2) - 2n\theta_2),2\right) - G\left((G^{-1}(\Phi(-g),2) - 2n\theta_2),2\right)\right\} > \{\Phi(g) - \Phi(-g)\}$. Let $a = G\left((G^{-1}(\Phi(g),2) - 2n\theta_2),2\right)$ and $b = G\left((G^{-1}(\Phi(-g),2) - 2n\theta_2),2\right)$. Now suppose $\{a - b\} > \{\Phi(g) - \Phi(-g)\}$. This can be true in one of three ways:

i) $a = 0$ and $-b > \{\Phi(g) - \Phi(-g)\}$.

ii) $b = 0$ and $a > \{\Phi(g) - \Phi(-g)\}$.

iii) $a > 0, b > 0$, and $a - b > \{\Phi(g) - \Phi(-g)\}$

<u>Case i</u>

Let $a = 0$. Then $G\left((G^{-1}(\Phi(g),2) - 2n\theta_2),2\right) = 0$. Now, $G(c,2) = 0$ whenever $c \leq 0$, so we have $G^{-1}(\Phi(g),2) - 2n\theta_2 \leq 0$, or $\theta_2 \geq \frac{G^{-1}(\Phi(g),2)}{2n}$. Next, let $-b > \{\Phi(g) - \Phi(-g)\}$. Then $G\left((G^{-1}(\Phi(-g),2) - 2n\theta_2),2\right) < -\{\Phi(g) - \Phi(-g)\}$. However, $G\left((G^{-1}(\Phi(-g),2) - 2n\theta_2),2\right)$ cannot be less than $-\{\Phi(g) - \Phi(-g)\}$, because $G(.,2)$ cannot be negative, while $-\{\Phi(g) - \Phi(-g)\}$ must be negative. Therefore, case I cannot occur.

<u>Case ii</u>

Let $b = 0$. Then $G\left((G^{-1}(\Phi(-g),2) - 2n\theta_2),2\right) = 0$. So, $G^{-1}(\Phi(-g),2) - 2n\theta_2 \leq 0$. Restated, $\theta_2 \geq \frac{G^{-1}(\Phi(-g),2)}{2n}$. Now let $a > \{\Phi(g) - \Phi(-g)\}$. Then $G\left((G^{-1}(\Phi(g),2) -\right.$

$2n\theta_2), 2\big) > \{\Phi(g) - \Phi(-g)\}$. Applying the χ_2^2 inverse function to each side gives us

$G^{-1}(\Phi(g), 2) - 2n\theta_2 > G^{-1}\{\Phi(g) - \Phi(-g), 2\}$, or $\theta_2 < \frac{G^{-1}(\Phi(g),2) - G^{-1}\{\Phi(g)-\Phi(-g),2\}}{2n}$.

So in Case ii, $\frac{G^{-1}(\Phi(-g),2)}{2n} \le \theta_2 < \frac{G^{-1}(\Phi(g),2) - G^{-1}\{\Phi(g)-\Phi(-g),2\}}{2n}$.

<u>Case iii</u>

Let $a > 0$. Then $G\big((G^{-1}(\Phi(g), 2) - 2n\theta_2), 2\big) > 0$. Applying the χ_2^2 inverse function to each side gives us $G^{-1}(\Phi(g), 2) - 2n\theta_2 > 0$, or $\theta_2 < \frac{G^{-1}(\Phi(g),2)}{2n}$.

Now let $b > 0$. Then $G\big((G^{-1}(\Phi(-g), 2) - 2n\theta_2), 2\big) > 0$. Applying the χ_2^2 inverse function to each side gives us $G^{-1}(\Phi(-g), 2) - 2n\theta_2 > 0$, or $\theta_2 < \frac{G^{-1}(\Phi(-g),2)}{2n}$.

Finally, let $-b > \{\Phi(g) - \Phi(-g)\}$. Then $\big\{G\big((G^{-1}(\Phi(g), 2) - 2n\theta_2), 2\big) - G\big((G^{-1}(\Phi(-g), 2) - 2n\theta_2), 2\big)\big\} > \{\Phi(g) - \Phi(-g)\}$. Note that $G\big((G^{-1}(\Phi(g), 2) - 2n\theta_2), 2\big) - G\big((G^{-1}(\Phi(-g), 2) - 2n\theta_2), 2\big) = \int_{G^{-1}(\Phi(-g),2)-2n\theta_2}^{G^{-1}(\Phi(g),2)-2n\theta_2} \frac{1}{2} e^{-\frac{x}{2}} dx$

$= e^{-\frac{[G^{-1}(\Phi(-g),2)-2n\theta_2]}{2}} \left[1 - e^{\frac{[G^{-1}(\Phi(-g),2)-G^{-1}(\Phi(g),2)]}{2}}\right]$. So,

$e^{-\frac{[G^{-1}(\Phi(-g),2)-2n\theta_2]}{2}} \left[1 - e^{\frac{[G^{-1}(\Phi(-g),2)-G^{-1}(\Phi(g),2)]}{2}}\right] > \{\Phi(g) - \Phi(-g)\}$. Dividing both sides by $1 - e^{\frac{[G^{-1}(\Phi(-g),2)-G^{-1}(\Phi(g),2)]}{2}}$ gives us $e^{-\frac{[G^{-1}(\Phi(-g),2)-2n\theta_2]}{2}} > \frac{\{\Phi(g)-\Phi(-g)\}}{\left[1-e^{\frac{[G^{-1}(\Phi(-g),2)-G^{-1}(\Phi(g),2)]}{2}}\right]}$. Taking the natural log of each side gives us $-\frac{[G^{-1}(\Phi(-g),2)-2n\theta_2]}{2} > \ln\left\{\frac{\{\Phi(g)-\Phi(-g)\}}{\left[1-e^{\frac{[G^{-1}(\Phi(-g),2)-G^{-1}(\Phi(g),2)]}{2}}\right]}\right\}$. Finally, we have $\dfrac{G^{-1}(\Phi(-g),2)+2\ln\left\{\dfrac{\{\Phi(g)-\Phi(-g)\}}{\left[1-e^{\frac{[G^{-1}(\Phi(-g),2)-G^{-1}(\Phi(g),2)]}{2}}\right]}\right\}}{2n} < \theta_2$. But

$\dfrac{G^{-1}(\Phi(-g),2)+2\ln\left\{\dfrac{\{\Phi(g)-\Phi(-g)\}}{\left[1-e^{\frac{[G^{-1}(\Phi(-g),2)-G^{-1}(\Phi(g),2)]}{2}}\right]}\right\}}{2n} = 0$, so $\theta_2 > 0$. Thus, for Case iii, we have $\theta_2 > 0, \theta_2 < \frac{G^{-1}(\Phi(g),2)}{2n}$, and $\theta_2 < \frac{G^{-1}(\Phi(-g),2)}{2n}$. Since $\frac{G^{-1}(\Phi(g),2)}{2n} > \frac{G^{-1}(\Phi(-g),2)}{2n}$, we see that case iii occurs when $0 < \theta_2 < \frac{G^{-1}(\Phi(-g),2)}{2n}$.

Combining the three cases, we see that bias occurs when $0 < \theta_2 < \frac{G^{-1}(\Phi(g),2)-G^{-1}\{\Phi(g)-\Phi(-g),2\}}{2n}$. When $g = 3.29$ and $n = 5$ as was the case in our simulation study, this means that there is bias when $0 < \theta_2 < 0.1386$.

C.6 Lack of ARL Bias in the SEMLE-ChiMax Chart

Suppose that some SEMLE-ChiMax Chart has *UCL* $g > 0$. Note that *ARL* bias would occur if for some shift size, $P(\mathcal{M} \le g|\theta_2, \lambda_2) > P(\mathcal{M} \le g|\theta_0, \lambda_0)$. Recall that the cumulative distribution function for the statistics which defines this chart is $P(T \le g \,\&\, D_1 > 0) =$ $\left\{G\left[\frac{2n}{\lambda_2}\left(\frac{\lambda_0 g}{2n} + \theta_0 - \theta_2\right), 2\right] - G\left[\frac{2n}{\lambda_2}(\theta_0 - \theta_2), 2\right]\right\} \times \left\{G\left\{\frac{\lambda_0}{\lambda_2} G^{-1}[G(g,2), 2n-2], 2n-2\right\}\right\}$ and that it simplifies to $\{G(g,2)\}\{G(g,2)\}$ when the process is *IC*. Now, suppose that $\theta_0 = 0$ and $\lambda_0 = 1$ and that there has been a shift in the location parameter but not in the scale parameter. Then, $P(T \le g \,\&\, D_1 > 0) = \left\{G\left[\frac{2n}{\lambda_2}\left(\frac{\lambda_0 g}{2n} + \theta_0 - \theta_2\right), 2\right] - G\left[\frac{2n}{\lambda_2}(\theta_0 - \theta_2), 2\right]\right\}$ $\times \left\{G\left\{\frac{\lambda_0}{\lambda_2} G^{-1}[G(g,2), 2n-2], 2n-2\right\}\right\} = \{G[g - 2n\theta_2, 2] - G[-2n\theta_2, 2]\} \times \{G(g,2)\}$.

We need to determine when $\{G[g - 2n\theta_2, 2] - G[-2n\theta_2, 2]\} \times \{G(g, 2)\}$ $> \{G(g, 2)\}\{G(g, 2)\}$. Dividing both sides by $\{G(g, 2)\}$ gives us $\{G[g - 2n\theta_2, 2] - G[-2n\theta_2, 2]\} > \{G(g, 2)\}$. Let $c = G[g - 2n\theta_2, 2]$ and $d = G[-2n\theta_2, 2]$.

Now suppose $\{c - d\} > \{G(g, 2)\}$. This can be true in one of three ways:

i) $c = 0$ and $-d > \{G(g, 2)\}$.

ii) $d = 0$ and $c > \{G(g, 2)\}$.

iii) $c > 0, d > 0$, and $c - d > \{G(g, 2)\}$

<u>Case i</u>

Let $c = 0$. Then $G[g - 2n\theta_2, 2] = 0$. Now, $G(c, 2) = 0$ whenever $c \leq 0$, so we have $g - 2n\theta_2 \leq 0$, or $\theta_2 \geq \frac{g}{2n}$. Now let $-d > \{G(g, 2)\}$. Then $-G[-2n\theta_2, 2] < \{G(g, 2)\}$. This simplifies to $\theta_2 < \frac{G^{-1}[-[G(g,2)],2]}{-2n}$. However, $\frac{G^{-1}[-[G(g,2)],2]}{-2n}$ does not exist. Therefore, case I cannot occur.

<u>Case ii</u>

Let $d = 0$. Then $G[-2n\theta_2, 2] = 0$, which gives us $\theta_2 \geq 0$. Now let $c > \{G(g, 2)\}$. Then $G[g - 2n\theta_2, 2] > \{G(g, 2)\}$. This simplifies to $\theta_2 < 0$. However, θ_2 cannot simultaneously be less than 0 and greater than or equal to 0, so case ii cannot occur.

<u>Case iii</u>

Let $c > 0$. Then $G[g - 2n\theta_2, 2] > 0$. Therefore, $\theta_2 < \frac{g}{2n}$. Now let $d > 0$. Then $G[-2n\theta_2, 2] > 0$. Therefore, $\theta_2 < 0$. Finally, let $c - d > \{G(g, 2)\}$. Then $[g - 2n\theta_2, 2] -$

$G[-2n\theta_2, 2] > \{G(g, 2)\}$. . Note that $G[g - 2n\theta_2, 2] - G[-2n\theta_2, 2] = \int_{[-2n\theta_2]}^{[g-2n\theta_2]} \frac{1}{2} e^{-\frac{x}{2}} dx =$ $e^{[2n\theta_2]/2}\left[1 - e^{[-2n\theta_2 - g + 2n\theta_2]/2}\right] = e^{n\theta_2}\left[1 - e^{-g/2}\right]$. So $e^{n\theta_2}\left[1 - e^{-g/2}\right] > \{G(g, 2)\}$. Solving for θ_2 results in $\theta_2 > \left\{\ln\left[\frac{\{G(g,2)\}}{[1-e^{-g/2}]}\right]\right\}/n$. However, since $\frac{\left\{\ln\left[\frac{\{G(g,2)\}}{[1-e^{-g/2}]}\right]\right\}}{n} = 0$, resulting in $\theta_2 > 0$. θ_2 cannot simultaneously be less than 0 and greater than or equal to 0, so case iii cannot occur.

APPENDIX D: SUPPLEMENTARY DERIVATIONS FOR CHAPTER 5

D.1 The distribution of ϒ

$$P(\Upsilon \leq g) = P(\max\{|R_1|, |R_2|\} \leq g) = P\{(|R_1| \leq g)\,\&(|R_2| \leq g)\}$$

$$= P(|R_1| \leq g)P(|R_2| \leq g) = P(-g \leq R_1 \leq g)P(-g \leq R_2 \leq g)$$

$$= P(-g \leq \Phi^{-1}\{\daleth(\hat{a}_2, a_0, b_0)\} \leq g) \times P\left(-g \leq \Phi^{-1}\left\{\mathrm{M}\left(\frac{n\hat{b}_2}{b_0}\right)\right\} \leq g\right)$$

$$= P\left(\daleth^{-1}(\Phi(-g), a_0, b_0) \leq \hat{a}_2 \leq \daleth^{-1}(\Phi(g), a_0, b_0)\right)$$

$$\times P\left(M^{-1}(\Phi(-g), a_0, b_0) \leq \frac{n\hat{b}_2}{b_0} \leq M^{-1}(\Phi(-g), a_0, b_0)\right)$$

$$= P\left(\daleth^{-1}(\Phi(-g), a_0, b_0) \leq \hat{a}_2 \leq \daleth^{-1}(\Phi(g), a_0, b_0)\right)$$

$$\times P\left(\frac{b_0}{b_2}M^{-1}(\Phi(-g), a_0, b_0) \leq \frac{n\hat{b}_2}{b_2} \leq \frac{b_0}{b_2}M^{-1}(\Phi(g), a_0, b_0)\right)$$

$$= \{(\daleth[\daleth^{-1}(\Phi(g), a_0, b_0), a_2, b_2]) - (\daleth[\daleth^{-1}(\Phi(-g), a_0, b_0), a_2, b_2])\}$$

$$\times \left\{M\left(\frac{b_0}{b_2}M^{-1}(\Phi(g), a_0, b_0), a_2, b_2\right) - M\left(\frac{b_0}{b_2}M^{-1}(\Phi(-g), a_0, b_0), a_2, b_2\right)\right\}.$$